EXPERIMENTAL INVESTIGATION AND MODELING OF MINIMUM HOT SURFACE IGNITION TEMPERATURE FOR AVIATION FLUIDS

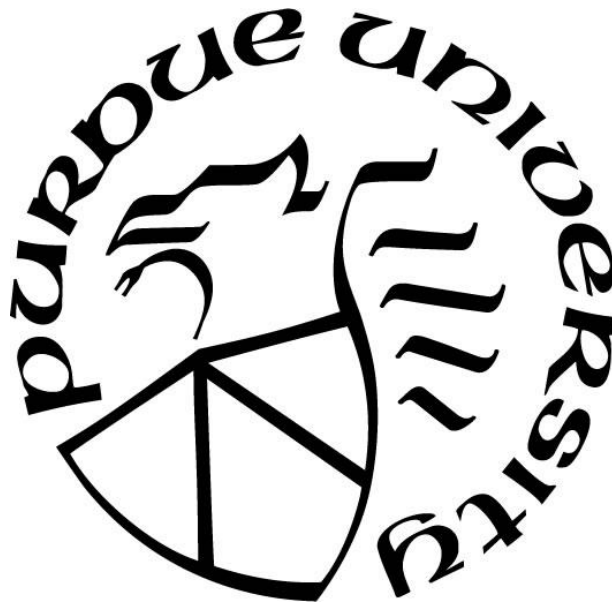by

Mehmed Sitki Ulcay

A Dissertation

Submitted to the Faculty of Purdue University

In Partial Fulfillment of the Requirements for the degree of

Doctor of Philosophy

School of Mechanical Engineering

West Lafayette, Indiana

May 2020

THE PURDUE UNIVERSITY GRADUATE SCHOOL
STATEMENT OF COMMITTEE APPROVAL

Dr. Jay P. Gore, Chair

School of Mechanical Engineering

Dr. Robert P. Lucht

School of Mechanical Engineering

Dr. Terrence R. Meyer

School of Mechanical Engineering

Dr. Li Qiao

School of Aeronautics and Astronautics

Approved by:

Dr. Nicole Key

Head of the Graduate Program

Dedicated to

To my Wife, Daughter and Parents

ACKNOWLEDGMENTS

TABLE OF CONTENTS

LIST OF TABLES

LIST OF FIGURES

NOMENCLATURE AND SYMBOLS

TC – Thermocouple

PT – Pressure Transducer

MHSIT – Minimum Hot Surface Ignition Temperature

HSIT – Hot Surface Ignition Temperature

HSIC – Hot Surface Ignition in Crossflow

AIT – Auto Ignition Temperature

AFRL – Air Force Research Lab

RR – Rolls Royce

N_2 – Nitrogen

HPL – High Pressure Lab

ZL – Zucrow Laboratories, an off-campus Purdue Laboratory mainly for combustion and propulsion research

VI – Virtual Instrument

GT – Gas Turbine

P&ID – Plumbing and Instrumentation Diagram

RHS – Right Hand Side of the Equation

LHS – Left Hand Side of the Equation

EES – Engineering Equation Solver (a software package)

Re – Reynolds Number

Pr – Prandtl Number

Gr – Grashoff Number

Ra – Rayleigh Number

P_{ratio} – Pressure ratio reference to atmospheric pressure

k_{parcel} – Shape constant for the parcel

Nu – Nusselt Number

k – Thermal Conductivity Coefficient [W/m-K]

h – Heat Transfer Coefficient [W/m^2-K]

g – gravitational acceleration [m/s^2]

d – parcel (ignitable mixture) size [m]

T_{surf} – Hot surface temperature [K]

μ - viscosity [N-s/m^2]

β – reciprocal of temperature in Kelvin [1/K]

τ_{ign} – Ignition delay [seconds]

IDT – ignition delay time

HCCI – homogeneous charge compression ignition

AENFTS – aircraft engine nacelle fire test simulator

ν – kinematic viscosity [m^2/sec]

Bi – Biot number

c_p – specific heat [J/kg-K]

ρ – density [kg/m^3]

A_c – Cross sectional area [m^2]

X% – ignition probability

A – Pre-exponential coefficient for ignition delay correlation

B – Exponential coefficient for ignition delay correlation

C – Activation energy coefficient for ignition delay correlation

R – Universal gas constant

D_H – Hydraulic diameter [m]

L_c – Characteristic length [m]

LHV – Lower Heating Value [kJ/kg]

P_{atm} – Atmospheric pressure

$A_{contact}$ – Contact surface area [m^2]

V – Volume [m^3]

$\dot{E}$ – Energy transfer [W]

a – acceleration [m/s^2]

m – mass [kg]

JP – Jet propellant

ABSTRACT

A hot surface is one of the ignition sources which may lead to fires in the presence of aviation fluid leakage. Bleeding ducts and exhaust pipes that are at elevated temperatures are potential sources of ignition. A database of Minimum Hot Surface Ignition Temperatures (MHSIT) resulting from experiments conducted three decades ago at the Air Force Research Laboratory (AFRL), Dayton, OH has served as a valuable source of estimating safe operating temperatures. However, MHSIT for some of the aviation fluids such as Jet-A and MIL-PRF-23699 (lubrication oil) are not readily available. Further, the ranges of the hot surface and flammable liquids' temperatures and the range of the air stream velocities need to be extended for use in higher pressure ratio and higher performance aircraft engines developed since the generation and interpretation of the original data. The air velocities (V_A) in the modern engines have increased by a factor of two and documenting their effects on the MHSIT for a range of test fluid temperatures and air temperatures (T_F, T_A) is important.

The objectives of this study are to develop a generic test apparatus to study MHSIT and to model an air-fuel mixture space to find the range of temperatures and velocities that lead to ignition. Among various leakage scenarios, the test apparatus simulates spray (atomized particles injected through a nozzle) and stream (dripping from a 3 mm tube) injection. A semiempirical ignition model was developed using an ignition temperature and delay time expression based on an energy balance between the heat lost to the cross-stream flow, the heat added from the hot surface and the heat released by the nascent chemical reactions to estimate the MHSIT.

MHSIT is measured including the effects of V_A, T_F, T_A and the effects of obstacles. Ignition probability is evaluated as a function of the hot surface temperature. The probabilistic nature of the hot surface ignition process was established. New flammable fluids (Jet-A & MIL-PRF-23699) have been tested and MHSIT database was expanded. A large number of ignition experiments were completed to evaluate ignition probability at various flow conditions of aviation fluids: (1) Jet-A, (2) Hydraulic oil (MIL-PRF-5606) and (3) Lubrication oil (MIL-PRF-23699). Uncertainty of the experimental measurements for these tests have been documented. Air velocities were

extended up to 7 m/s. Effects of flammable liquid and air temperature on MHSIT were studied. The empirical constants for the semi-empirical model were determined using these experimental data.

The ignition probability is strongly correlated with hot surface temperature and progressively weakly correlated with air velocity, fluid parcel size, air temperature, and test fluid temperature. Parameters investigated in this study are useful design choices considering MHSIT for a given flow condition.

1. INTRODUCTION AND LITERATURE REVIEW

1.1 Motivation

Energy demand increases with technological innovations. Innovations often require higher power consumption. In both the aviation and automotive industries, it is important to deliver power from energy sources, using more efficient and safer designs. The industry still relies on combustion for power generation while the world becomes more digital. A century long combustion knowledge cannot be neglected while designing for future engine concepts to decrease emissions, produce power from clean and renewable energy sources, and increase the power output while maintaining safe operation of the equipment.

Experimental and computational investigations are both valuable areas of research. Often computational research is validated with experiments. Experiments can be expensive, however laboratory scaled targeted experiments are very important and less costly in comparison to the operational costs of the aviation industry.

As technology evolves the aviation industry utilizes modern technology. New aircrafts use the latest technology to manufacture critical components. The aviation industry also uses newer aviation fluids which experience higher bypass ratios. An experimental study was aimed to extend the Minimum Hot Surface Ignition Temperature (MHSIT) database and allow for safer designs while conducting fundamental research.

1.2 Hot Surface Ignition

Ignition is a process of an exothermic chemical reaction that propagates into flames or detonation. Hot surface ignition is defined as the process of a flammable liquid coming in contact with a hot surface followed by evaporation, mixing, and reacting with the surrounding oxidizer with self-supporting heat release (combustion) [1]. A special type of ignition is the vaporization of a flammable liquid drop by a hot surface [2]. Bleeding ducts or exhaust pipes are commonly encountered surfaces that are at elevated temperatures in the aviation and automotive industries.

The flammable liquid evaporates after contacting a hot surface and forms an ignitable mixture while mixing with the surrounding oxidizer. The ignitable mixture will continue to receive energy from the hot surface. Ignition will occur if the energy received is enough to break the chemical bonds within the ignitable mixture. Ignition kernels will agglomerate and proceed to combustion, if the surrounding ignitable mixtures' local equivalence ratios are within the flammability limit.

Hot surface ignition temperature (HSIT) measurements are costly and time consuming. Ignition temperature varies with a myriad of parameters; therefore, it is not a property of the substance/flammable liquid like autoignition temperature (AIT).

Hot surface ignition (HSI) of flammable liquids has been studied extensively for the automotive and aviation industries [3]. Hot surfaces are often exposed to airflow, including natural convection. Flammable vapor mixed with air is heated by heat transfer from a hot surface. Bleed ducts or exhaust pipes that are at elevated temperatures may be a source of ignition. Although ignition of the flammable liquids by a hot surface has been studied, limited data are available in the literature. The past work for MHSIT is three decades old and is based on a complicated apparatus that led to large apparatus specific uncertainties [4]. Newer aircraft designs lead to higher airflow rates and result in usage of new aviation fluids for which MHSIT is not experimentally measured. The present work is motivated by these facts. Air-fuel ignitable vapor mixtures in contact with a hot surface can lead to hot surface ignitions. This can lead to fires within the engine compartment.

The explosion of Trans World Airlines Flight 800 in 1996 was the most extensive and costly investigation in U.S. history of its time. One of the causes leading to ignition was that the flammable air-fuel mixtures in the center wing fuel tank received high heat flux from hot air conditioning packs located in the surrounding area [5]. This investigation improved the safe design of the aircrafts against ignition by flammable mixtures. Another incident regarding hot surface ignition happened in November 2010, Qantas Flight 32. The aircraft was forced to make an emergency landing due to a ruptured lubricant line leading to an oil fire in the engine [6], [7].

One of the most recent incidents of an aircraft engine failures regarding hot surface ignition happened in 2019. In this case a stalled compressor reduced the additional airflow for cooling the engine. This caused surface temperatures to rise and resulted in hot surface ignition [8], [9].

It is important to know the fluid's ignition characteristics when designing aircraft or automotive hardware. Minimum AIT have been useful in the past [10]. The American Petroleum Institute recommends a general rule that MHSIT is assumed to be 200 K greater than the minimum AIT under some assumptions [11]. However, there is no standardized method to evaluate the MHSIT of a flammable liquid.

The Department of Defense Test Method Standard 511.5, regulates the use of explosives and the ignitable mixtures resulting from mixing with the surrounding oxidizer at atmospheric pressure. Considering the environment, a laboratory test method is defined: (1) to select materials and safe operating conditions for the fuel-air mixtures without causing ignition, and (2) to contain a burning reaction occurring within the encased material without propagating outside the test item [12].

1.3   Literature Review

The combustion process releases chemical energy, and gas turbines convert it into useful mechanical energy. Combustion can initiate from an ignition source or if conditions allow autoignition may also occur. An ignition source can be a spark, laser, plasma or hot surface. Combustion will occur when combustible vapors mix with the oxidizer and receive enough energy to initiate chain reactions, leading to propagation, and sustained flames.

Ignition is a necessary step for combustion to initiate, although there are circumstances where ignition is not wanted. Hot surface ignition can happen from leakage of flammable liquids onto the hot surfaces. Hot surface ignition of the flammable liquids is a risk that must be mitigated for ground and air transportation vehicles [2]. Safe handling of the flammable liquids near hot surfaces is extremely important and interaction between the hot surface and the flammable liquids must be well understood to ensure safe design of engine compartments.
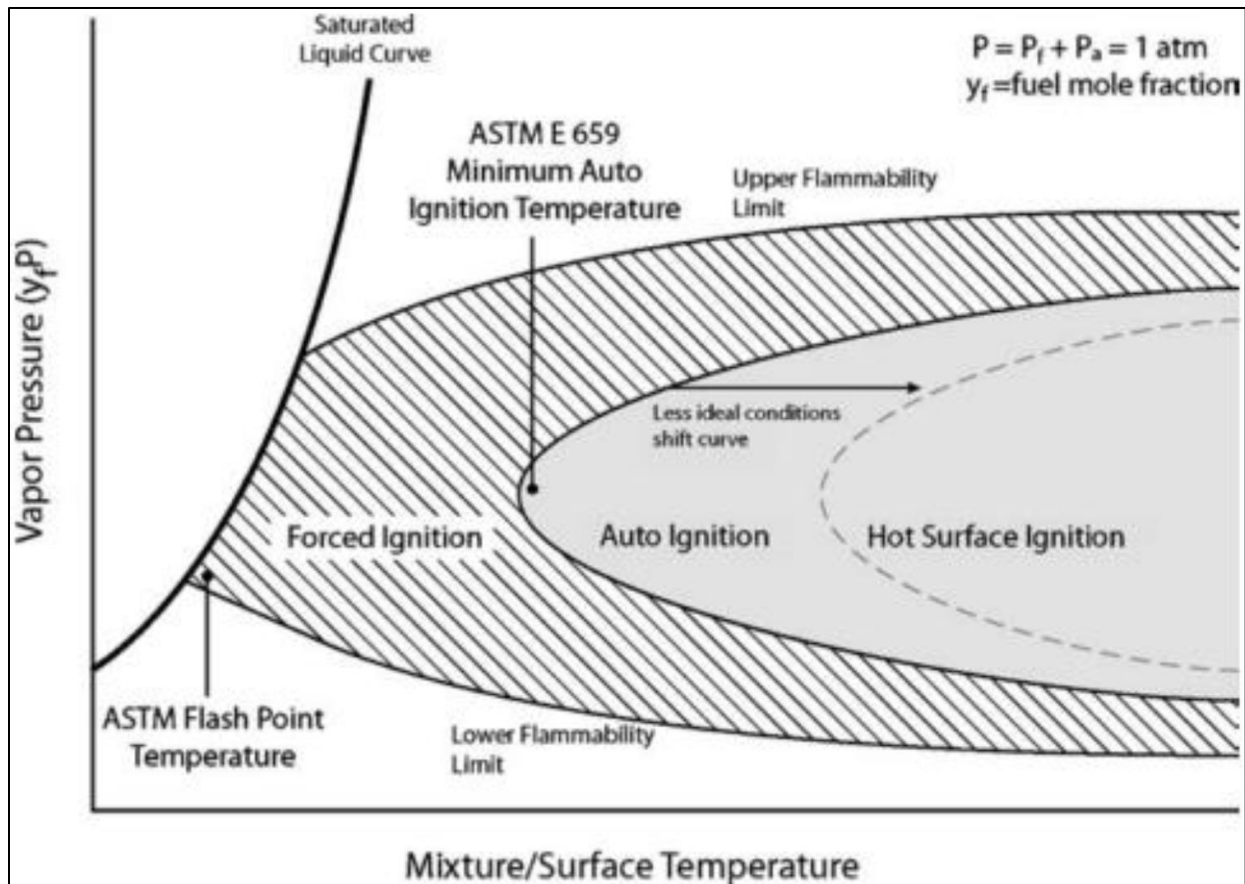
Figure 1-1 Flammability limit and ignition regimes as a function of surface temperature

The literature shows progress from autoignition to hot surface ignition with buoyant flows and hot surface ignition with real flows. Forced ignition is when an air-fuel vapor mixture is ignited using an external ignition source like a spark or laser. AIT is an important property of the flammable liquid. According to ASTM definition, autoignition is the ignition of a substance commonly in air as the result of heat liberation due to an exothermic oxidation reaction in the absence of an external ignition source such as a spark or flame [13]. This temperature is required to provide the activation energy needed for combustion. Unlike AIT, which is well defined by ASTM E 659 standard, the MHSIT is not a fundamental property of a substance. It depends on various factors such as: physical properties of the hot surface, liquid drop size, and the local air flow rate [14]. Because of these effects, the hot surface temperature required for ignition can vary greatly depending on flow conditions or the geometrical parameters.

Ignition is the leading process to combustion. Combustion initiates with ignition and if conditions are adequate, reactants can burn completely and convert into products. Ignition propagates to a self-sustaining combustion process if enough fuel-oxidizer mixture is provided.

Laurendeau et. al. studied factors affecting the MHSIT and listed the following parameters that have an effect on ignition temperature: fuel structure, surface material, surface temperature, fuel/air stoichiometry, surface size and orientation, initial fuel and air temperatures, contact or residence time, condition, pressure, and heating rate of the surface [15]. They also correlated size of the hot surface with ignition temperature.

1.3.1 Effect of Apparatus

Johnson et. al. made a large contribution to the MHSIT database in the 1989 at Air Force Research Laboratory (AFRL) for aircraft manufacturers to improve the safety of gas turbine design and identify candidate replacement fluids which are less susceptible to ignition [4]. Experimental conditions were greatly varied to investigate MHSIT for aviation fluids under various flow conditions in an engine compartment while a fluid leakage event is possible. Johnson et. al. varied pressure, ventilation air temperature, ventilation air velocity, injection type (stream or spray), injection location (upstream, downstream or at specific locations), hot surface heating method and orientation. However, his work did not consider the effect of ignition probability as a function of the hot surface temperature. Ignition probability is an important parameter in identifying the safe surface temperature for fire safety applications. It is also important to identify a surface temperature to an igniter for consistent and reliable ignitions.
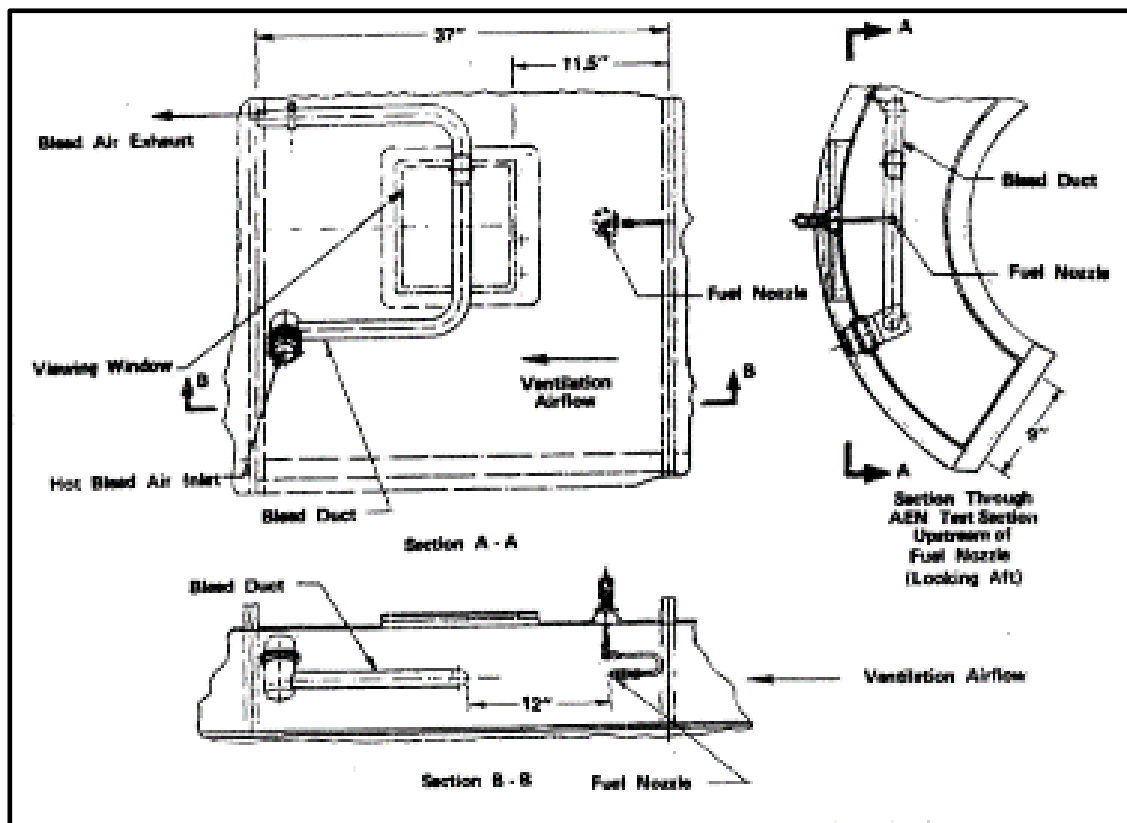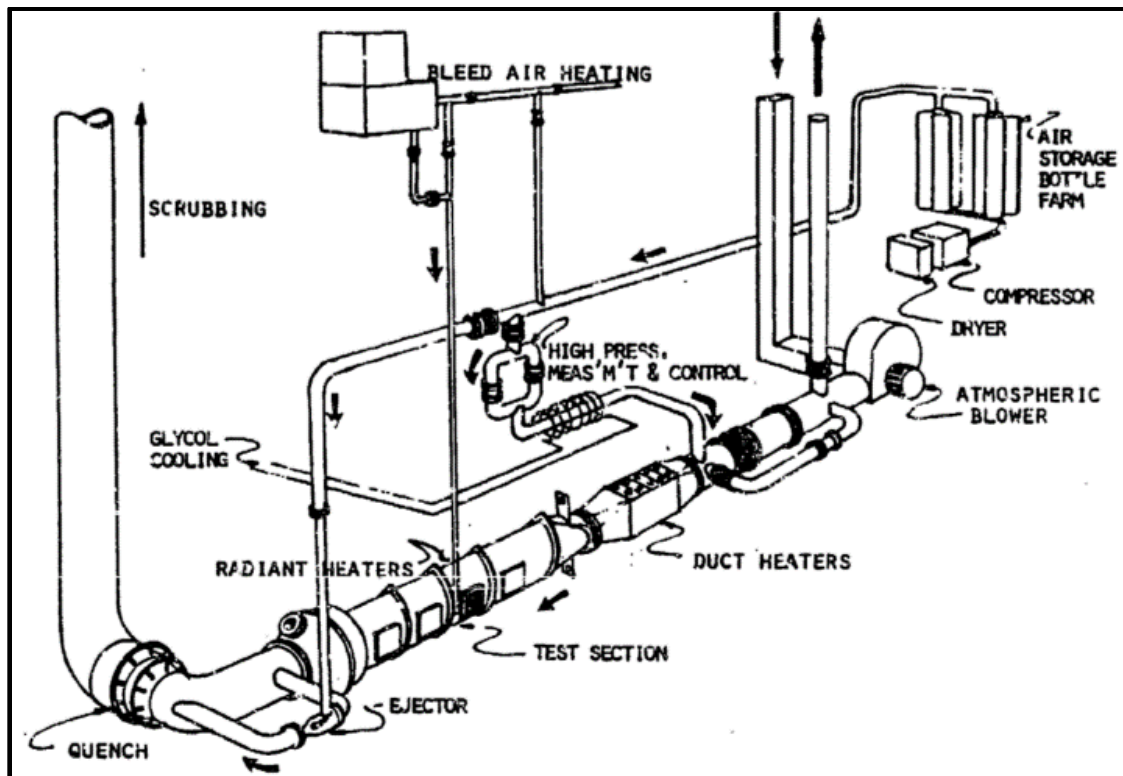
Figure 1-2 Experimental apparatus: section of F-16 engine compartment located at Wright Patterson Air Force Research Laboratory

Johnson et. al. performed MHSIT experiments for five common aircraft fluids of the time (MIL-PRF-5606, MIL-PRF-83282 hydraulic oils, JP-4 and JP-8 kerosene-based fuels, and MIL-PRF-7808 lubricating oil). Experiments were conducted at Wright Patterson Air Force Research Laboratory using the Aircraft Engine Nacelle Fire Test Simulator (AENFTS). AENFTS consists of a 114 degrees section of the annular F-16 engine compartment with actual heated bleed-air duct and the complex geometries surrounding it. They conducted experiments varying ventilation air velocities up to 3.3 m/s, and ventilation air temperatures up to 590 K. Pressure was also varied from 0.3 – 1.4 bars. Results of their experiments covered a large range of flow conditions. However due to complex geometry, MHSITs were apparatus specific and the data needed interpolation to apply different configurations and flow conditions.
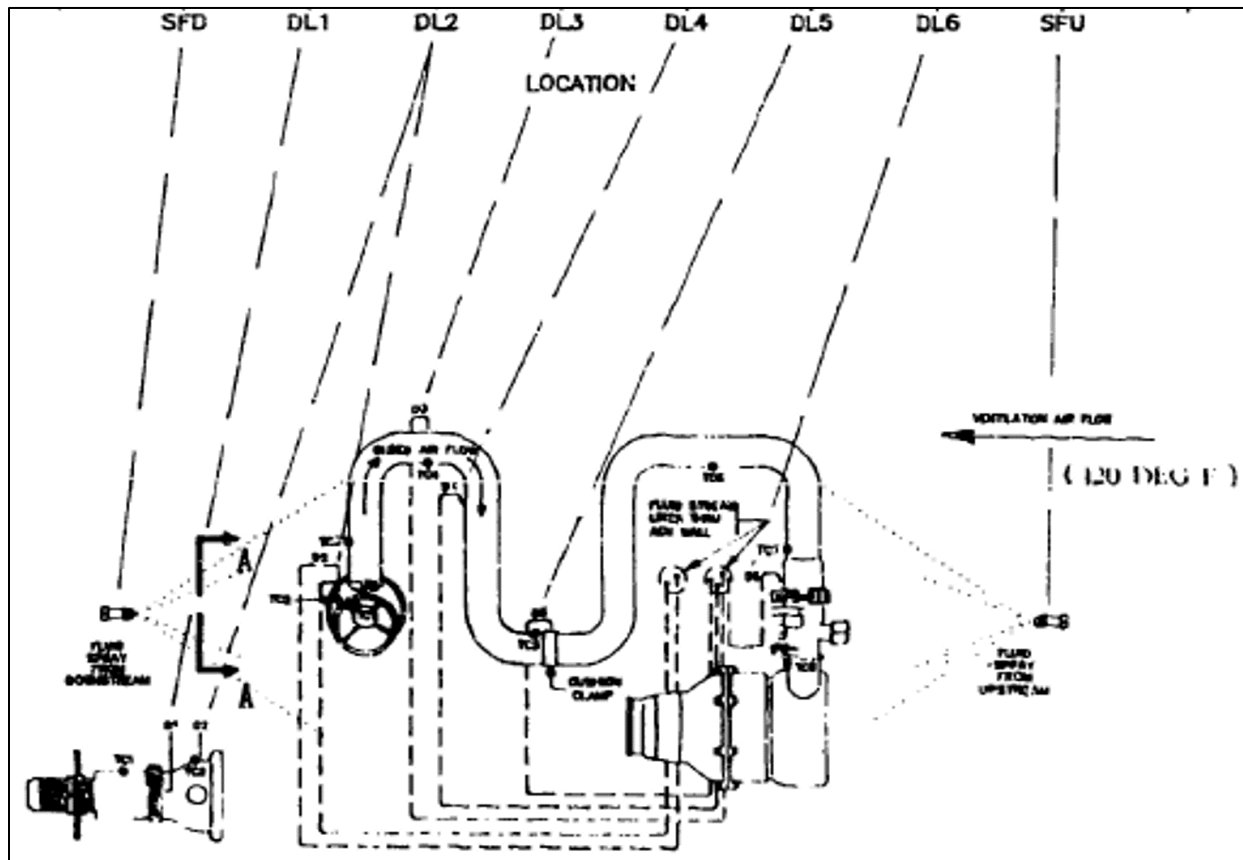
Figure 1-3 High realism test article used at Air Force Research Laboratory, Dayton, OH

Geyer et. al. conducted hot surface ignition temperature tests using actual flow conditions and physical parameters using a F402 Pegasus Turbofan engine [16]. As valuable as this data is, it was not generic, but rather specific to the prescribed engine physical parameters.
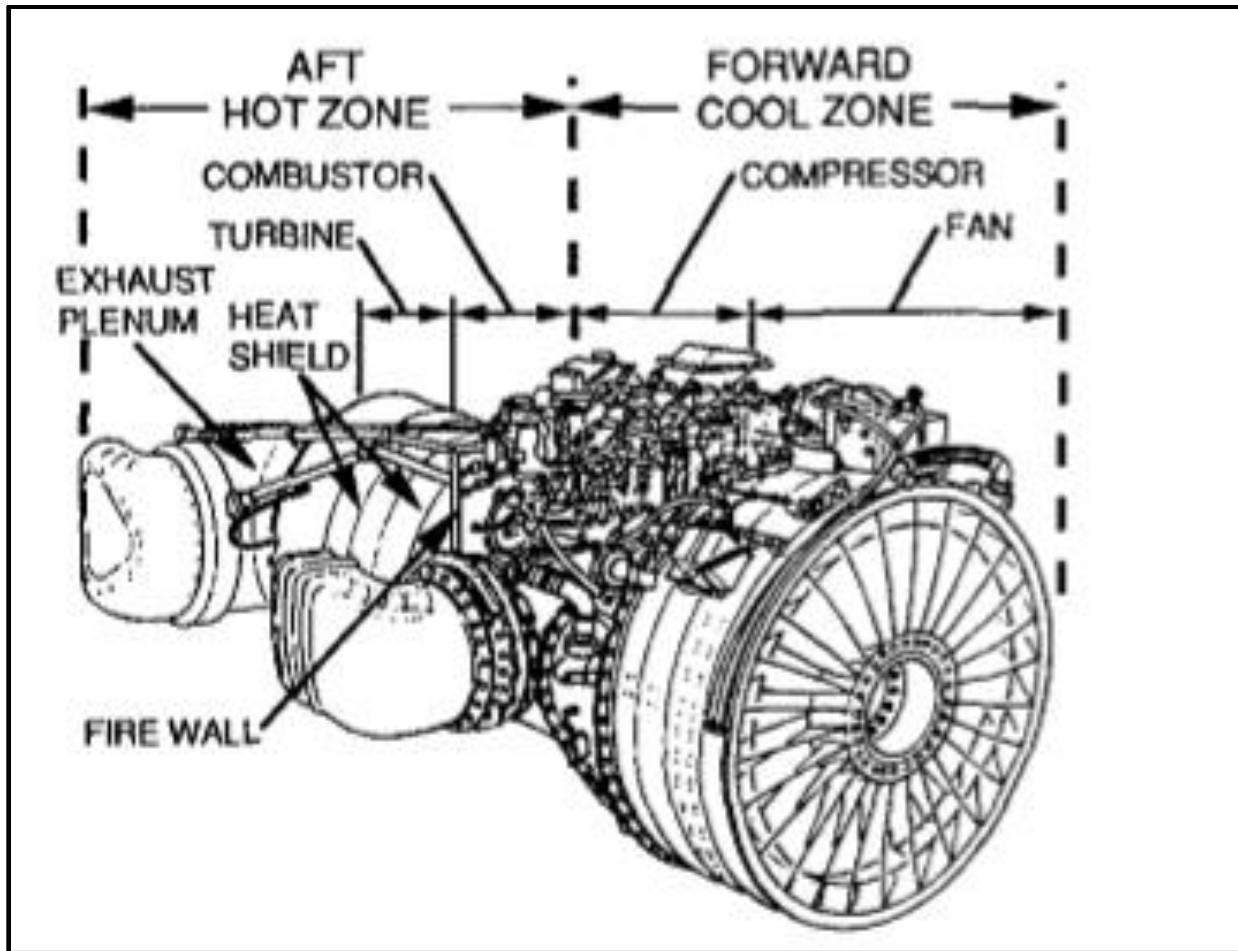
Figure 1-4 F402 Pegasus Turbofan engine

Finally, Clodfelter et. al. [17] noted that many of the experiments in the AFRL study [4] and other hot surface ignition studies at Air Force Research Lab didn't account for flammable test liquid temperature. They also added that current engine compartments experience fuel temperatures as high as 435 K, 410 K for hydraulic oils and 450 K for lubricants.

Aircraft manufacturers use the existing MHSIT database generated three decades ago which can lead to complicated calculations from the data to adapt for the modern aircraft designs. This can increase the uncertainty in the MHSIT estimates from the apparatus specific data. Estimates of the current MHSIT for the modern engines also lead to temperature margins as low as 10 K along the aircraft nacelle.

1.3.2 Ignition Modeling

Numerical modeling of the ignition of spray liquid drops have been extensively investigated. However quiescent and low airflow conditions were preferred due to the complications that arose by the convective effects and the turbulence in the presence of higher crossflows [18]. Often experiments are conducted for comparisons between measurements and real-world applications for predictions.

Models have been developed to correlate the minimum ignition energy required and the hot surface size for the minimum hot surface ignition temperature for various flow conditions [19] and [20]. Laurendeau [21] analyzed thermal ignition of methane-air mixtures and developed an ignition model considering some flow parameters. He modeled ignition by equating energy release by chemical reaction and heat loss from the hot surface.

Mizimoto et. al. [22] analyzed ignition of a drop by a hot surface and the subsequent relevant processes, such as evaporation of the drop and the effect of the drop size, surface roughness on the hot surface ignition.

Bennett et. al. suggested nondimensionalization and including the following fundamental parameters such as fuel-vapor concentration, temperature profile, convection velocity, ignition delay time since the ignition is a transient process, and the AIT [23], [24].

Khaled et. al. developed an ignition delay time (IDT) correlation with detailed chemistry for combustion phasing in homogeneous charge compression ignition (HCCI) predictions [25]. IDT correlation consists of pre-exponential coefficient times equivalence ratio raised to a constant times pressure raised to a power times exponential of a constant (E_a/R) divided by the surface temperature T.

1.3.3 Ignition Probability

The FAA regulates the flammable liquids used in the construction of aircrafts. The design must minimize the probability of the occurrence and spread of fire during normal operation and failure

conditions. It also must minimize the effect of such an event leading to fire. Hence, the design and construction of aircraft engines must minimize the probability of the occurrence of an internal fire that could result in structural failure or other hazardous effects [26].

Clodfelter [17] reported limited ignition probability data in tabular form for some of the aviation fluids investigated by Johnson et. al. Although the MHSIT data didn't capture the effect of ignition probability due to the experimental technique utilized, the importance of the ignition probability as a function of the hot surface temperature was established.

Colwell et. al. investigated MHSIT of aviation and automotive fluids using logistic curves. Despite highly reproducible data generated, his data was limited to ambient test liquid and air temperature, and pressure with no air crossflow over hot surface [11].

Hot surface ignition of spray fuel in crossflow is of interest. Numerous experimental studies have been conducted for various aviation and automotive fluids, simulating leakage scenarios. This problem involves conduction and convection heat transfers along with the chemical reaction occurring.

Davis et. al. conducted hot surface ignition temperature tests with various flammable fluids and interpreted results using logistics curves to capture ignition probability as function of hot surface temperature [27]. Goyal et. al. also tested aviation fluids, Jet-A, JP-5, JP-8, 100LL Avgas and piston-based engine fuel [1]. In these experiments the ambient air and fuel were at room temperature with no air crossflow. Hence results were interpreted using logistic curve functions to demonstrate ignition probability as a function of surface temperature. Davis et. al. also conducted experiments using performance fuels with flat plate at room temperature with no crossflow and interpreted ignition probability as a function of the hot surface temperature [28].

Ignition is a stochastic process, meaning that if conditions are within partial ignition probability (0% < X% < 100%), air-fuel mixture may ignite for some cases and may not ignite for other cases under same surface temperature and flow conditions. The stochastic nature of ignition is valid for hot surface ignition mechanism as well.

Ignition of the flammable liquids by the hot surface is a complex process involving the liquid droplet evaporating and mixing with the surrounding air [2]. Colwell et. al. showed ignition events caused by a hot surface were probabilistic by conducting 2000 ignition experiments and the results were interpreted using logistics curve. Colwell et. al. stated that increasing airflow increases the heat loss from the hot surface and results in higher MHSIT [11]. Both Colwell et. al. and Smyth et. al. emphasized the extensive experimentation required to explain the ignition probability [29]. Davis et. al. also conducted hot surface ignition temperature tests with performance fuels: high-octane leaded gasolines from VP Racing Fuels Inc. and more. He measured ignition probability as function of hot surface temperature [28].

1.3.4 Effect of Pressure

Kopecek et. al. related minimum pulse energy required for ignition with pressure [30]. The results showed that increasing pressure resulted in lower laser pulse energy for ignition. Pressure was varied from 5 – 40 bars. Menon et. al. conducted experiments with n-hexane as a surrogate fuel instead of jet fuel for MHSIT measurement and compared the results with heptane simulation. Due to the reduced chemical mechanism with heptane simulation [31] they conclude that since the reduced mechanism over predicts ignition delay time, it is likely to expect the original larger chemical mechanism to estimate lower ignition temperature, and therefore simulation and experimental results would be much closer. He also conducted vacuum conditions up to atmospheric pressure.
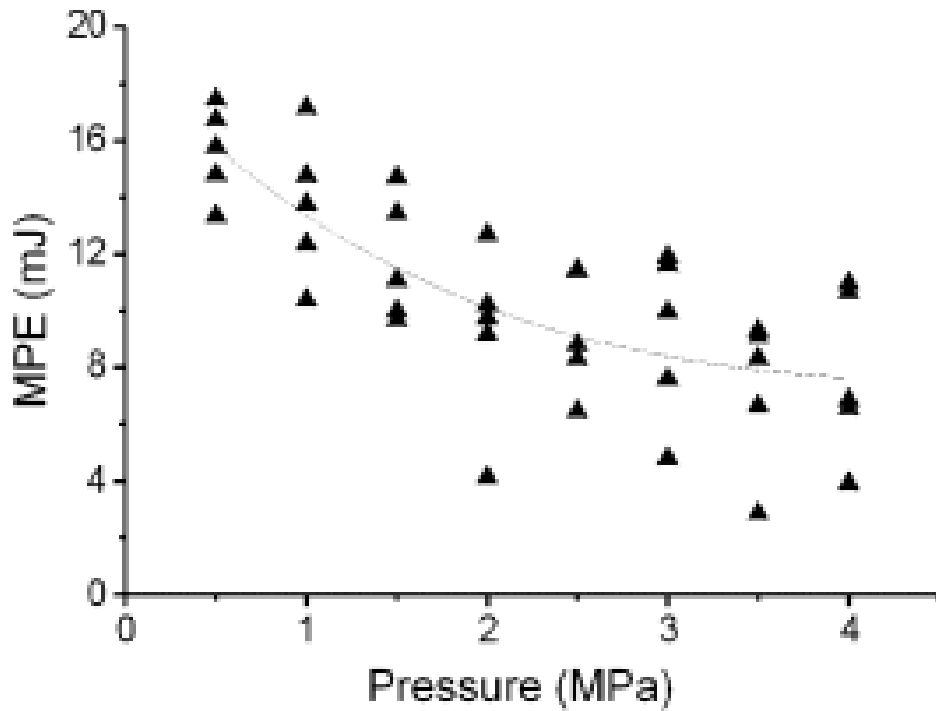
Figure 1-5 Minimum pulse energy vs. pressure by Kopecek et. al.

Pederson et. al. simulated the effect of pressure on hot surface ignition temperature and increased pressure up to 10 bars [32] of methane-air mixtures. The results from Pederson et. al. showed lower MHSIT for methane-air mixture with increased pressure. All pressure studies showed similar pressure trends on MHSIT. However, no experimental pressure study was found in the range of 1-5 bars using aviation fluids for MHSIT evaluation.

Experiments by McTaggart-Cowan et. al. for the design of an igniter [33] used natural gas as the fuel. Tests were conducted at two pressure levels; atmospheric and 4.5 bar. Hot surface ignition temperature was correlated with ignition delay time. For approximately 10 ms ignition delay time between 1 bar and at 4.5 bar, hot surface ignition temperature decreased by ~100 K.
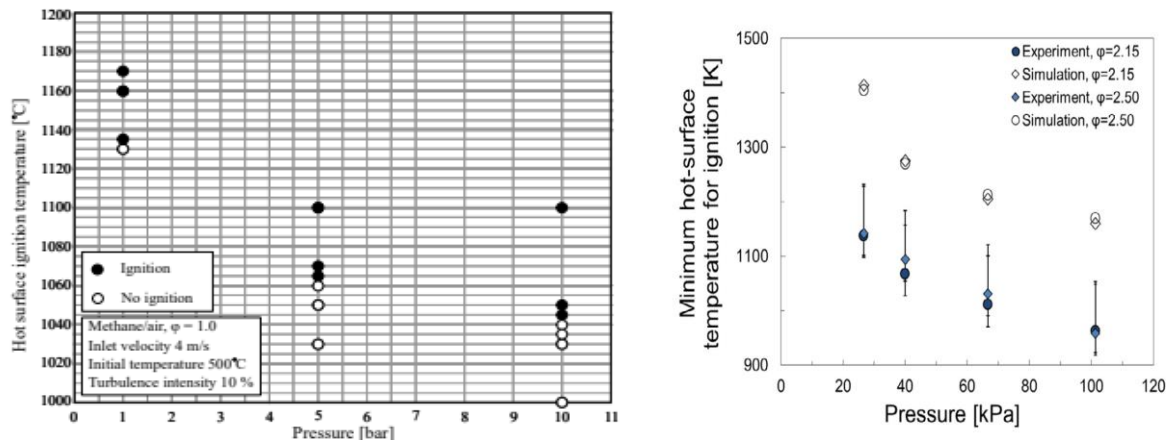
Figure 1-6 (left) Simulation results from Pederson et. al. for methane-air mixture hot surface ignition temperature as a function of pressure, (right) experimental n-hexane vs. simulation hot surface ignition temperatures for n-heptane as a function of pressure by Menon et. al.
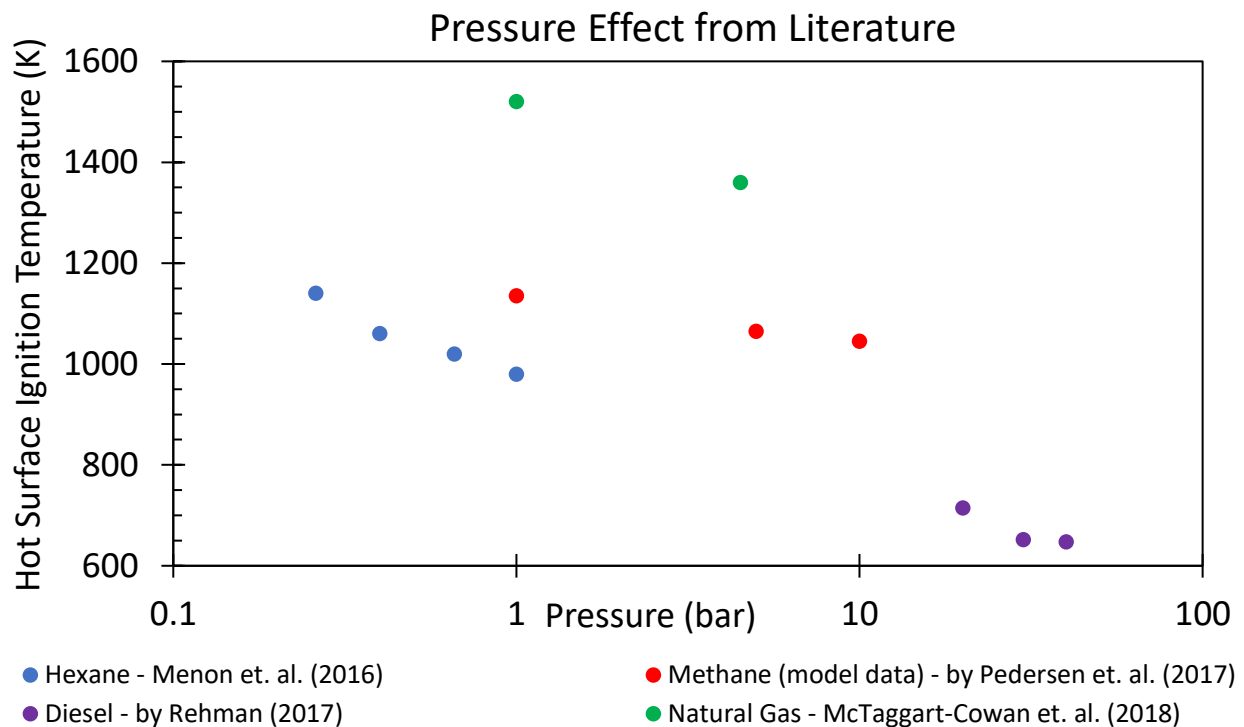
Figure 1-7 Effect of pressure on hot surface ignition temperature from the literature

Menon et. al. [31], sponsored by Boeing, conducted their study with hexane as a surrogate for jet fuel, as shown in Figure 1-7. The effect of pressure on minimum hot surface ignition is summarized for a range of pressures from 0.2 to 1 bar. This showed that the hot surface ignition temperature decreases

from 1150 K to 975 K with an increase in pressure from 0.2 to 1 bar. Neither Menon et. al. nor McTaggart et. al. studied the effects of crossflow nor extend their data to pressures of the range of 1 to 5 bar. In fact, the literature review did not yield any data focused on the effect of pressure on the MHSIT for jet fuels or other hydrocarbon fuels in the pressure range of interest.

The remaining three studies referenced in Figure 1-7 address the effect of pressure on MHSIT for natural gas and methane and the range from 1 to 5 bar is not covered by the authors. There are reasons associated with detailed chemistry and formation of stable compounds like H_2O_2 that may in fact increase the MHSIT with increasing pressure in the interim range. This phenomenon is called the negative pressure coefficient in the basis combustion literature. However, reliable experimental data documenting the negative pressure coefficient particularly including the effects of crossflow are not available in the literature.

1.3.5   Thesis Structure and Objective

Design of a generic experimental apparatus to measure MHSIT of controlled leaks on to uniformly heated cylindrical hot surface is presented in chapter 2. An improved experimental technique is also described in this chapter. An empirical ignition model is presented in chapter 3. Experimental data is used to solve for empirical constants in the energy balance proposed for the kernel-based empirical ignition model. An ignition regime classification based on global equivalence ratio is proposed in chapter 4. Its implications on ignition probability and importance of identifying false ignition is described. Appendix A illustrates the apparatus drawings.
.

2. MINIMUM HOT SURFACE IGNITION TEMPERATURE EXPERIMENTALS

Hot surface ignition of flammable fluids is a risk that must be mitigated for ground and air transportation vehicles. Hot surfaces are typically exposed to airflow, and leaking fuel or oil heated by these surfaces can vaporize and mix with the air flow. Past work on Minimum Hot Surface Ignition Temperature (MHSIT) data is three decades old and is based on a complicated apparatus. Newer propulsion system designs lead to flow conditions beyond those available in the data base. The present work is motivated by these facts. An experimental apparatus was designed to observe ignition of controlled leak of a liquid jet or spray by increasing surface temperature of a uniformly heated Inconel 718 cylinder surrounded by an air duct (forming an annulus around the cylinder) for a range of air velocities and a variety of aviation fluids. Multiple controlled leaks of fluids were utilized to evaluate ignition probability at relevant air flow conditions. The results of the experiments verify the probabilistic behavior of the hot surface ignition process. This chapter describes the experimental apparatus and highlights the experimental methods developed to minimize uncertainty and maximize repeatability in these measured values of the MHSIT.

An experimental apparatus was designed to observe ignition of a controlled leak of flammable fluids by increasing surface temperature of a uniformly heated cylinder surrounded by an annular flow for a range of air velocities and flammable leaking fluids. A 3D model of the apparatus along with a photograph of the actual installation is shown in Figure 2-1. Details of the components can be found in Adams' study [34]. Several modifications have been made to the initial test apparatus configuration to effect improvements to measurement accuracy, repeatability, and effort required to conduct each test.
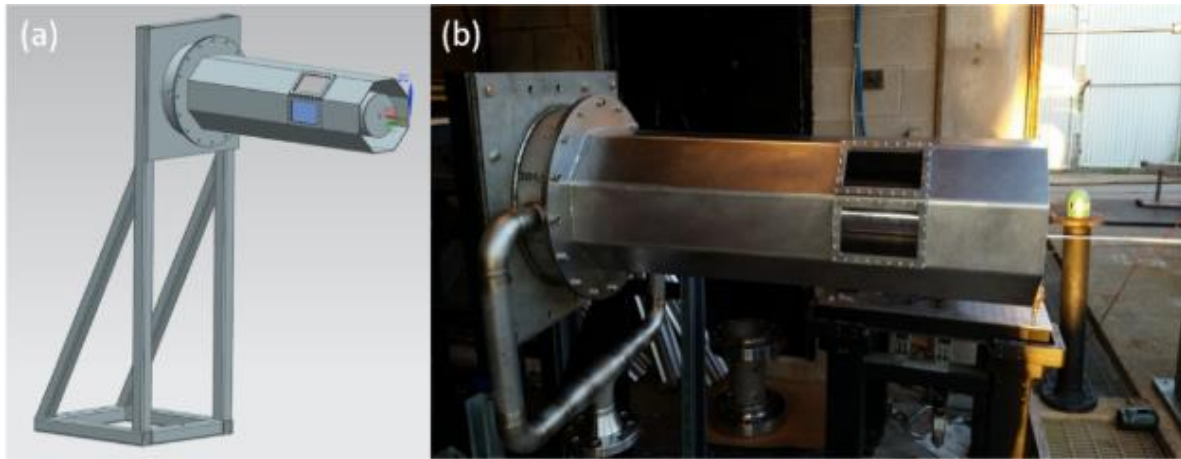
Figure 2-1 Hot Surface Ignition Test Apparatus (a) 3D Model (b) Photograph

The following figure illustrates the features of the flow path within the experimental apparatus. Air is preheated and flows over the hot surface and then exits to atmosphere. The fluid of interest is injected and mixes with the flowing air, leaving the apparatus as vapor or liquid depending on the flow conditions and ignition status.
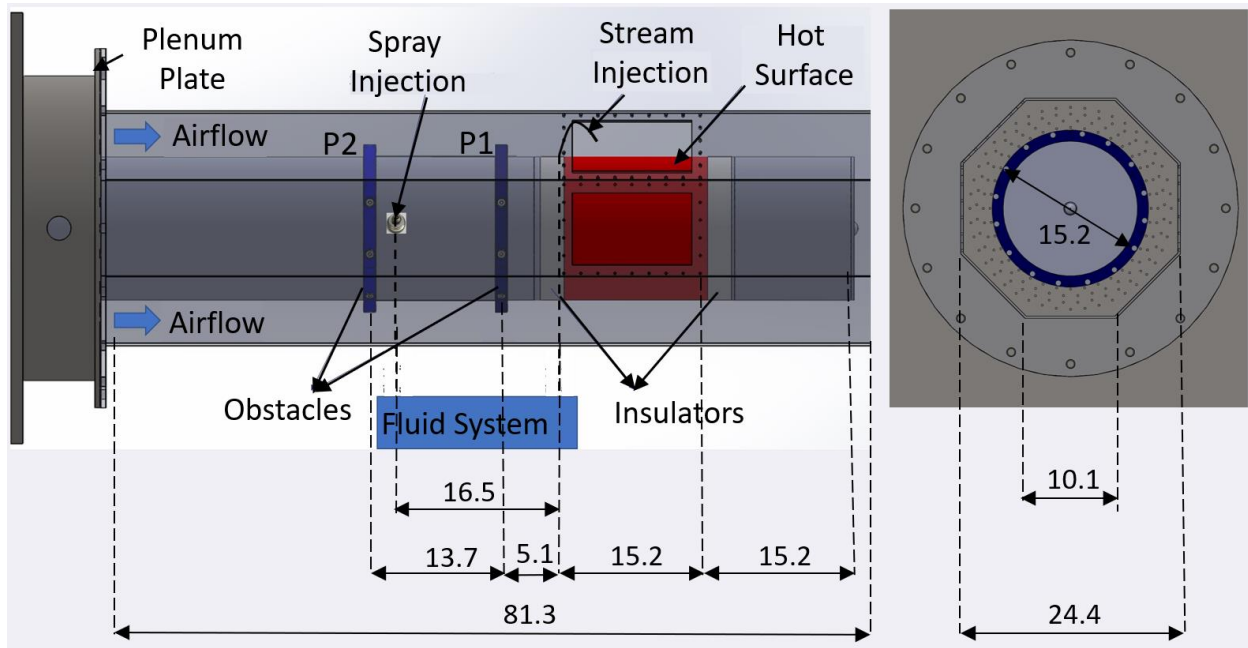
Figure 2-2 MHSIT apparatus test section with relative dimensions (all dimensions in cm)

The air supplied to the hot surface ignition apparatus is heated to desired temperatures with an air heater and its temperature is monitored with thermocouples located on the supply pipes.

2.1   Experimental Apparatus

2.1.1   Octagonal Test Duct

An octagonal shape was chosen as test duct cross sectional area to allow flat surface for installing windows for flame visualization. Geometric proportions of Wright-Patterson test apparatus were applied to sizing of the hot surface ignition test duct and the central body, which formed inner radius. Central body was chosen to be a hallow structure to allow electrical and instrumentation wiring to extend to hot surface without exposing them to flames and high temperature harsh environments. Inner wall radius of the annulus was determined to be 7.6 cm, while it ensured enough space for instrumentation and allowed the weight of the central body and therefore the hot surface material to be manageable. Experimental annular section dimensions on hot surface ignition of aircraft fluids done at Air Force Wright-Patterson Laboratories [4], were 0.76 m inner and 1.22 m outer radius.
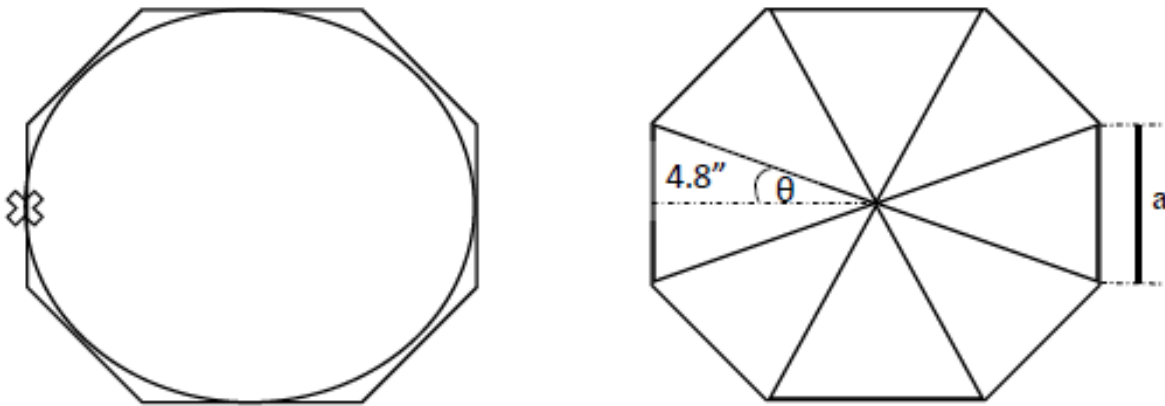
Figure 2-3 Scaling down the test duct to octagonal shape while maintaining same geometric proportion as previous work [4]

Outer diameter was chosen to be 0.122m so same geometric proportion was maintained for the annular flow section same as AFRL study.
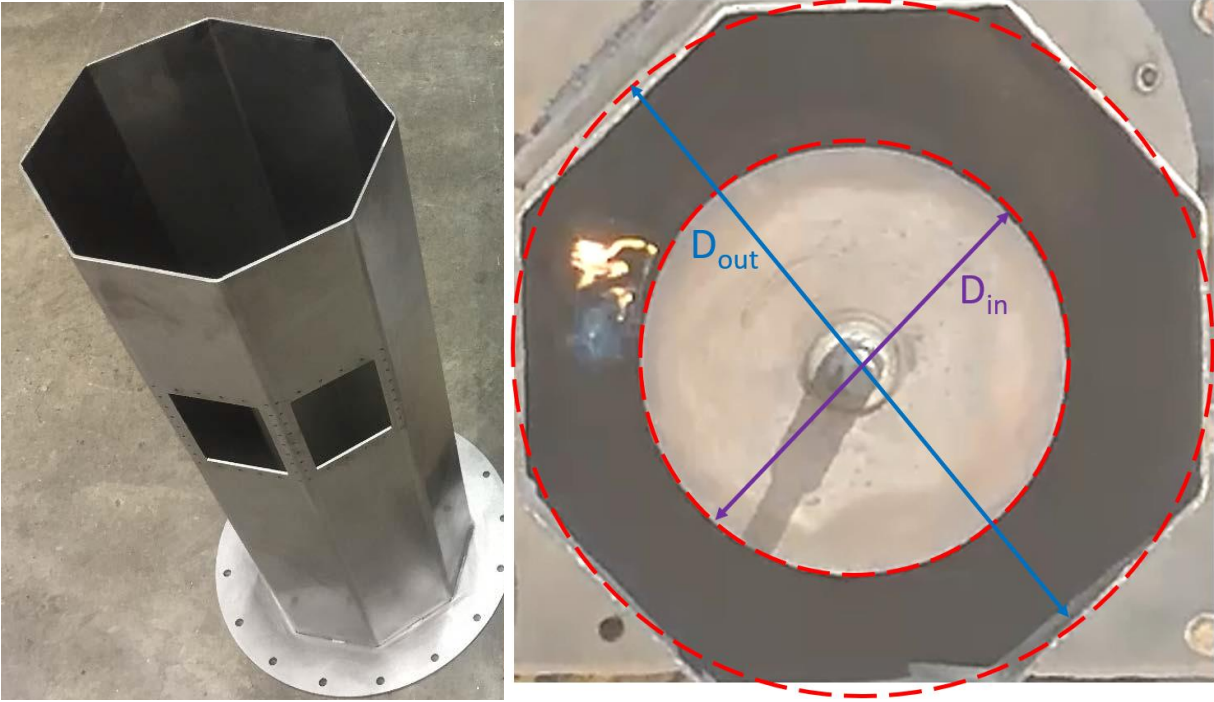
Figure 2-4 Octagon cross-sectional test duct (left) after manufacturing (right) exit view during test with approximate annular cross-section approximation

2.1.2 Exhaust Tube/Bypass Duct

HSIC apparatus is designed to inject multiple fluids with various injection methods. Combustible fuel vapors mixed with air upon ignition and leave soot as a residue. Other fluids like hydraulic and lubrication oil are heavier hydrocarbon and have more additives within. When these fluids burn, they generate mist and or leave unburned fluid.

A waste capture system was designed to collect the mist generated during the experiment and flown away from the lab space towards courtyard (open space surrounded concrete walls, seen in figure below).

Figure 2-5 Exhaust tube in construction for test fluid waste capture system in courtyard behind test facility (HPL, Zucrow Laboratories)
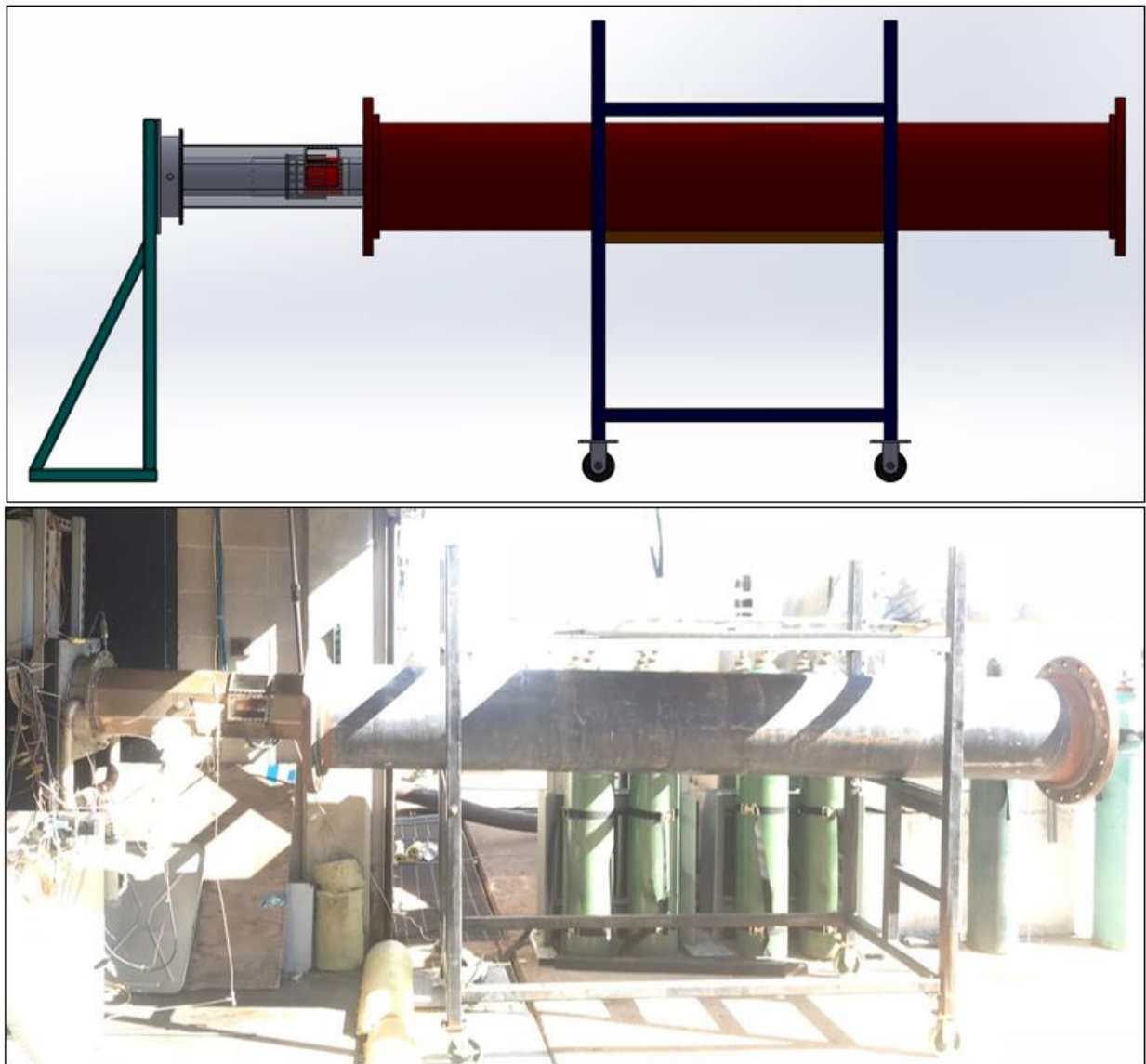
Figure 2-6 Exhaust Tube constructed and in place of testing position

The waste capture system was built with a bypass line of airflow to form suction within the exhaust tube to pull away the unburned fluid mist and flow it away from the test area. An experiment was conducted both with and without the exhaust tube to show that the exhaust tube has no effect on MHSIT measurements.

2.1.3 Cylindrical Hot Surface

The structural backbone of the experimental apparatus is an arbor welded to the structural support stand at the back plate of the air plenum. The arbor is a thick-walled hollow cylinder that allows for routing of heating and instrumentation leads to the hot surface in a protected manner. This arbor locates and supports the hot surface body segments that slide over it. These segments are held together with a tie bolt running through the center of the arbor. The actual heated test surface segment is insulated with ceramic rings to minimize heat loss due to conduction in the axial and radially inward directions.

The heated test section shown in Figure 2-7 is made from Inconel 718 as it is a common material used in gas turbine engine cases. This figure also shows the arrangement of the 15 cartridge heaters used to heat the test section. The total maximum power was 15 kW. Each heater is 1.27 cm diameter and 20 cm long to ensure that the entire length of the hot surface is evenly heated. The hot surface temperature is measured at the circumferential locations shown in Figure 2-7c using three-junction thermocouple probes as shown in Figure 5c.
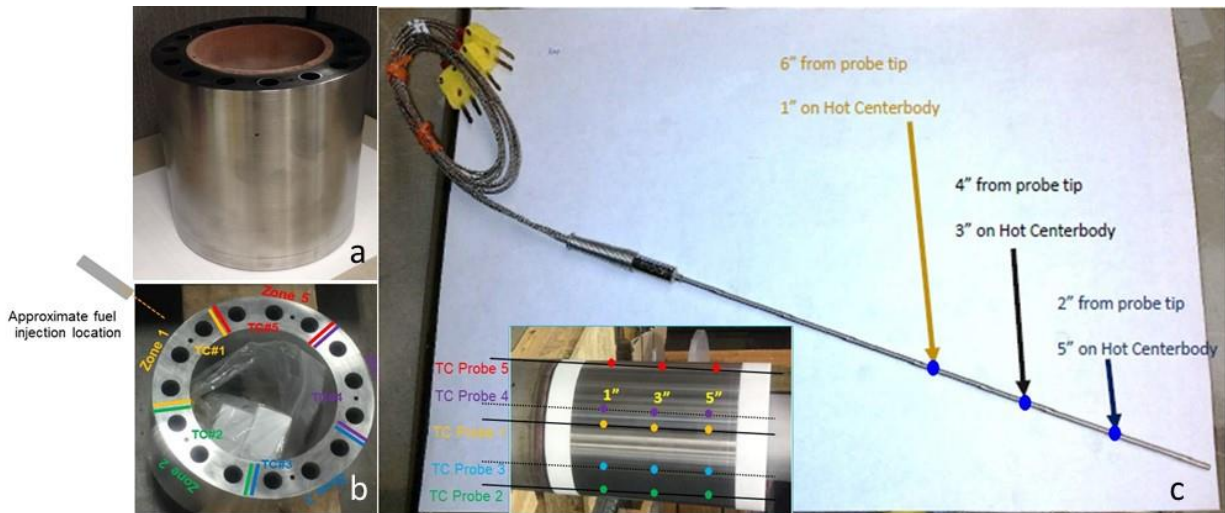
Figure 2-7 a) Inconel 718 hot surface body b) thermocouple and cartridge heater holes along with zoning configuration c) hot surface thermocouple configuration

The most critical parameter for evaluating MHSIT is to accurately measure the hot surface temperature. The temperature of the hot surface was controlled by a CN616 temperature controller

unit, which can control up to 6 zones per unit. Hot surface temperature was controlled using 5 zones as shown in Figure 2-7. The CN616 temperature controller was initially operated in the default on-off mode. This resulted in high variation in spatial and temporal surface temperature uniformity. Such variation made it difficult to adjust surface temperature in small enough increments to produce an accurate logistic curve. Operating the controller in the PID mode improved spatial temperature uniformity from approximately 20 K to 5 K, as shown by analysis in Figure 2-8. Furthermore, the temperature variation with respect to time decreased from 15 K to 3 K. A total of 15 thermocouples were used to monitor the hot surface temperature.
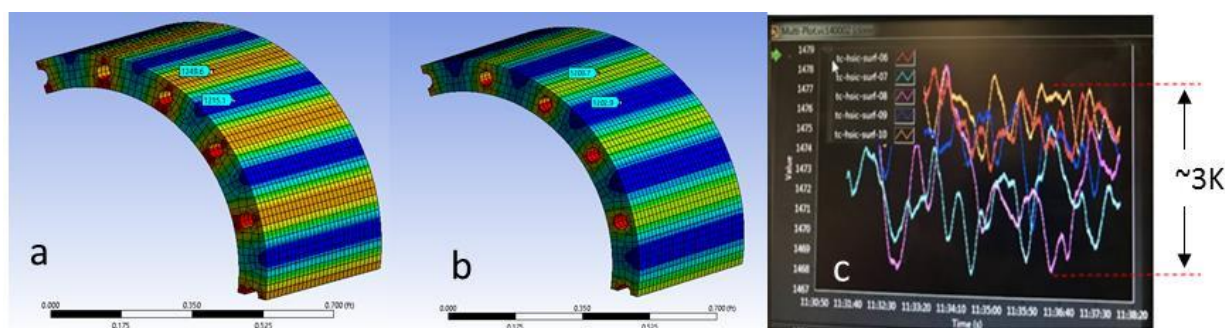
Figure 2-8 a) on-off control b) PID control cc) time varying temperature with PID.

2.1.4   Test Fluid Supply and Injection System

Figure 2-9 shows a schematic for plumbing and instrumentation diagram of the system used to inject flammable test liquids (fuel and oil) into the area upstream of the hot surface. Test liquids can be heated up to 475 K using a 720-watt heat tape wrapped around the supply tank. Heat loss between the tank and the injection point is reduced by using a 120-watt heat tape wrapped around the line. Liquid temperature was measured at a location 7.5 cm upstream of the injection port. Nitrogen is used to pressurize the storage tank, actuate flow control valves, and purge the fluid injection lines. Stream injection is 2.54 cm directly above the hot surface. Spray injection is introduced as a crossflow and is 16.5 cm upstream on the hot surface.
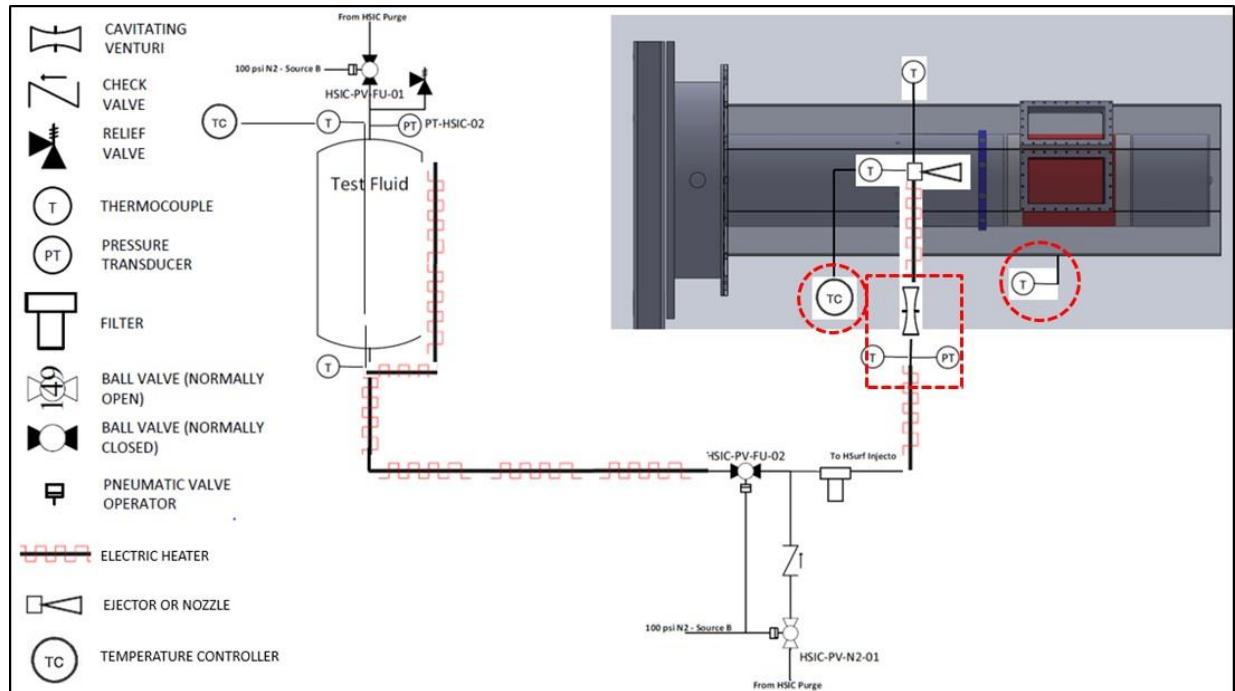
Figure 2-9 P&ID diagram showing test fluid heating sub-system

Injection system is capable of simulating spray and stream type leaks. Spray injection is achieved using an MT series 10/24 thread and 0.4 mm orifice stainless steel nozzle manufactured by AmFog, positioned 16.5 cm upstream of and 5.3 cm above the hot surface at an angle of 90° relative to the air flow direction. The nozzle atomizes the test fluid to 50µm diameter spherical drop sizes and the atomized spray particles are mixed with the air flow over the hot surface for 10 seconds or until ignition event is observed. Air-fuel mixture is vaporized by the heat received from the hot surface. Flammable vapor pockets ignite on the hot surface. Stream injection is achieved using a 0.32 cm (1/8") tube positioned 2.54 cm downstream from the leading edge of and 2.54 cm above the hot surface at an angle of 90° relative to the air flow direction. The stream leak is simulated by continuous drops of the diameter size set by the 0.32 cm tube diameter. Test fluid flow rates are set using the criteria described by Adams [34].

2.1.5 Air Heating System

Airflow over MHSIT apparatus was tested for its air velocity and temperature limits. Air can be heated and maintained up to 553 K and 11 m/s air velocity.
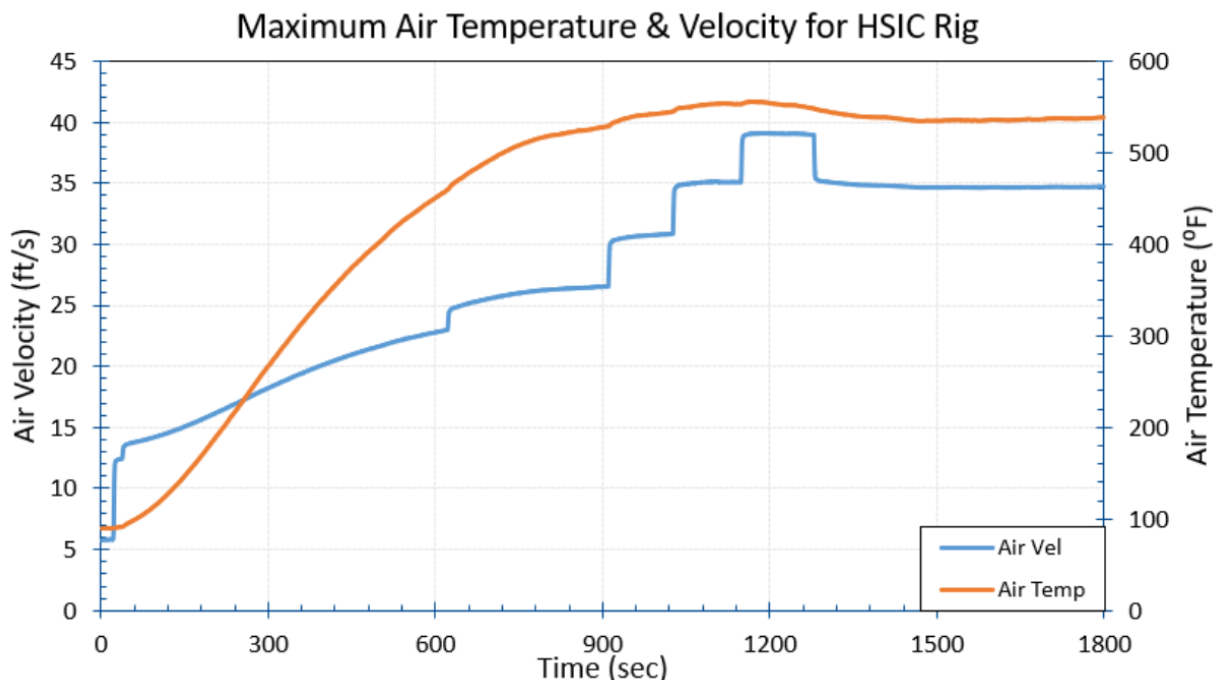
Figure 2-10 Air temperature and velocity limits

Air is compressed and stored in facility tanks up to 140 bars. Air heater is installed in-line with air flow. Air heater was manufactured by H.E.A.T. Inc. (Heat Exchange and Transfer Inc). Model number for the heater is CHP0824S-80-80Y-483. Power capacity is 3-phase power of 80kW with 480V and 60Hz. Heater is capable of maximum temperature of 920 K.

Air heating system was changed to another air heating system over the course of testing period due to a facility construction. New air heater was designed for higher mass flow rates, and therefore above conditions were met with no problem and exceeded. Test conditions were selected based on air temperature and velocity limits as displayed in the above figure.

The current air heater by Thermal Transfer Corporation of Monroeville, Pennsylvania was originally built for heating hydrogen and used three burners with propane to heat hydrogen flow using convective and radiative heating with the burners. Over the course of its operation at Zucrow Laboratories, the heater was adapted to operate as air heater with natural gas from grid as source of heat in the burners instead of propane. Heater's specifications can be found in the following figure.

Hydrogen Heater Specifications

Total Heat Input	. .BTU/HR	20.0×10^6
Design Operating Pressure	PSIG	325
Excess Combustion Air	%	50
Waste Gas Volume	S.C.F.M.	3,190
W. G. Temp.-entry	°F	2,700
exit	°F	1,400
Thermal Efficiency	%	30
Hydrogen Flow	#/sec	0.5
Hydrogen Temp.-entry	°F	70
-exit	°F	1040

Figure 2-11 Current air heater specifications [35]

Air temperature was measured at the heater, multiple locations on air lines, upstream of venturi, where flow is chocked, and its flow rate was calculated. Air temperatures reported at the test apparatus throughout during this study was measured at the plenum plate, as shown on Figure 2-2.

Figure 2-12 Air heater used for this study located at Maurice J. Zucrow Laboratories

2.1.6 Ignition Observation/Cameras

Multiple cameras were utilized to observe ignition event. Axis cameras were located both on the side of the test apparatus and at the exit. Side camera viewed through the viewing port and exit camera was positioned at the exit when possible, so ignition event occurred at any circumferential location on the hot surface was captured. Observations from the exit view were more reliable to detect an ignition event. Ignition location can axially vary as well as circumferentially. Window is 12.7 cm long and the second window only allows an additional 45° view of the hot surface. Window flange thickness between the two windows also creates an obstruction to observe the ignition event. Following side and exit camera views were obtained using AXIS P1435-LE network cameras.
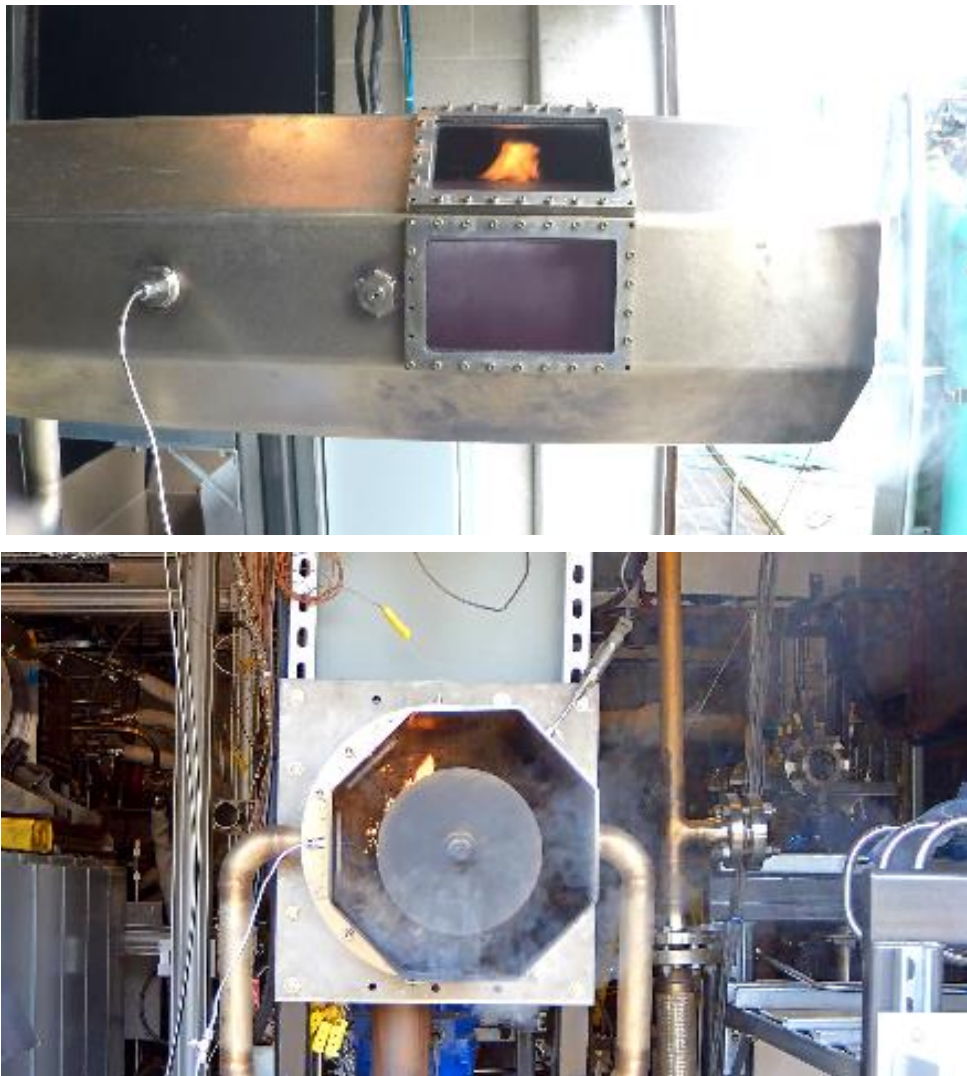
Figure 2-13 (a) Side (b) Exit views using Axis P1435-LE camera

41

Ignition events are complex and may not always be visible to the axis camera. Therefore, a high-speed camera was also used in this process. Following figure shows the experimental setup with high-speed camera. High-speed camera was placed on the side of the apparatus and monitored hot surface with a mirror installed at the exit to avoid exposure of oil/fuel mist generated after injection.
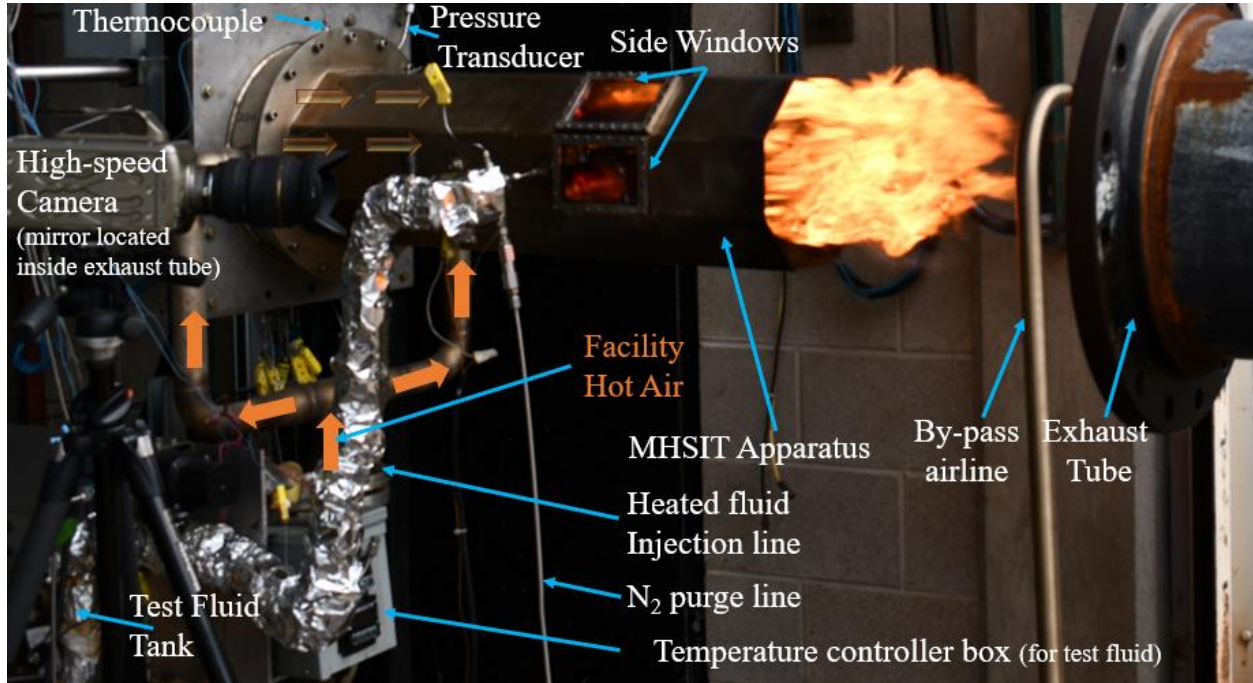
Figure 2-14 Test apparatus setup with high speed phantom camera

High-speed phantom camera was used for detailed ignition initiation visualization. Camera settings are shown in following table.

Table 2.1 High speed phantom camera settings

Camera	Phantom
Video file type	.cine
Resolution	320 x 240
Sample rate, fps	1750
Exposure time, μs	567.75
Number of frames	18206
Recoding duration, seconds	10.403

Injection duration for this study was fixed and didn't vary. Contact time was 10 seconds. Storage space and injection time was taken under consideration for determining these settings to allow recording of enough time to capture the ignition event.

2.1.7 Instrumentation/User interface control program

Test apparatus was controlled by LabVIEW program. Facility data acquisition system was used and a user interface to monitor test parameters during test was built using NI as shown in Figure 2-15.

Multiple computers were used while operating an experiment. Main VI was loaded using one PC in test control room. At least 3 more PCs were utilized; (1) High speed camera (2) Regular AXIS camera, low speed for additional video recording and (3) CN616 Temperature controller for hot surface heating.
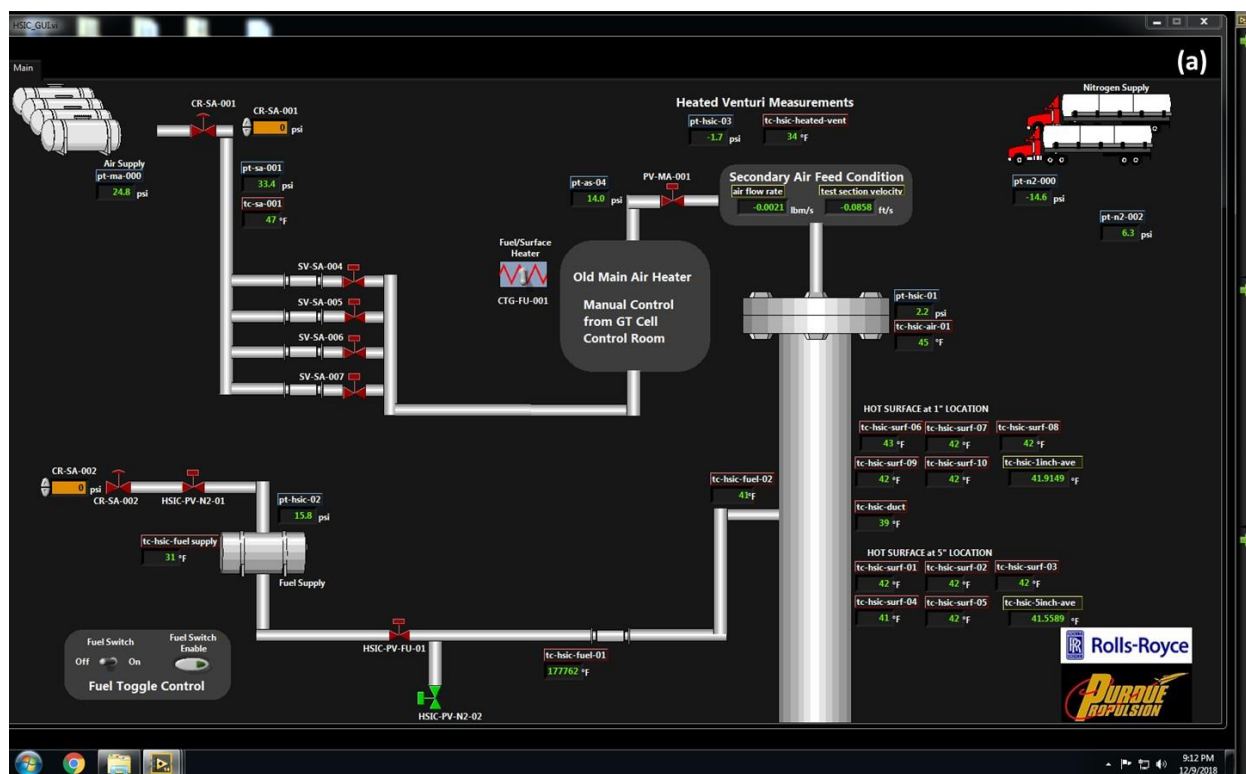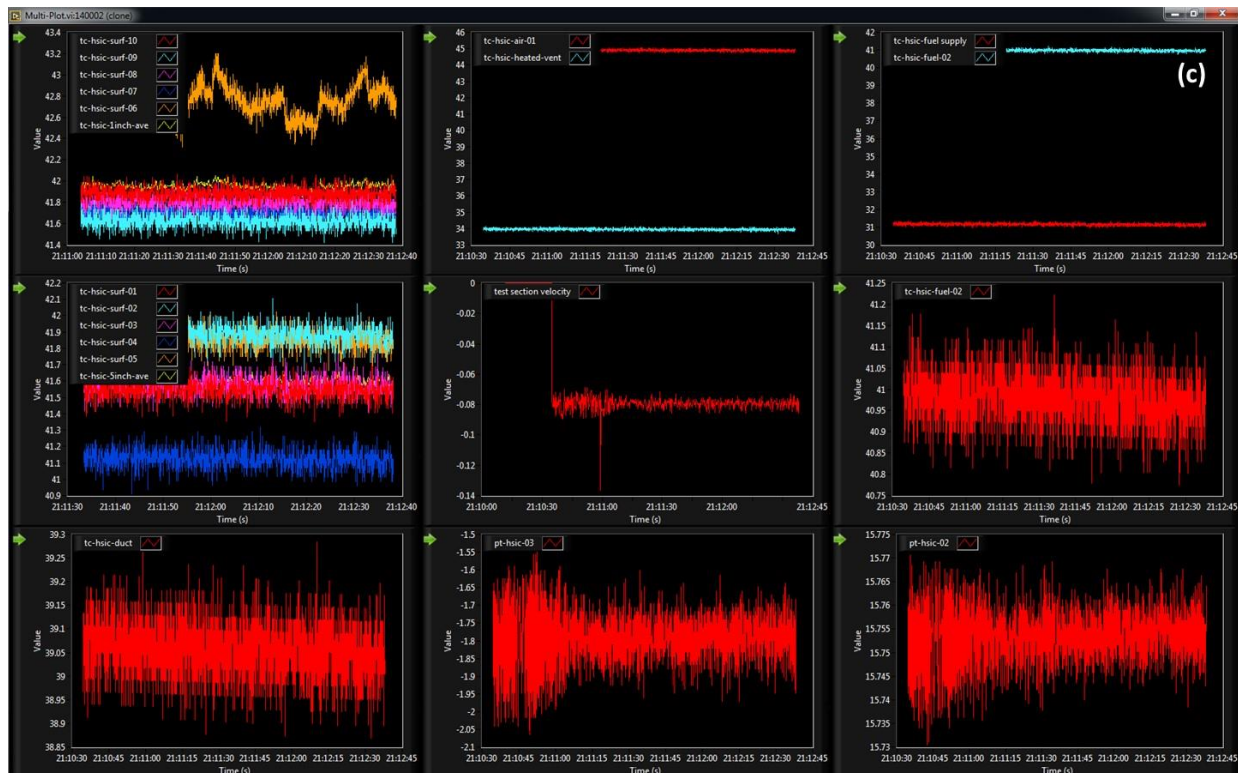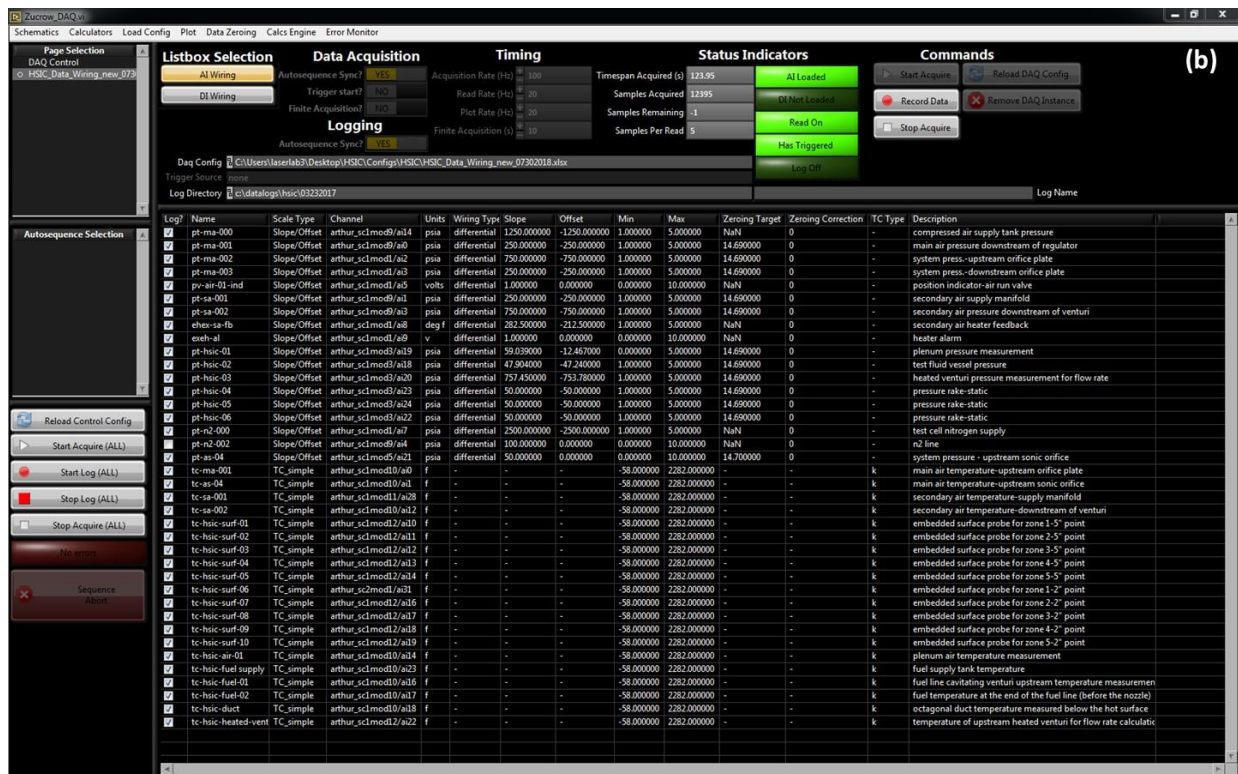
Figure 2-15 LabVIEW graphic user interface (GUI) for HSIC test apparatus (a) Main Window, displaying all process variables (b) DAQ window, where control valves and data processing variables are loaded, (c) Plot screen, where process variables are live plotted and monitored

User interface shown on the above figures were the main screens for the MHSIT apparatus control program. Facility air and N_2 pressure was monitored using thermocouples and pressure transducers located on the apparatus and air/ N_2 supply pipes. The VI was also used for actuating pneumatic valves for controlling air, N_2 and test fluid flows for the experiment.

Detailed instrumentation and plumbing diagram of the MHSIT test apparatus and HPL facility systems used for these experiments can be seen from following figure. Test fluid heating system was added to MHSIT apparatus after it was operational, and its P&ID can be viewed from Figure 2-16. Pressure transducer and thermocouple located upstream of the venturi on air supply line, was used to calculate mass flow rate of the air using choked mass flow equation [36].

$$\dot{m} = \frac{A_{cross} \cdot P_{total}}{\sqrt{T_{total}}} \cdot \sqrt{\frac{\gamma}{R}} \cdot \left(\frac{\gamma+1}{2}\right)^{-\frac{\gamma+1}{2 \cdot (\gamma-1)}}$$ 2-1
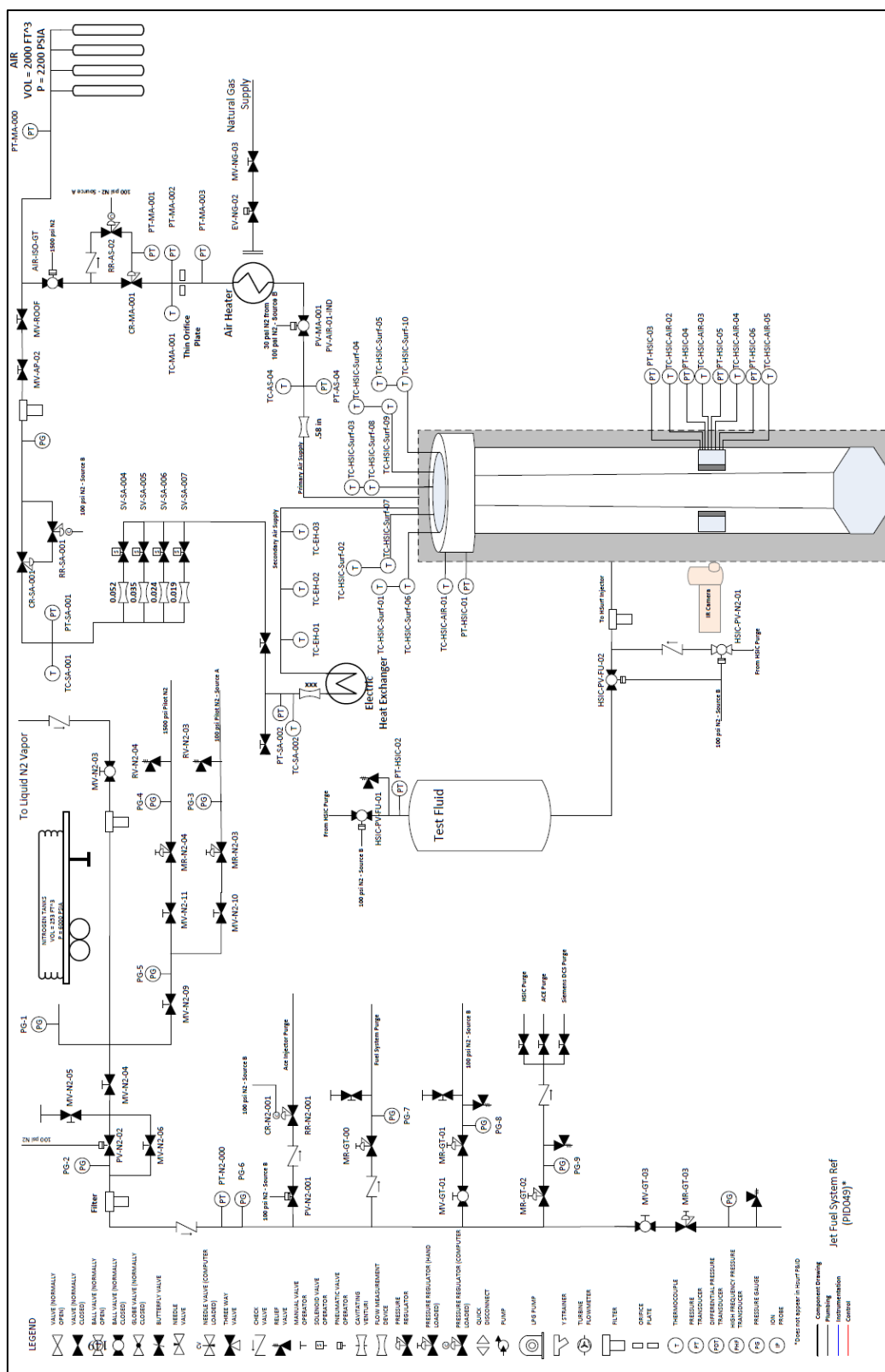
Figure 2-16 Plumbing and Instrumentation Diagram of MHSIT Test Apparatus with Facility Systems at HPL

2.1.8 Fluid Properties

Three aviation fluids were selected for this study. JP-8 was used to validate the test apparatus against AFRL data. Aviation fuel was then switched to commercial aviation fuel, Jet-A. Hydraulic and lubrication oil were chosen to be the same fluids as Rolls Royce uses significantly on their current products. Hydraulic oil (MIL-PRF-5606) is the same type of hydraulic oil used for AFRL study. However, lubrication oil used in AFRL study was MIL-PRF-7808 and this was no longer being used by Rolls Royce. Lubrication oil was switched to MIL-PRF-23699 F. Lubrication oil was a standard synthetic turbine engine lubricant that is currently in use by Rolls Royce. This was also useful for updating existing data and expanding it to include more test fluids and higher air velocities. Both hydraulic and lubrication oils were purchased from Aviall. Jet fuel was purchased from Purdue airport. Flammable fluids' thermal, chemical, and physical properties were needed later in the modeling.

Some thermal properties like specific heat for Jet-A was also found from handbook of aviation fuel properties [37]. Lubrication and hydraulic oils properties were provided from Rolls Royce.

Table 2.2 Test fluid properties [11], [38], [39], [40], [41]

Fluid	Brand	Flash Point (K)	Auto Ignition (K)
Jet-A	Local airport	310	483
MIL-PRF-5606	ROYCO 756	>365	492[1*]
MIL-PRF-23699	ROYCO 500	525	638[2*]

[1*]AIT provided for MIL-PRF-5606 is for ROYCO 567G brand, [2*]AIT for lubrication oil is for MIL-PRF-7808.

2.1.9 Operating Conditions, Test Parameters & Test Matrix

Air velocity and temperature limits were shown on Figure 2-10. MHSIT apparatus is designed to have 2 types of injection mechanisms to replicate 2 different leak scenarios: (1) Spray, leaks with micron sized parcels from 16.5 cm upstream of the hot surface and (2) Stream/jet, leaks with millimeter sized parcels from directly above the hot surface. There injection mechanisms weren't changed over the course of this study.

Test fluid contact time was determined to be 10 seconds and injections were stopped after 10 seconds. If ignition occurred before the fixed duration, test fluid injection was stopped immediately upon observation of ignition event. Test fluid flow rate was experimentally determined at ambient test fluid temperature conditions. Test fluid tank was pressurized, and fluid flow rate was experimentally measured. Test fluid tank pressure was constant to maintain a fixed flowrate throughout this study. MSHIT of aviation fluids study in this document was all done at atmospheric pressure.

Table 2.3 Operating conditions and test parameters

Test Fluid	Temperature (K)		Air Velocity (m/s)
	Air	Test Fluid	
Jet-A/JP-8 Hydraulic Oil (5606) Lubrication Oil (23699)	320 – 505	Ambient – 485	0 – 7.3
Fixed Test Parameters			
Test Fluid Contact/Residence Time (sec)	10		
Pressure (bar)	Ambient ~1		
Test Fluid Injection Type	Spray or Stream		
Hot Surface Size	0.15 m OD x 0.15 m Length		
Hot Surface Material	Inconel 718		
Hot Surface Heating Method	Electric cartridge heating		

2.2 Experimental Technique

Major steps in the experimental procedures are shown in the figure below. Air is conditioned using the facility air heater then flows to the apparatus through a venturi to calculate the air mass flow rate. Hot surface is made from Inconel 718 and is heated by 15 electric heaters with each 1 kW power. Surface temperature is controlled using CN616 temperature controller. There are 15 thermocouples to monitor the surface temperature.

Figure 2-17 Test procedure and experimental technique

MHSIT is the highest surface temperature where no ignition is observed for a given flow condition, and it is described with near 0% ignition probability. It is best practice to capture and use partial ignition probabilities between 0 and 50% to fit an S-curve (logistic function). The MHSIT can be determined after enough injections are repeated at a given surface temperature and flow condition. Therefore, a minimum of 10 trials was performed in this study to determine the MHSIT and to investigate the so-called low end of the S-curve. This number was determined so that the time to complete an MHSIT experiment for a given flow condition was manageable. Furthermore, such a technique is consistent with that used in recent studies by Colwell et. al. [11] and Goyal et. al. [1]. It is also important to vary the hot surface temperature in small increments because ignition probability is highly sensitive to the surface temperature. Several levels of ignition probability between 0% and 50% are required to construct an informative S-curve. The temperature increment used for in this study was as low as 3 K.

Air is preheated before each experiment. Before starting the air heater, air flow is initiated so that the heat from the air heater can be dissipated by the flowing air. This process usually takes about one hour. During the air heating process, both test fluid and surface heaters are powered and set to their desired temperatures. Once the hot surface, air and test fluid temperatures have reached acceptable levels of thermal equilibrium (±5, ±5, and ±10 K respectively) and circumferential uniformity (±5K), the supply tank is pressurized, and test fluid is injected for 10 seconds.

The hot surface temperature is increased until an ignition event is observed. Once the ignition event is observed, the surface temperature is reduced in relatively large temperature increments until no ignition events are observed. This initial search with large increments is done to locate the temperature range between 0% and 100% ignition probability and save time instead of repeatedly applying ~5 K temperature increments. The surface temperature is then increased in increments of 5K to identify the lowest partial ignition probability levels, up to 50%, with 10 trials at each surface temperature and flow condition. Ignition events are observed using two Axis P1435-LE cameras viewing the test apparatus from flow discharge and through the side window. A Phantom, black and white high-speed camera was also utilized to detect ignition events in more detail. An ignition event was counted if ignition is followed by sustained burning. Intermittent ignition kernels that were extinguished were not counted.

Following each injection, cool nitrogen gas is used to purge the injecting lines. Each trial lasted about 5 minutes, depending on the surface temperature and flow conditions. A typical experiment consists of at least 50 injections. After each experiment, the test apparatus was disassembled for cleaning the hot surface, windows, octagonal air duct and surrounding test apparatus. This cleaning removes any test fluid residue that may aid ignition and affect data accuracy. An experiment conducted with the technique described here takes about two 8-hour days to complete including data processing.

2.3   Results and Discussion

Results from Johnson et. al. [4] are compared to results generated by the current study at similar conditions in Figure 8. Orange and blue dots pertain to preliminary ignition data at 0 and 0.3 m/s air velocity prior to the development of the experimental technique described in section 2.2. Orange and blue diamond symbols pertain to ignition data improved by the experimental technique. S-curves were fitted to ignition data from the current study. AFRL data are plotted by orange, blue, and purple stars. However, the experimental technique used by Johnson et. al. prevented the assessment of ignition probability. Therefore, ignition data from the AFRL study are plotted without an s-curve.

MHSIT reported in the current study is comparable to MSHIT reported by Johnson et. al. However, any ignition counted in the AFRL study was interpreted as 100% ignition probability and all ignition data were plotted on y=1 line on Figure 2-18. Therefore, the hot surface temperatures with increasing ignition probabilities from the current study aren't comparable to the hot surface ignition temperatures reported from the AFRL study.

Preliminary data from the current and AFRL study measured MHSIT by observing 4 and 3 consecutive no-ignitions, respectively. Also, preliminary data span a temperature range that covers ignition data from the AFRL study. The similar number of trials used between the two studies resulted in similar temperature ranges for reported ignition data. The MHSIT in this study has shifted over 100 K for both 0 and 0.3 m/s air velocities between 4 and 10 trials. Ignition data with partial probabilities obtained using the developed experimental techniques discussed here are more comparable with the recent studies [1], [11]. The improved experimental technique was applied to analyze the effect of air velocity on the hot surface ignition temperature.

The effect of air velocity on MHSIT is widely discussed in the literature. For example, Laurendeau [15] listed fuel/air stoichiometry affecting ignition temperature. Increasing airflow limits the flammable vapors' contact time with the hot surface and reduces exposure time which increases the temperature required for ignition [11], [21] and [29]. Therefore, fuel leaks in the presence of higher air velocities are expected to ignite at higher surface temperatures. As a result, the MHSIT at 0.3 m/s air velocity with 10 trials is higher than the MHSIT with no crossflow (0 m/s). However, the effect of the air velocity on the MHSIT wasn't clearly observed at low air velocities from the AFRL and preliminary data due to the applied experimental technique. The MHSIT reported by Johnson et. al. at 0.6 m/s air velocity is lower than the MHSIT at 0.3 m/s. Similarly, the MHSIT at 0.3 m/s air velocity is lower than the MHSIT at 0 m/s from the preliminary data.
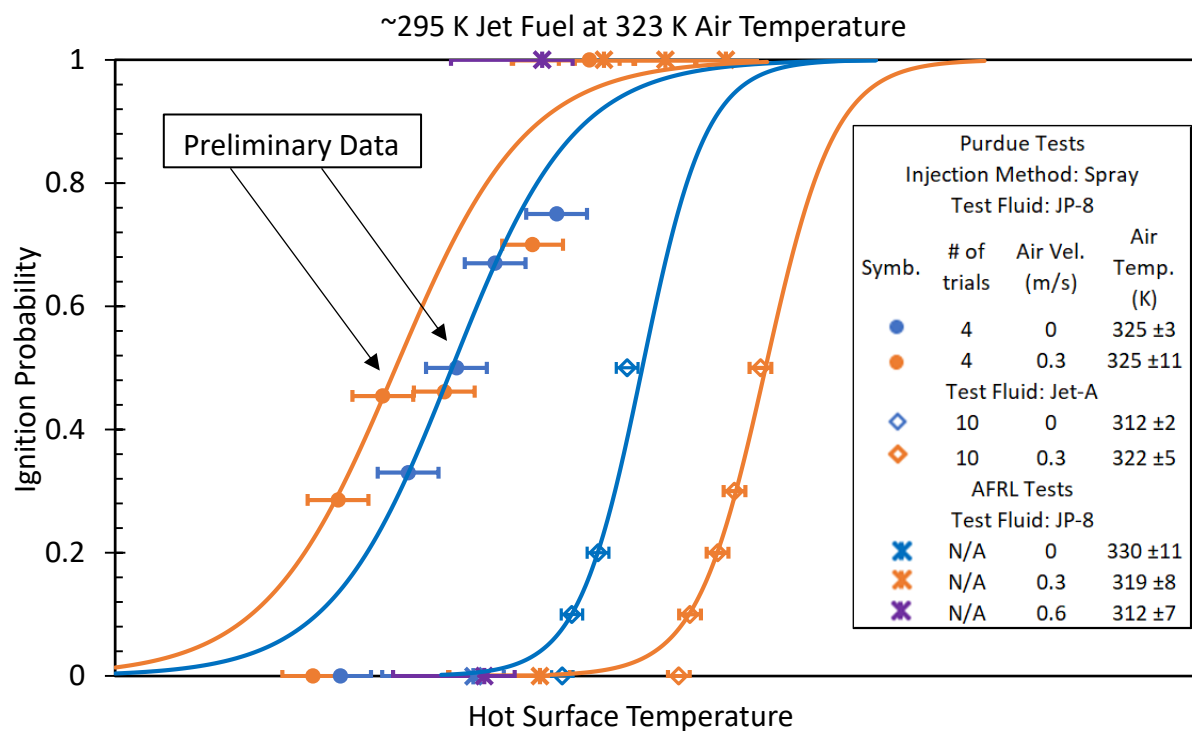
Figure 2-18 Ignition probability graph for Jet fuel using 4 trials vs. 10 trials. Ignition data for air velocities 0-0.6 m/s presented with spray injection method

The ignition probability margin in the AFRL study was higher than the current study due to the experimental technique applied. It is possible for an additional fourth injection performed after three consecutive non-ignitions can ignite and change the ignition probability from 0% (0 out of 3 trials) to 25% (1 out of 4 trials). This added high uncertainty for reported MHSIT values in the AFRL study. Both the number of trials performed at a desired surface temperature and temperature increments are important to determine the MHSIT. The current study was conducted to further explore these factors.

Experiments were conducted to observe the MHSIT for various leak conditions. Therefore, several levels of ignition probabilities above the MHSIT were measured, up to 50%. S-curves for the 0 and 0.3 m/s air velocities with 10 trials in Figure 2-18, were fitted to the lowest two partial ignition probabilities. The blue s-curve was fitted between 10% and 20%, and the orange s-curve was fitted between 10% and 20% ignition probabilities. However, the s-curves in the current study underestimated the MHSIT compared to experimental ignition data by ~40 K, which was also observed by Goyal et. al. [1].

52

Thermocouples used by the AFRL study were larger compared to the current study and led to higher surface temperature uncertainties. Ignition data by Johnson et. al. is hardware specific and requires additional processes before applying to different geometries and flow conditions. Thermocouples measuring the hot surface temperature are placed closer to the ignition point in the current study.

A generic experimental apparatus to investigate the minimum hot surface ignition temperature was developed in this study. An improved experimental technique for evaluating MHSIT for aviation fluids was documented. As a result of the improved technique, uncertainty on the hot surface temperature in this study is ±5 K, in comparison to +14 K and -42 K from the AFRL study. Results from the apparatus were compared to ignition data from previous studies.

The effect of the number of injection trials was demonstrated. At least ten trials were performed at each flow condition to evaluate ignition probability. Ignition data resulted from the ten trials lowered the uncertainty associated with ignition probability. Ignition detection criteria was improved by using a high-speed camera. Surface temperature control was improved with the use of PID control, and temporal uniformity of the hot surface temperature was better managed. Because of the PID control on the hot surface temperature, temperature increments as low as 5 K were achieved. This resulted in a detailed investigation of the hot surface temperatures as a function of ignition probability. This technique allowed for more accurate MHSIT determination for aviation fluids.

3. THEORY OF IGNITION AND IGNITION HEAT TRANSFER MODEL

3.1 Theory of Ignition

Hot surface ignition in crossflow is modeled by an energy balance over the smallest flammable fluid/parcel on the heated surface. The parcel receives energy from the heated surface, evaporates, and mixes with the surrounding airflow to form an ignitable mixture. Ignition initiates a chain reaction leading to combustion, by breaking the bonds within the molecular structures which stores the chemical energy. The energy balance is built between the chemical energy and the energy lost from the hot surface to the ignitable parcel by convection. This model has been proposed in the past [18], [19], [21], [22], [24], [42], [43], [44], [45] and [46].

The ignition criterion defined by Williams is immanently reasonable [47]. The heat liberation rate by chemical reactions inside a slab must approximately balance the heat loss from the slab by thermal conduction.

3.2 Empirical Modeling for Hot Surface Ignition of Aviation Fluids

An empirical model is proposed in this section to estimate minimum hot surface ignition temperature (MHSIT) for aviation fluids. MHSIT in the current study is defined as the highest temperature where no ignition is observed for a set number of injections at a given flow condition. MHSIT is condition specific and performing experiments for each condition is costly and time consuming. A well-established empirical model that considers the flammable fluid and local air flow properties to estimate MHSIT in the design and evaluation process can be very useful for safe handling of these aviation fluids. The empirical model for flammable fluid ignition is based on an energy balance between convective heat loss to the ignitable parcel from the hot surface and the energy released by the incipient chemical reaction. This empirical model considers the air temperature, pressure, and velocity, flammable fluid temperature, and its chemical and physical properties to estimate the MHSIT at a given flow condition. MHSIT estimates from the empirical model are within $\pm 5\%$ on average of the experimental data.

The current study was motivated by the need to design a generic apparatus and develop a model based on the ignition data from this apparatus to estimate the MHSIT as a function of flow conditions such as air velocity, air temperature, and fluid temperature.

High speed ignition images from an experiment is shown below. Ignition initiates on the hot surface and propagates in the airflow direction as well as towards the source of flammable fluid leak.
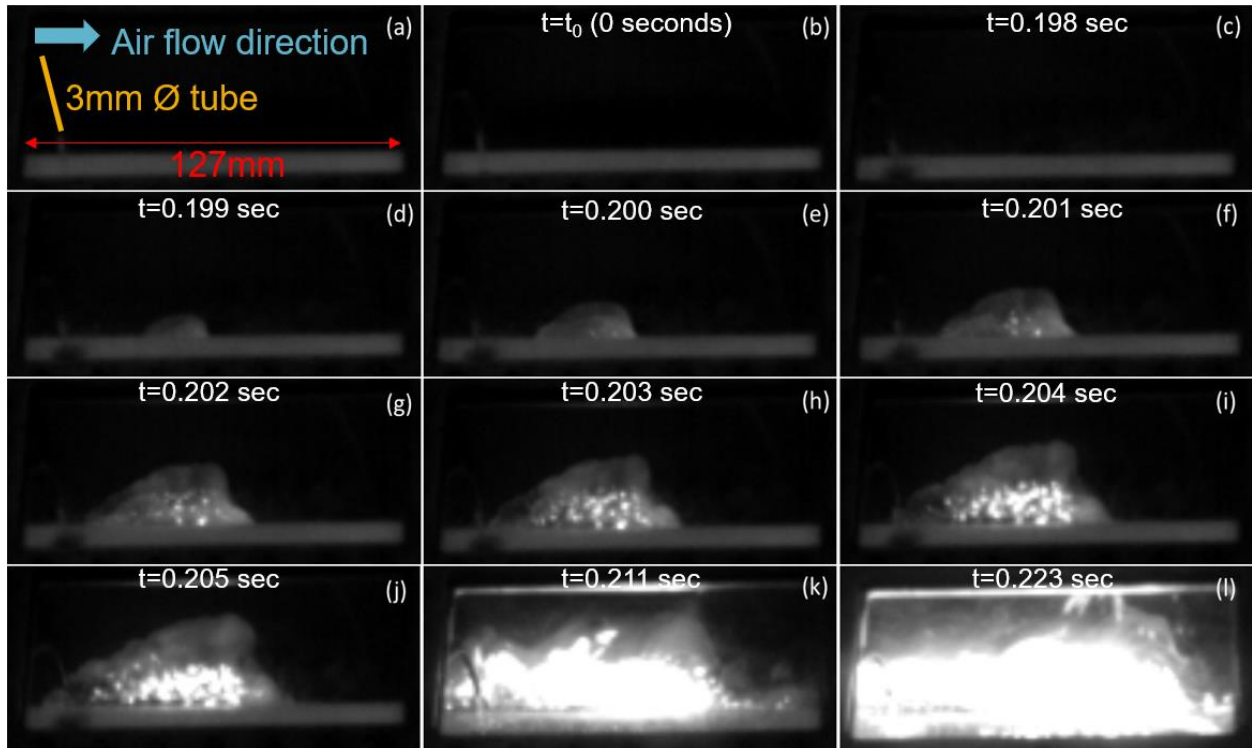
Figure 3-1 High speed camera images from stream injected lubrication oil

127 mm section of the hot surface material is shown on each frame in Figure 3-1. Frame (a) shows lubrication oil leaking from the tube. At this point oil hasn't reached to hot surface yet. Frame (b), shows the first black mark on the hot surface by relatively colder oil temperature contacting to the hot surface. Frame (b) is considered as t=t_0 (0 seconds). Frame (c) is taken at t=0.198 seconds. Hot surface temperature is decreased locally at the point of colder temperature oil contact. Frame (d) at t=0.199 seconds, shows first oil vapor and air mixture nucleus (ignition kernels may have formed, but it is not visible to the naked eye). Frame (e) at t=0.200 seconds, 2 ignition kernels ~200µm are spotted. Spotted ignition kernels are both on the surface. Initial kernels are axially, about in the

middle of the cylindrical Inconel 718 hot surface material (approximately 3" from either end of the hot surface material). Frame (f) at t=0.201 seconds, kernels propagate. Frame (g) at t=0.202 seconds, one can observe the increase in number of ignition kernels. It is also observed that ignition kernel diameters increase in comparison to initial kernel formations from frame (e). Frame (h) shows ignition kernel agglomeration at t=0.203 seconds. Frame (i) at t=0.204 seconds, ignition kernels continue to agglomerate and grow under oil-air mixture vapor dome. Frame (j) at 0.205 seconds, ignition kernels are propagating in both directions. The flame propagates at relatively the same speed in both directions (in-parallel with and against to airflow direction). Frame (k) at t=0.211 seconds, the kernels form a continuous flame. Frame (l) at t=0.223 seconds, a self-sustaining flame is formed (if oil continues to leak, flames will be sustained and continue to burn). The flames propagated until fuel sources. The flame reaches to total length of 127 mm in Δt=0.022 seconds, between frames (e) and (l). This corresponds to about 5.8 m/s flame speed.

3.2.1   Empirical Ignition Model for Hot Surface Ignition

Hot surface ignition of the flammable fluid leak is modeled in this chapter. The flammable fluid parcel sizes can range from micron to millimeter depending on the leakage scenario. It was observed from thousands of ignition videos that ignition always initiated on the hot surface. This model is for hot surface ignition only and doesn't apply for auto-ignition. The model is generic to various aviation flammable fluid leakage scenarios. The hot surface is surrounded by 3 insulator rings to minimize heat loss via conduction from the hot surface: two insulators parallel to the airflow direction positioned before and after the hot surface and the third insulator sleeve is located inside the hot surface insulating radially inwards.
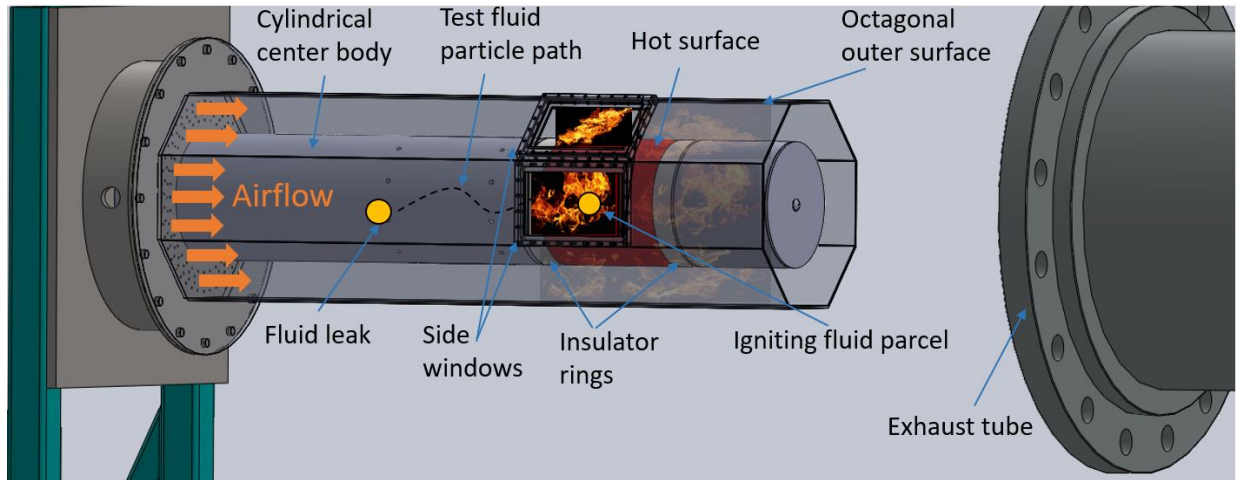
Figure 3-2 MHSIT apparatus and components inside the duct with airflow and fluid leak shown
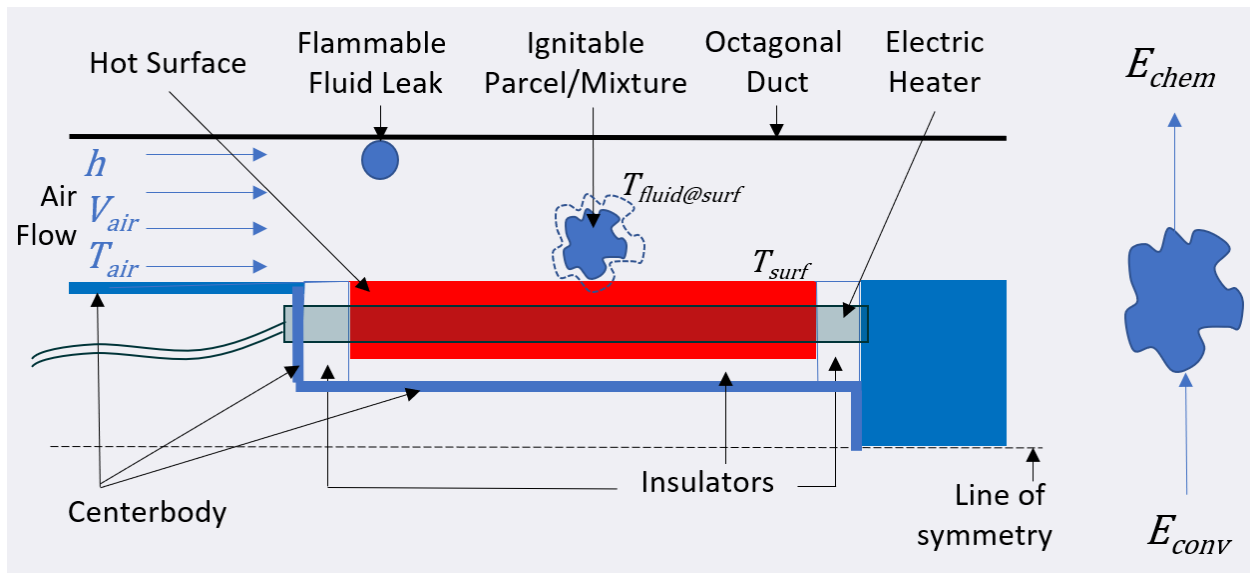
Figure 3-3 Ignition model diagram (bottom), fluid parcel travel path, its heating/cooling with the airflow, and the energy balance on the flammable parcel

The convective heat transfer is calculated using the temperature difference between the hot surface temperature and the flammable fluid parcel temperature at the surface. The fluid parcel temperature is measured before entering the octagonal duct. The parcel can be heated or cooled depending on the airflow condition once in the octagonal duct. Various flow conditions are possible in an engine compartment depending on the geometry and location.

The parcel evaporates by the energy received from the hot surface and the vapor diffuses and mixes with air. Heat transfer occurs from the hot surface to the ignitable parcel/mixture in contact with the hot surface. The model considers the lower heating value of the flammable fluid at the time of ignition due to evaporation. The latent heat of vaporization does not contribute to the energy released due to chemical reaction (the combustion event).
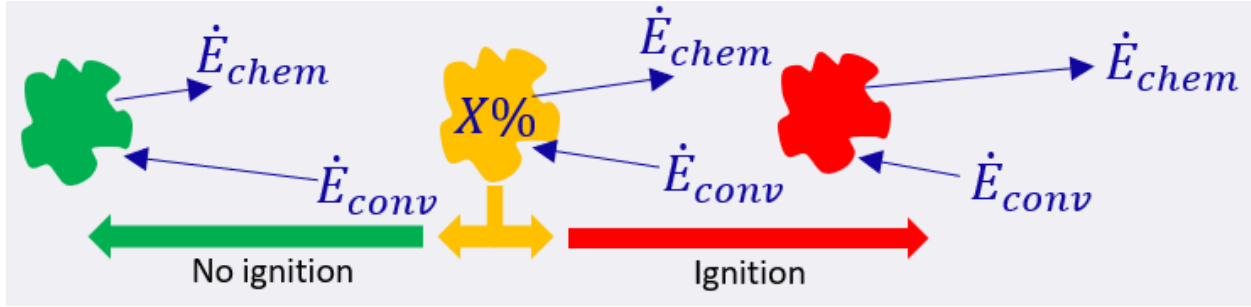
Figure 3-4 Ignition model schematic

$$\dot{E}_{conv} = \dot{E}_{chem} \tag{3-1}$$

$$h \cdot A_{parcel,contact} \cdot (T_{surf} - T_{parcel@surface}) = \frac{\rho_{parcel} \cdot V_{parcel} \cdot LHV}{\tau_{ign}} \tag{3-2}$$

Above equation simplifies into the following form, where k is the geometry factor resulting from the fluid/parcel volume to contact surface area ratio:

$$k_{parcel} \cdot h \cdot (T_{surf} - T_{parcel@surface}) = \frac{\rho_{parcel} \cdot d_{parcel} \cdot LHV}{\tau_{ign}} \tag{3-3}$$

Where, τ_{ign} is the ignition delay time:

$$\tau_{ign} = A \cdot T_{surf}{}^{B} \cdot P_{ratio}^{-0.5} \cdot e^{C/T_{surf}} \tag{3-4}$$

Heat transfer coefficient for energy balance between hot surface and the parcel at the surface is calculated using following Nusselt number correlation. This is modified Dittus – Boelter correlation. Constant 2 was added to the correlations, to account for near no airflow conditions, to account for natural convection.

$$Nu = 2 + 0.023 \cdot Re^{0.25} \cdot Pr^{0.3} \tag{3-5}$$

$$Nu = \frac{h \cdot D_h}{k} \tag{3-6}$$

The heat transfer coefficient between the hot surface and the parcel is directly related to the airflow rate, which is related to the global equivalence ratio within the octagonal duct. The ignition delay expression doesn't account for equivalence ratio directly, but the global equivalence ratio within the duct is accounted for in the model, embedded into the heat transfer coefficient h as shown in equation 3-2.

No chemical reaction takes place until the parcel reaches to the hot surface. Evaporation rate of the parcel is accounted, hence LHV is used to compute the amount of energy release per unit of mass during combustion. The parcel volume is assumed to be constant through its travel to the hot surface when calculating reactant mass to simplify the model.

Test fluid parcel temperature is measured during its injection before entering the test section (octagonal duct). Ignition always takes place at the hot surface. $T_{parcel@surface}$, parcel temperature at the hot surface is different than what was measured at the thermocouple location before the parcel entering the test section. $T_{parcel@surface}$ is calculated using the relevant heat transfer correlation based on the conditions.

The parcel acceleration was calculated using the following set of equations to determine proper Nu number correlation for calculating $T_{parcel@surface}$, parcel temperature at the hot surface. Micron sized parcels (spray injected) acceleration was calculated using following equation with Jet-A properties. Millimeter sized parcel (stream injection) acceleration was calculated with lubrication oil properties.

$$F_x = \frac{1}{2} \cdot C_d \cdot \rho \cdot v^2 \cdot \pi \cdot \left(\frac{D}{2}\right)^2 \qquad \text{3-7}$$

$$a = \frac{F_x}{m_{droplet}} \qquad \text{3-8}$$
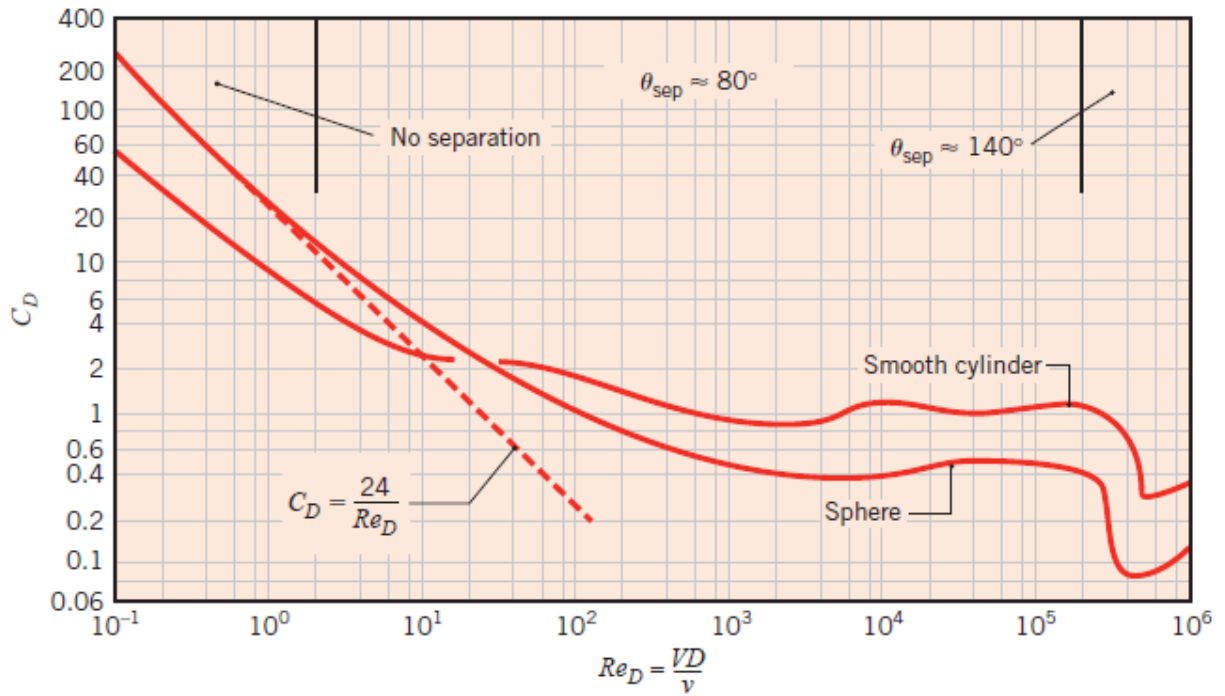
Figure 3-5 Drag coefficient graph for spheres and smooth cylinders [48]

Table 3.1 Parcel acceleration calculations and assumption for Nu number correlation of the parcel heating/cooling

	Jet-A (spray parcel acceleration)		Lube Oil (stream parcel acceleration)	
	Case 1	Case 2	Case 1	Case 2
V_{air} (m/s)	0.3	6	0.3	6
Re	1	17	19	346
C_d	24	3	3	1
a (m/s^2)	49	2061	0.01	1.2

Micron sized parcel acceleration is 49 m/s^2 for the lowest airflow rate. This indicates micron sized parcels will travel at the same speed as the airflow. It is assumed that parcel velocity reaches to the air velocity very quickly and therefore heat transfer between the parcel and the air is mainly natural convection to calculate the parcel temperature at the hot surface.

Millimeter sized parcel acceleration is 0.01 m/s^2 for low air velocities and relative velocity between the airflow and larger parcels is small as shown in Table 3.1. This and the thousands of ignition

tests allowed to assume that jet injection is continuous and cylindrical in shape. Therefore, heat transfer between millimeter sized (stream injected) parcel and airflow is of the heat transfer of a cylinder in crossflow with forced convection. Following figures illustrate the two different leak types. Two Nu number correlations were used to calculate the heat transfer between the parcel and the airflow depending on the leak type.
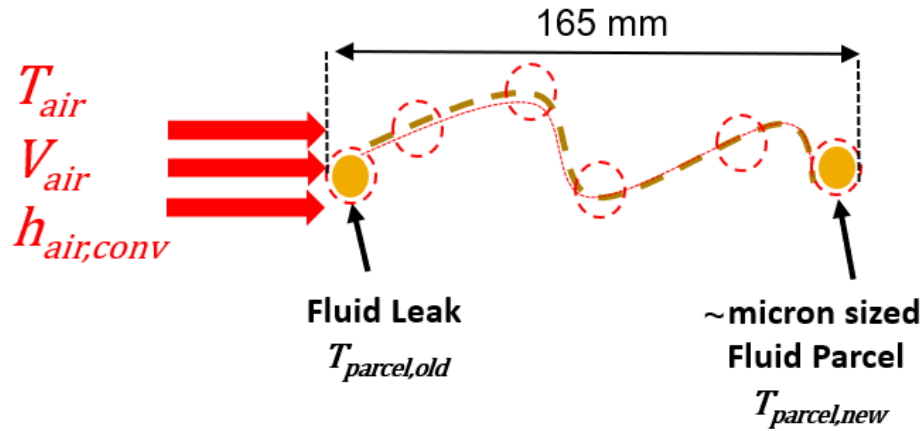
Figure 3-6 Micron sized fluid leak scenario (spray injection – 165 mm upstream of the hot surface) and parcel travel path while heating/cooling due to airflow

Free-Convection Heat Transfer between Air and Micron Sized Parcel (Spray Injection), Yuge Correlation

$$Nu = 2 + 0.435 \cdot Ra^{0.25} \qquad\qquad 3\text{-}9$$
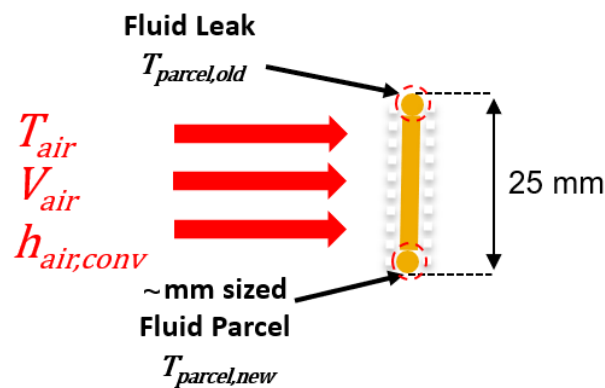
Figure 3-7 Millimeter sized fluid leak scenario (stream injection – 25mm above the hot surface) and parcel travel path while heating/cooling due to airflow

Heat Transfer between Air and Millimeter Sized Parcel (Stream Injection) for a Cylinder in a Crossflow with Forced Convection

$$Nu = 0.3 + \frac{0.62 \cdot Re^{0.5} \cdot Pr^{1/3}}{[1 + (0.4/Pr)^{2/3}]^{1/4}} \cdot \left[1 + \left(\frac{Re}{282000}\right)^{\frac{5}{8}}\right]^{\frac{4}{5}} \qquad \text{3-10}$$

The lumped capacitance model with only convective boundary condition is applied to the parcel traveling to the hot surface for the fluid leak scenarios described above. The parcel is assumed to be in spherical shape for this analysis.

$$\dot{E}_{in} + \dot{E}_{gen} - \dot{E}_{out} = \dot{E}_{st} \qquad \text{3-11}$$

$$\dot{E}_{in} = \dot{E}_{gen} = 0 \qquad \text{3-12}$$

$$-\dot{E}_{out} = q''_{conv} \cdot A_{parcel} \qquad \text{3-13}$$

$$\dot{E}_{st} = \rho_{parcel} \cdot V_{parcel} \cdot c_p \cdot \frac{dT}{dt} \qquad \text{3-14}$$

$$-h_{conv} \cdot A_{parcel} \cdot \Delta T = \rho_{parcel} \cdot V_{parcel} \cdot c_p \cdot \frac{dT}{dt} \qquad \text{3-15}$$

$$\left(T_{air} - T_{parcel,old}\right) \cdot \int_{t_0}^{t_1} dt = \frac{\rho_{parcel} \cdot V_{parcel} \cdot c_p}{h_{conv} \cdot A_{parcel}} \cdot \int_{T_{parcel,old}}^{T_{parcel,new}} dT \qquad \text{3-16}$$

t = 0.001 seconds, to allow proper convergence of the solution. $T_{parcel,new}$ is calculated step-by-step advancing the temperature of parcel using following equation.

$$T_{parcel,new} = T_{parcel,old} + \left(T_{air} - T_{parcel,old}\right) \cdot \frac{\Delta t \cdot h}{\rho_{parcel} \cdot d_{parcel} \cdot c_p} \qquad \text{3-17}$$

Test fluid leakage leading to hot surface ignition study was performed in an octagonal duct/enclosure. This is referred to as annular flow. The flow is turbulent with Re>2300 even with lowest experimental air velocity of 0.3 m/s. Reynolds, Prandtl, Grashoff, and Rayleigh non-dimensional numbers were calculated using the following formulas.

$$Re = \frac{4 \cdot \dot{m}_{air}}{\pi \cdot D_H \cdot \mu_{air}} \qquad \text{3-18}$$

$$Pr = \frac{\mu_{air} \cdot c_p}{k} \qquad \text{3-19}$$

$$P_{ratio} = \frac{P}{P_{atm}} \qquad \text{3-20}$$

$$Gr = \frac{g \cdot \beta \cdot \Delta T \cdot L_c{}^3}{v^2} \qquad \text{3-21}$$

$$Ra = Gr \cdot Pr \qquad \text{3-22}$$

The simplified energy balance for the empirical ignition model equation is combined and organized into the following form so, T_{surf} terms were all grouped on the LHS of the equation below. This equation is equivalent to equation 3-23.

$$\ln(T_{surf} - T_{parcel@surface}) + B \cdot \ln(T_{surf}) + {}^C\!/_{T_{surf}}$$
$$= \ln(\rho_{parcel}) + \ln(d_{parcel}) + \ln(LHV) - \ln(8) - \ln(h) - \ln(A) - 0.5 \cdot \ln(P_{ratio})$$

3-23

This equation is solved iteratively, varying T_{surf} by 0.05 K at each step until the system is converged. The system reaches convergence when both sides of the equation are equal or the error (difference between LHS and RHS) is minimized. Ignition delay equation constants are needed to solve the above equation. Hot surface ignition temperatures from the experiments were used to determine ignition delay constants. Details of ignition delay constants determination will be explained in the next chapter.

Regression analysis was used to obtain correlations for change in the hot surface ignition temperatures with obstacles and no obstacles. Approximate parcel size, air and flammable fluid temperatures were used to determine a correction factor to be added or subtracted from the estimated MHSIT found from the model described in this section.

3.2.2 Empirical Ignition Model Constants

Ignition events from the experiments showed that ignition delay time and the ignition probability decrease with increasing hot surface temperature. However, ignition delay times aren't experimentally measured. Therefore, ignition delay expression with constants A, B and C was fitted to the data to estimate hot surface ignition temperatures with assigned ignition probabilities using the empirical kernel-based ignition model described in this chapter.

There are 7 variables, A, B_0, B_1, B_2, B_3, C, k and T_{surf}, to be empirically solved for using the experimental data. k is the geometric factor and this value was determined based on the fluid leak

type. This parameter was also used as a tuning parameter in the model. First, A and C constants were solved using EES with the assumption of $B=0$ and $P_{ratio}=1$ for the hot surface temperatures (1) the highest surface temperature with no ignition - MHSIT and (2) the lowest hot surface temperature at which ignition is highly probable (~100% ignition probability). Constant B is used for estimating hot surface ignition temperature as a function of ignition probability. Subscripts 0, 1, 2, and 3 are referring to different ignition probabilities based on the number of injections performed at each hot surface temperature and flow condition. B_0 is used for MHSIT and the consecutive numbers refer to increasing ignition probabilities. Constant C represents activation energy for the flammable test fluid. Therefore, an Arrhenius form of the ignition delay expression was utilized. Constant A represents a form of pre-exponential coefficient within the ignition delay correlation. It is correlated with the heat transfer coefficient between the hot surface and the parcel. EES was used to solve the following equation 3-23, which is equivalent to equation 3-2. Empirical constants are calculated using the model described in this section, and the MHSIT estimates from the model are within 5% in average of the experimental MHSIT values.

3.2.3 Empirical Ignition Model Results using AFRL Study

Energy balance used in the model for the hot surface ignition of the smallest flammable parcel is independent of any apparatus. The model can be applied to ignition data from any experimental hardware. The model will estimate MHSIT based on the size and the number of variables in the data.

MHSIT depends on the flow condition and is not a fluid property like AIT. This led researchers to build complicated application specific test apparatus. Processing the ignition data to apply to other leak scenarios was difficult and resulted in high apparatus-specific uncertainty to estimate the MHSIT.

The following figure was taken from an AFRL report [4]. It shows the complex heated bleed duct shape and various stream and spray injection locations to study hot surface ignition temperature of aviation fluids. For a constant surface temperature and flow condition, the reported hot surface ignition temperature between location 1 and 6 differed by ~200 K. This illustrates the difficulty to generalize ignition criteria from a hardware specific ignition data.

64

HIGH REALISM TEST ARTICLE
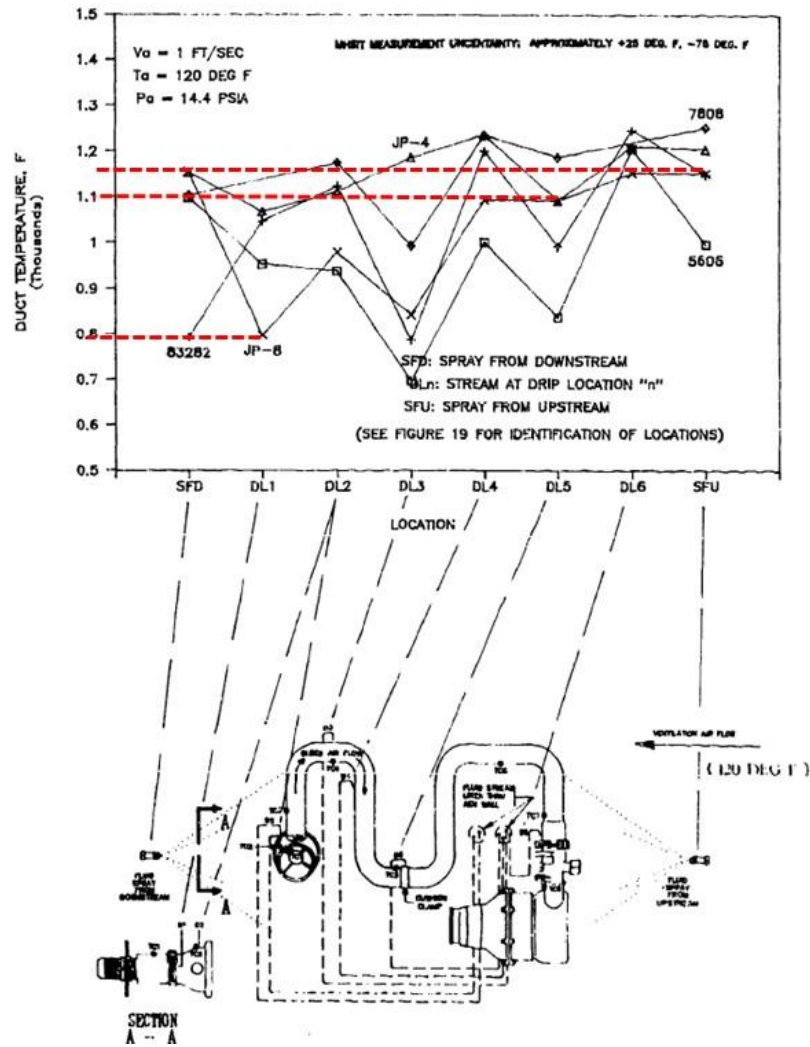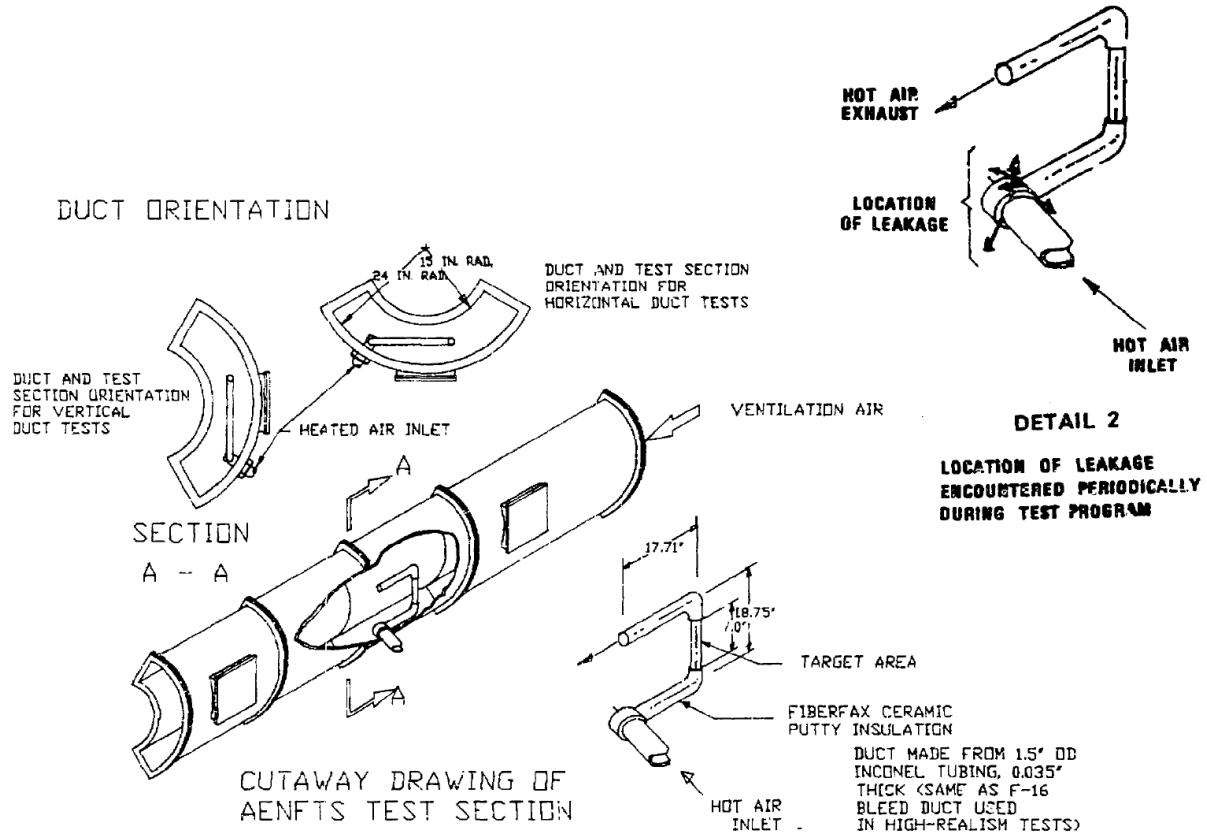
Figure 3-8 AENFTS located in Dayton, OH

Same model described in section 3.2.1 was used ignition data by Johnson et. al. and compared to experimental results. JP-4 fuel was selected as the flammable fluid using the simple test configuration at the Air Force Research Laboratory to demonstrate the empirical ignition model First, the fluid either heats up or cools down while traveling through the air stream towards the hot surface depending on the difference between the air and fluid temperature at the point of leak. The smallest particle is considered as it travels to the hot surface as this particle is most likely to evaporate and ignite after impinging on the surface. This process is shown in equation 3-24 and accounts for the parcel size and fluid chemical and physical properties. During experimentation it was noted that the fuel always ignites on the surface, and thus auto ignition is not considered in this model. Fluid parcel size was found to be ~65µm, thus the lumped capacitance model can be applied.

$$m_{parcel}c_p\frac{dT_{parcel}}{dt} = h_{parcel}A_{parcel}(T_{air} - T_{parcel}) \qquad \text{3-24}$$

A baseline spherical shape is considered for a representative leaked fluid parcel with the greatest potential to ignite. This assumption leads to the following modification to equation 3-25, where k_{parcel} is an empirical constant that accounts for the surface area to volume ratio of the particle including departures from the spherical shape.

$$d^3_{parcel}\rho_{parcel}c_p\frac{dT_{parcel}}{dt} = k_{parcel}h_{parcel}d^2_{parcel}\left(T_{air} - T_{parcel}\right) \qquad \text{3-25}$$

$$\frac{dT_{parcel}}{dt} = \frac{k_{parcel}}{\rho_{parcel}c_p d_{parcel}}h_{parcel}\left(T_{air} - T_{parcel}\right) \qquad \text{3-26}$$

This equation can be solved to determine the temperature of the fluid parcel at the time that it impinges on the hot surface. In this study the fluid trajectory to the hot surface following the leak is assumed to produce small enough parcels for the trivial solution to equation 3-26 to be true; this solution being the solution of utmost engineering interest.

$$T_{parcel,final} = T_{air} \qquad \text{3-27}$$

The fluid particle then interacts with the boundary layer on the hot surface and continues to heat up. Radiative heat transfer is not considered in this model. This process is represented below in equation 3-28; a spherical particle is assumed, and the equation is simplified to equation 3-29.

$$m_{parcel}c_p\frac{dT_{parcel}}{dt} = h_{parcel,final}A_{parcel}\left(T_{surf} - T_{air}\right) \qquad \text{3-28}$$

$$\frac{dT_{parcel}}{dt} = \frac{k_{parcel}}{\rho_{parcel}c_p d_{parcel}}h_{parcel,final}\left(T_{surf} - T_{air}\right) \qquad \text{3-29}$$

Upon ignition, the energy transfer reverses direction from the hot surface to the fuel/air parcel and now the energy flows from the ignition kernel to the hot surface. This is written as:

$$k_{parcel}h_{parcel,final}A_{contact}\left(T_{surf} - T_{air}\right) = \frac{m_{parcel}LHV}{\tau_{ign}} \qquad \text{3-30}$$

The ignition delay term takes an Arrhenius form and is combined with equation 3-30 to write equation 3-32

$$\tau_{ign} = AT_{surf}{}^{B}P_{ratio}{}^{-0.5}e^{\frac{C}{T_{surf}}} \qquad \text{3-31}$$

$$\kappa_{parcel}h_{parcel,final}A_{parcel,contact}\left(T_{surf} - T_{air}\right) = \frac{m_{parcel}LHV}{AT_{surf}{}^{B}P_{ratio}{}^{-0.5}e^{\frac{C}{T_{surf}}}} \qquad \text{3-32}$$

Equation 3-32 allowed for estimating ignition probability and accounts for the effects of parcel temperature, air temperature, pressure, velocity, and fluid type. Equations 3-2 and 3-32 describe the present MHSIT model that is independent of the test apparatus as long as the underlying assumptions are satisfied. A similar energy balance was created by Laurendeau and defined an ignition criterion for auto ignition, by equating heat release from chemical reaction to heat loss to the surrounding by convective heat transfer [49]. While the autoignition criteria is relevant to ignition in a combustor, the MHSIT is relevant to accidental fluid leaks igniting within boundary layers on solid surfaces.

Data from Johnson et. al. [4] were used to calculate the constants in equation 3-32. As a first step, B is set to 0, all data are at atmospheric pressure, ignoring the effect of pressure and ignition probability. This allowed the MHSIT to be calculated for the given flow conditions. The MHSIT value is determined by varying T_{surf} until the equation 3-32 is converged.

The number of experimental points increases the accuracy of the empirical model [50]. The data used to determine the empirical constants A and C from equation 3.32 are from the AFRL study using unheated JP-4. Therefore, the JP-4 is assumed to be at room temperature in this section.

The JP-4 is injected 0.3 m upstream of the hot surface. Details of the test apparatus can be found from the Hot Surface Ignition Tests for Aircraft Fluids report by Johnson et. al. The following tables summarize the fuel properties and other parameters used in this model. Due to under-developed experimental methods employed for data gathering, estimations can only be done for MHSIT. The empirical constants can't be used for other fluids or conditions beyond the range of

the data. In Table 1, low hot surface temperature refers to the temperature at which no ignition was observed for 3 repetitions and high hot surface temperature refers to the next temperature when ignition was observed for the first time. It was found that smaller temperature increments and a greater number of repetitions improved the accuracy the model [50].

The heat transfer coefficient was computed based on the fuel leak scenario and air flow conditions seen in the study. EES software was utilized to solve equation 3.32 parametrically for a set of flow conditions. Fuel properties were obtained from the handbook of aviation fluids [51]. Some of the parameters used for the empirical model are listed in Table 2.

Table 3.2: Empirical model parameters and calculated values for JP-4

h (W/m^2-K)		JP-4 Density	$T_{fluid,final}$	Hot Surface Temp (K)		Output Constants		Estimated
low	high	(kg/m^3)	(K)	low	high	A (sec)	C (K)	MHSIT (K)
127	129	733	329	992	1017	0.224	2351	1031
234	239	735	326	995	1021	0.124	2330	1045
377	385	736	324	1061	1086	0.069	2503	1057
532	544	737	323	1072	1102	0.054	2405	1065
659	673	739	320	1081	1113	0.046	2353	1071

Equation 3.32 was solved iteratively by changing T_{surf} and it was further refined by varying the parcel size until a correlation can be developed between empirical constants and heat transfer coefficient.

Table 3.3: JP-4 properties

LHV (J/kg)	43.9 E+7
Density (kg/m^3)	-0.75 x (K) + 771
Parcel Size (μm)	65

Hot surface ignition temperatures were estimated using the model described above for the flow conditions in the AFRL study. Experimental hot surface ignition temperatures and empirical model estimations are shown in Figure 3-9. Blue open squares with connected line show the model estimations. In contrast, blue solid squares are for the experimental hot surface temperatures with no ignitions, while red solid squares are the hot surface temperatures where ignition was observed.
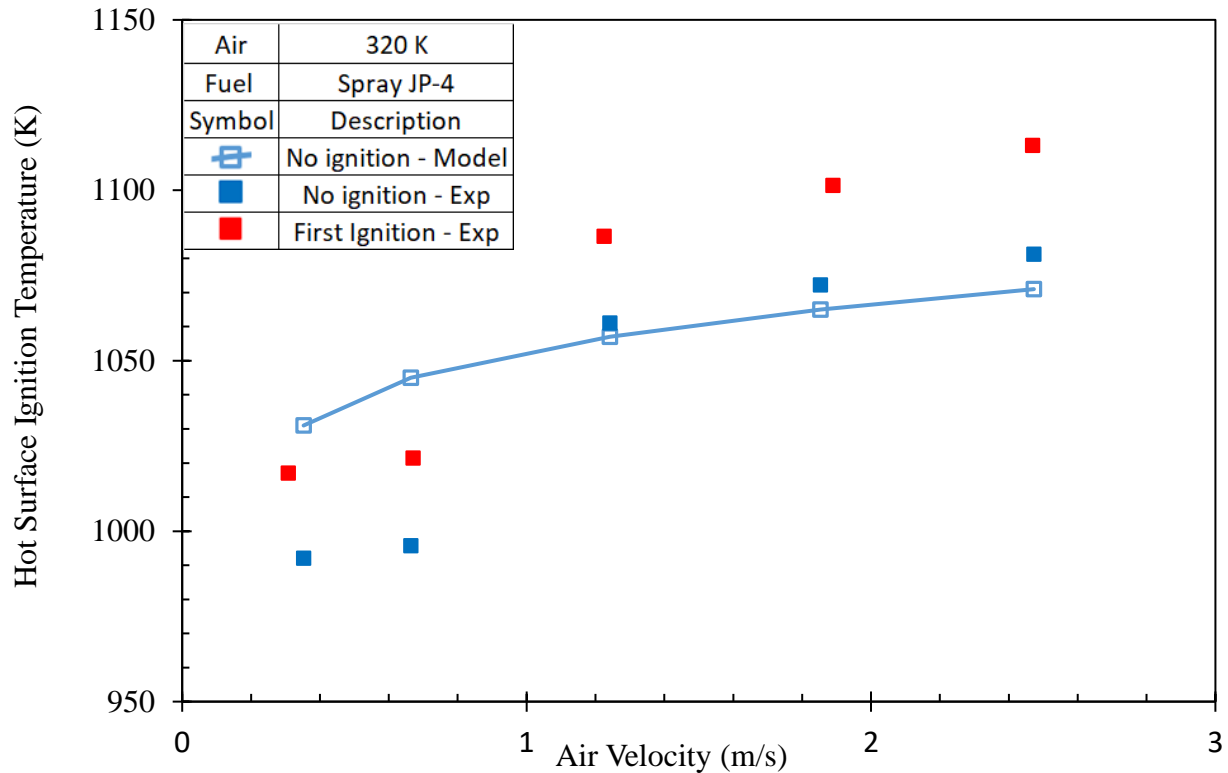
Figure 3-9 MHSIT and hot surface ignition temperatures from the experiment and the model

Model estimations are all within ±5% of the experimental results. However, the model is stronger at higher air velocities yielding as low as ±2% difference. A data set with improved experimental methods will obviously yield even better estimations than those shown in Figure 3-9.

The model shown here can be adjusted for various aviation fluids if experimental data are provided. It is important to note that the model is valid only for the range of conditions set by the experiments. The model here is consistent with the study of Laurendeau [21]. The model will reduce cost associated with experiments and a well-established model can estimate MHSIT in the design evaluation process. This can be very useful for safe handling of aviation fluids.

3.3 Effect of Air Velocity
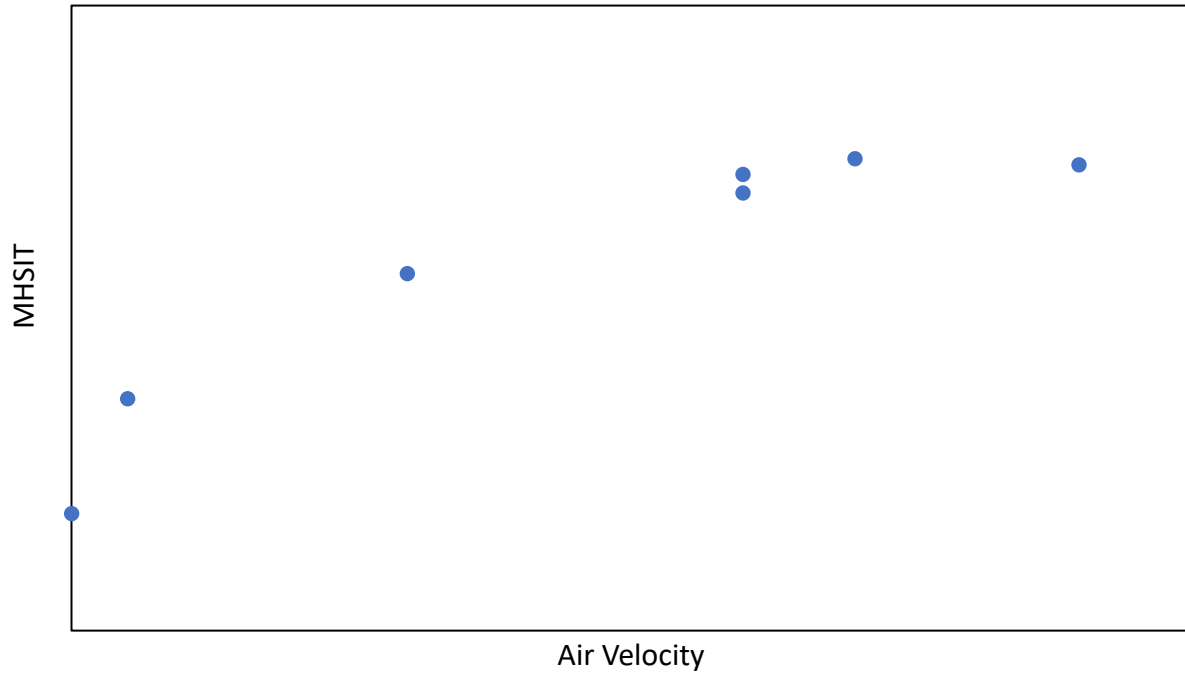
Figure 3-10 Effect of air velocity on MHSIT

MHSIT increases with increasing air velocity. This is also evident from the kernel-based ignition model. Increased air velocity leads to increasing convective heat losses from the hot surface. The required minimum ignition energy also increases proportionally. It is important to note that, the benefit gained by increasing air velocity diminishes as air velocity increases. Benefit gained on the hot surface ignition temperature by increasing air velocity from higher velocities is less than the benefit gained at lower velocities.

The above figure is an example to demonstrate the effect of air velocity on the MHSIT. Data on the figure is for the surface temperatures at which no ignition was observed for a number of injections performed at each air velocity and surface temperature. The effect of air velocity is shown on the x-axis. Surface temperatures are shown on y-axis. The increase in MHSIT saturates as air velocity increases and reaches to a limit. This is where the ignition experiments were stopped.

3.4   Effects of Air and Test Fluid Temperature

3.4.1   Air Temperature

Flammable fluid parcel temperature at the hot surface depends on air flow temperature and the fluid leak type. Stream injection represents a leak type of dripping the fluid from a pipe 25 mm above the hot surface, and spray injection represents a leak type from a spray nozzle with micron sized parcel. Spray nozzle is located 165 mm upstream of the hot surface. Therefore, micron sized parcels have a longer travel time compared to millimeter sized parcels until reaching to the hot surface. Air temperature is more effective in heating or cooling the micron sized. The millimeter sized parcel temperature (stream injection) doesn't change much due to change in air temperature. Therefore, the fluid temperature is more effective on MHSIT for stream injection method in the current study.

The test fluid temperature and air velocity play a significant role for the effect of air temperature on MSHIT. Therefore, the temperature difference cannot be generalized (a general temperate shift cannot be approximated for all air velocities and fluid temperatures), however the change in MHSIT trend can be generalized. Increased air temperature results in decreased MHSIT for a fixed air velocity and test fluid temperature. Ignition temperatures and probabilities shift to lower hot surface temperatures with increased air temperatures. Similar effect can be observed for air temperature on stream injected lubrication oil MHSIT. Increased air temperature decreases stream injected lubrication oil MHSIT.

Effect of changing air temperature on MHSIT for two different injection methods at the same air velocity was different. Change of air temperature is more effective on MHSIT for micron sized parcel leak than for the millimeter sized parcel leak. This difference shifts of MHSIT due to air temperature may be explained by the following: (1) Micron sized parcels heat or cool more effectively than millimeter sized parcels. (2) Parcel distance path between the two different leak types.

3.4.2   Effect of Fluid Temperature

Test fluid temperature is another major factor on MSHIT. Referring to the empirical kernel-based ignition model, convective losses are measured between hot surface temperature and fluid parcel temperature at the hot surface. However, the lumped capacitance model showed that fluid temperature is also affected by the air temperature.

Change in the flammable fluid temperature for micron sized parcels with longer travel path showed minimum effect on MHSIT for a given flow condition. This shows the effective heating or cooling process between the air and the test fluid parcel when the fluid leak lead to micron sized parcels. Hence hot surface ignition temperatures for different fuel temperatures are similar, and the effect of fuel temperature on micron sized parcels with longer travel paths is not significant in the current study.

Effect of the fluid temperature is evident for millimeter sized parcels with short parcel travel path. Hot surface ignition temperatures may decrease as high as 110 K for lubrication oil for a given flow condition. This shows that air heating or cooling is less effective for stream injection method.

Lubrication and hydraulic oils are heavier hydrocarbons compared to jet fuel, which is 99% kerosene. Jet-A is approximated as $C_{11.4}H_{22.1}$ by Edwards [41], whereas exact chemical formula for lubrication and hydraulic oil is not readily available. It is reported that oils are heavier hydrocarbons starting around $C_{20}H_{42}$ with irregular molecular pattern (carbon atom count average is 36, but the range is about 18 – 44) [52], [53]. This can also be related to evaporation rate of jet fuel vs. heavier hydrocarbons like lubrication oil.

3.5   Effect of Number of Injections

Ignition probability is measured based on the number of injections performed at a constant surface temperature with all other variables unchanged. If ignition probability is calculated out of 4 injections at a given condition, the error on ignition probability will reduce if the number of injections increase. However, increasing the number of injections is harder; it requires more time, air, and fuel. Hence it is more expensive. A reported MHSIT (hot surface temperature with near

0% ignition probability) based on 4 injections refers to 0 ignitions out of 4 injections. However, if a fifth experiment is conducted at the same condition, it can either ignite or not. If it ignites the effective ignition probability will be 1 ignition out of 5 injections, hence 20%. However, if the fifth injection doesn't ignite, ignition probability remains the same, 0 ignition out of 5 injections. Therefore, the error on ignition probability for MHSIT with 4 injections is +20% and -0%. When number of injections are increased to 20, the ignition probability uncertainty reduced, and the accuracy of the ignition probability is improved.
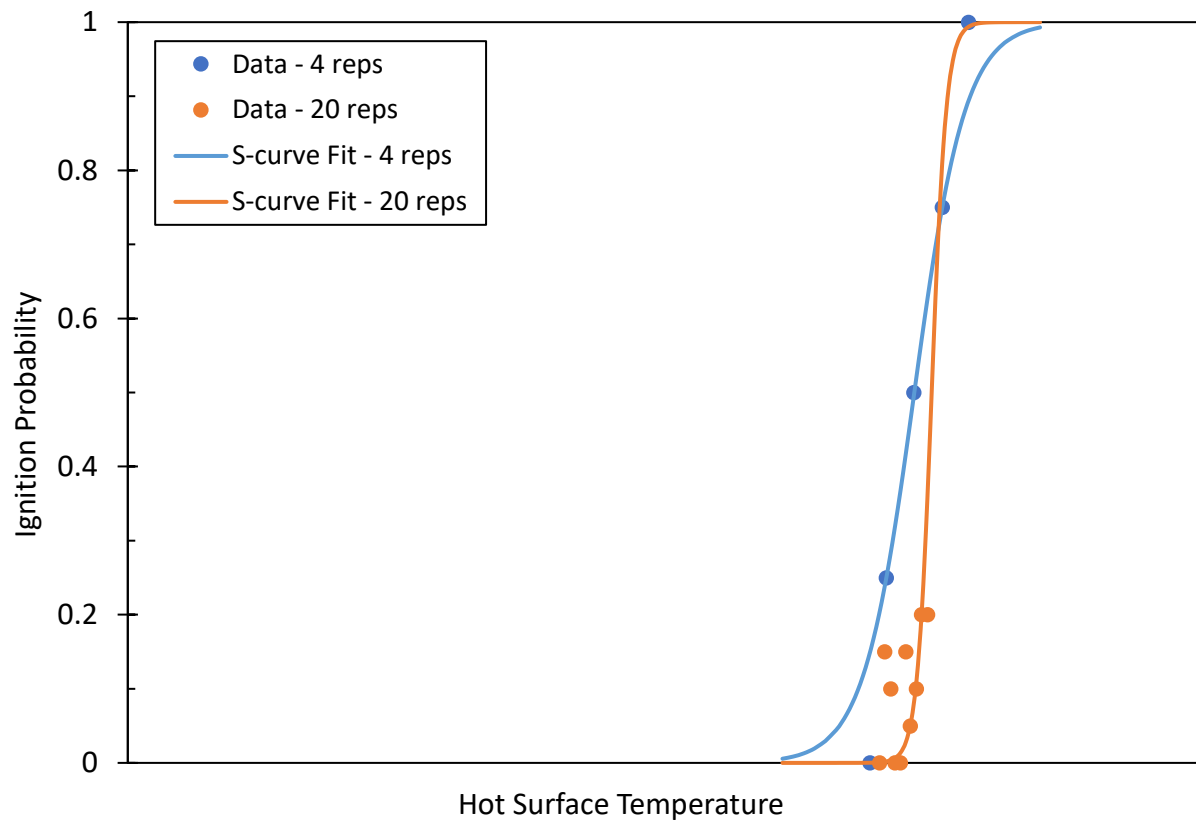
Figure 3-11 Comparison between 4 vs. 20 injections at each surface temperature for improved ignition probability measurement

An S-curve was fitted to data with both 4 injections (between 25%-75% partial ignition probabilities) and 20 injections (5%-20% partial ignition probabilities). The low-end tail of the S-curve for data with 4 injections is therefore extended to much lower hot surface temperature than the experimental MHSIT data. MHSIT differs approximately by 40 K between the measured MHSIT and the S-curve fit. However, experimental data with 20 injections can measure the

ignition probability more accurately. Investigators are more concerned about MHSIT for fire safety reasons, therefore detailed experimental investigation is conducted at lower ignition probabilities. Improved experimental test method, increased number of ignition tests at each surface temperature will produce more reliable and accurate hot surface ignition temperatures. Data resulting from the method, can be used to further improve constants embedded in ignition delay expression for kernel-based empirical ignition model for better hot surface ignition temperature estimates.

3.6   Effect of Obstacles

Obstacles represent any equipment or hardware component installed along the flow path to the heated surfaces. This can be valves or flanges installed on heated ducts. These features perturb the flow and cause changes in flow patterns. MHSIT test apparatus in the current study can accommodate different obstacle location, geometry, and size. Two different types of obstacles were designed to investigate the effect of obstacles. (1) Flange (2) Claw obstacles. These obstacle designs can be seen from Figure 3-12 and Figure 3-13. Flange obstacles were designed with 3 different blockage ratios to investigate the effect of obstacle size.
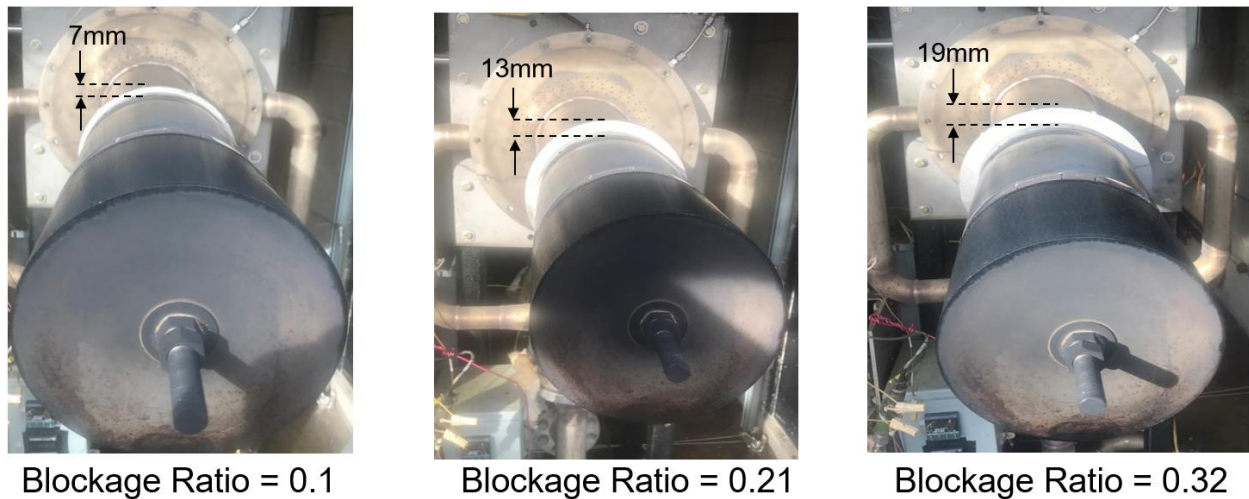
Figure 3-12 Flange obstacles with three different blockage ratios installed on the test apparatus

Figure 3-13 Claw obstacle installed at position 1 (P1) on the test apparatus
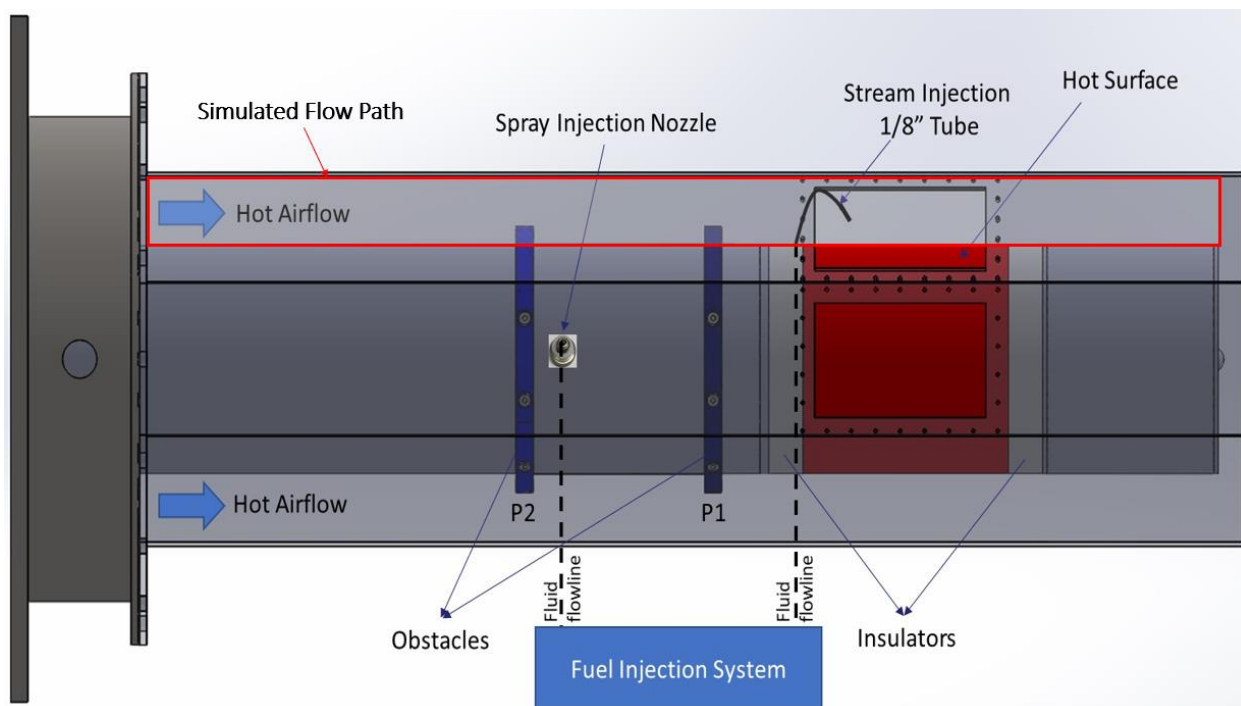
Figure 3-14 MHSIT test apparatus showing the flow obstacles, injection methods and locations, and the hot surface with respect to hot airflow

Effect of flange obstacles with 10% blockage ratio was investigated in a 2D enclosure featuring same dimensions to the MHSIT apparatus and the octagonal duct using ANSYS Fluent. Red boxed area as shown in Figure 3-14 was used as the domain in the 2D simulation. A flange obstacle with 7 mm height was simulated to see the effects of the obstacle.

Rectangular domain was designed with uniform square mesh elements. Inlet boundary condition was uniform velocity at 7 m/s and outlet was at ambient pressure. No slip boundary condition was applied on all interior walls.
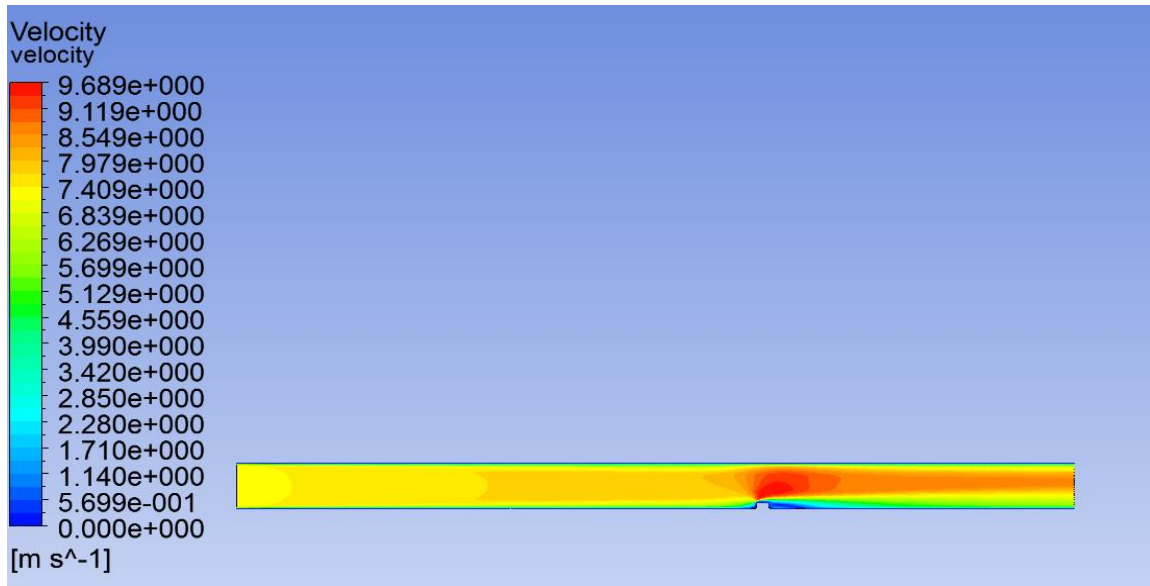
Figure 3-15 Flow path simulation over the hot surface in the presence of an obstacle

Simulation shows reduction in airflow speed near the hot surface to the right of obstacle. A series of experiments conducted to study the effect of obstacle height, location, air temperature, velocity, and test fluid leak type.
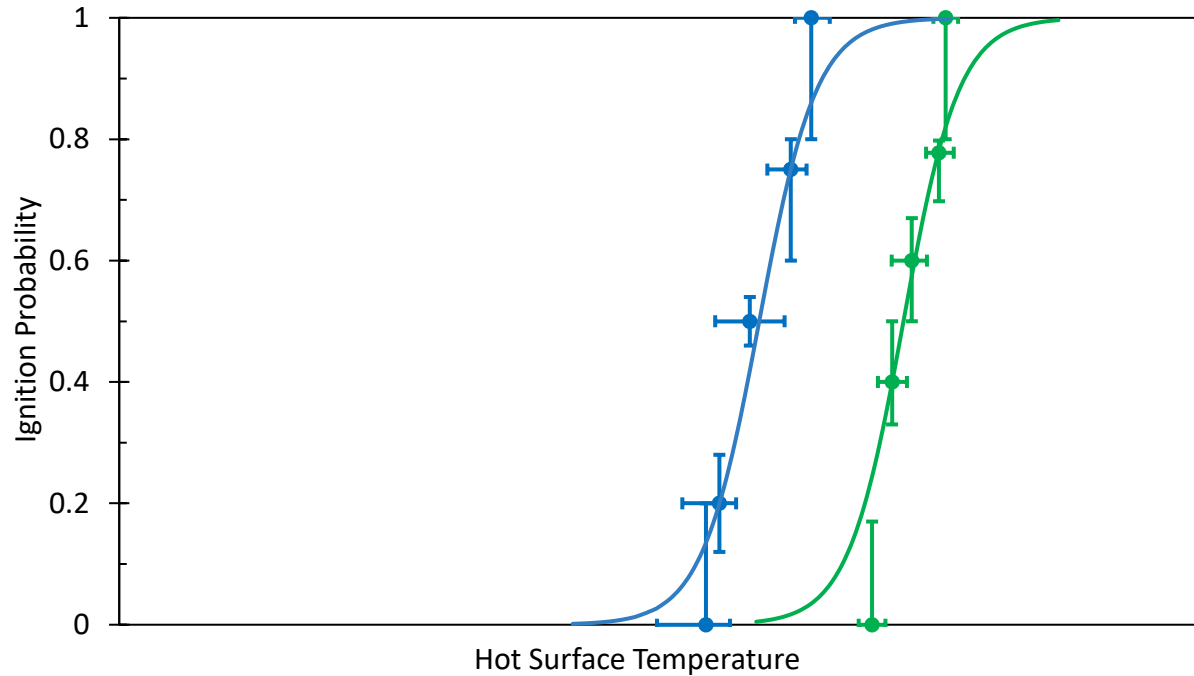
Figure 3-16 Preliminary results showing effect of flange obstacle on MHSIT

The hot surface ignition temperature with flange obstacle was reduced as conjectured from the simulation results. Figure 3-16 shows the reduction in ignition temperature due to 13mm flange obstacle installed at P1 location with stream injection method employed as the fluid leak type. The reduction in MHSIT is ~90 K between the no obstacle and obstacle flow condition. However, this ΔT cannot be generalized for all flow conditions as all MHSIT is measured for each obstacle size, location, and flow condition.
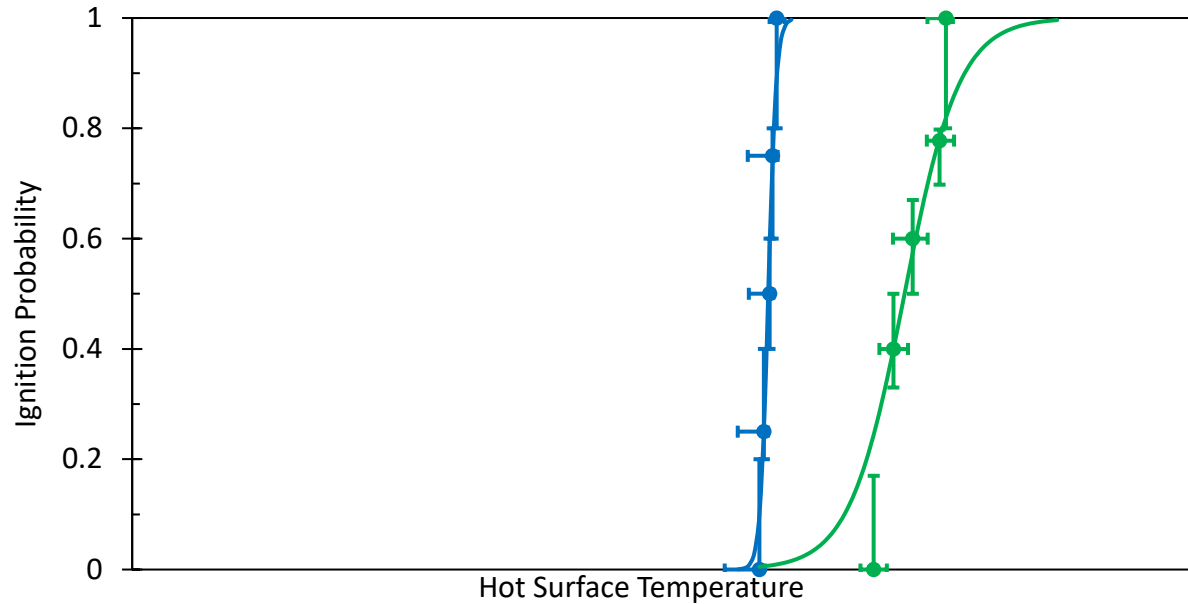
Figure 3-17 Preliminary results showing effect of claw obstacle on MHSIT

Preliminary results with claw obstacle showed steeper S-curve fit between lower and higher ignition probabilities for tests with 13 mm flange obstacle. Figure 3-17 show ignition temperatures and S-curve fits for same flow condition with and without the claw obstacle at position P1. Ignition temperature was reduced however the slope of the S-curve was steeper compared to flange obstacle and no obstacle ignition temperature fits. The presence of the pins, shown in Figure 3-13, may have advanced the turbulence and reduced the ignitable mixture formations near the hot surface. It is conjectured that the temperature range between maximum no ignition and minimum all ignition surface temperatures is reduced.

Initial experiments with obstacles and simulation results showed that obstacles form wake zones post obstacle location. This is true when high air velocities are experienced. These wake zones result in lower air velocities near obstacle and therefore may increase the residence time of the ignitable mixture on the hot surface. This allows enough energy to be received by the ignitable mixture and break the molecular bonds to release the chemical energy and initiate combustion. In other words, for such conditions MHSIT can be reduced. However, location of the obstacle and fluid leak are important design criteria. Flammable fluid leak location, obstacle size and location can influence whether the parcel is deflected and does not contact the hot surface or stay longer

over the hot surface. The latter condition is a result of the wake zones formed by the obstacle. More experiments were conducted to study the effects of each parameter in the flow condition.
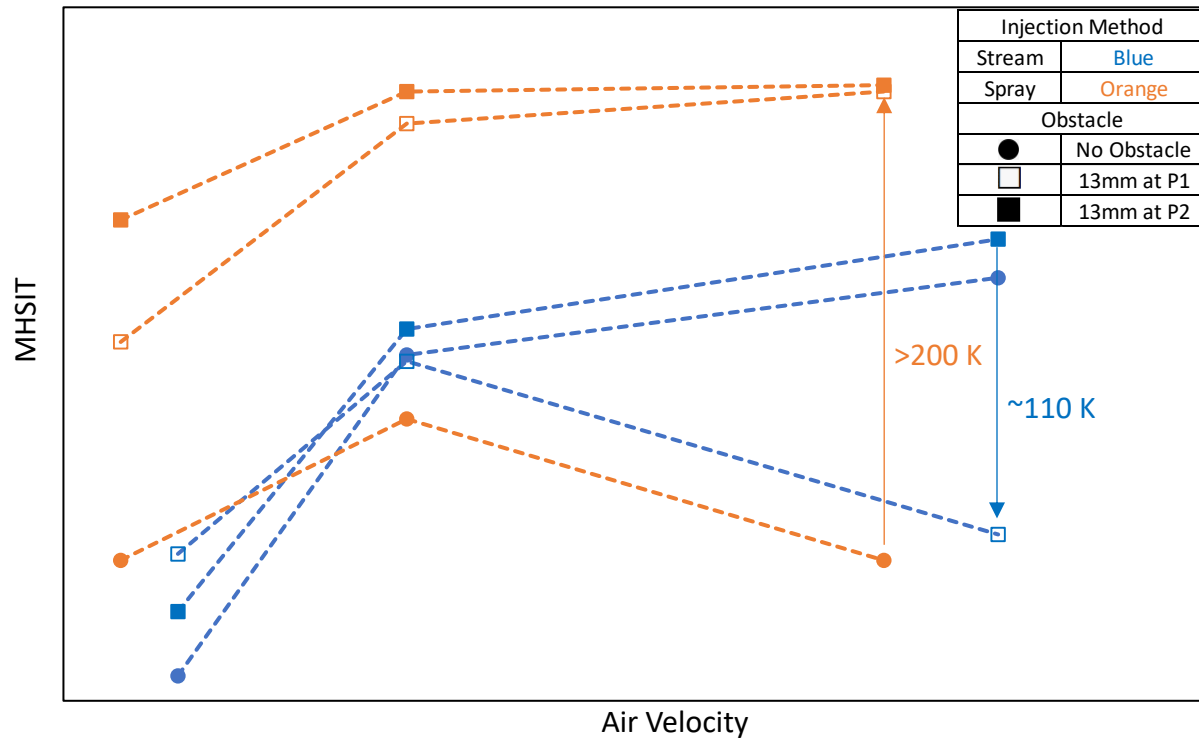
Figure 3-18 Summary of effect of 13 mm flange obstacle at 322 K air

Effects 13 mm flange obstacle as a function of the fluid leak type and the air velocity is summarized in Figure 3-18. This is an initial effort taken towards understanding the complex interaction between the obstacles, flow path, and the flammable fluid and air mixing.

The air velocity is displayed on x-axis and the corresponding MHSIT for each flow condition is shown on y-axis. Range of air velocities and hot surface ignition temperatures aren't shown due to data confidentiality. The effects of changes in air velocity and the fluid leak types are shown in Figure 3-18. It is conjectured from the current study that MHSIT increases with increasing air velocity for all microns sized parcel leaks (spray injection) and decreases for millimeter sized parcel leaks (stream injection) at higher air velocities. Data with obstacles will be further analyzed to understand the effects of various parameters and their complex interactions.

4. GLOBAL EQUIVALENCE RATIO BASED HOT SURFACE IGNITION REGIMES IN INTERNAL FLOWS

ASTM standardized methods for ignition phenomena are limited to stagnant drops falling downward (autoignition). Past studies have shown that MHSIT increases with increasing air velocity in the relatively low velocity range. However, data for higher crossflow velocities are desired. The data from this study show that the MHSIT increases significantly but non-linearly with increasing crossflow velocity. It was experimentally found, that by holding all other variables constant, that increasing air velocity caused the hot surface ignition of Jet-A to traverse several ignition regimes. A categorization of the MHSIT regimes in crossflow is presented. The results are plotted as a function of air velocity and categorized by the global equivalence ratio.

Zeldovich identified ignition regimes independent of the ignition energy source and transport mechanism from the source to the flammable mixture volume based on temperature gradients [54]. Gupta et. al. attempted classifying ignition regimes in HCCI engines using computational simulations following upon Zeldovich's classical work for autoignition [55]. More recently, Grogan et. al. [56] studied ignition using a rapid compression machine that is applicable to chemical kinetics studies of ignition in internal combustion engines. The authors emphasized the role of turbulence in causing longer times for ignitions. Clearly, ignition regime classification has been attempted and its importance is established in the basic and applied reciprocating engines literature. However, the applied reciprocating engine studies are not relevant to continuous flow machines used in propulsion applications involving flows that are parallel to the local direction of the surface. Similarly, studies with obstacles and their wakes are rare.

Ignition characteristics depend on a local energy balance with the energy provided to a combustible mixture Kernel by conduction, convection and radiation. All three modes of heat transfer in a turbulent flow have been established to be significantly different in laminar and turbulent flows. Vortical structures in boundary layer turbulence over curved surfaces and within the leading and trailing edge boundary layers and wakes of obstacles also affect flame ignition and propagation [57]. Airflow rate is therefore a significant design parameter when considering safety. The current study is motivated by a need to understand the relationship between airflow and hot surface

ignition temperature in aircraft and other propulsion applications. The next section describes the design of an experimental apparatus, operating conditions and instrumentation for maintaining this relevance. The experimental data are then summarized followed by a model for their interpretation and extension to a broader range of parameters. The success and limitations of this model are discussed prior to drawing conclusion regarding application and extension of the present work towards an impact on fire safety of practical propulsion vehicles.

4.1   Hot Surface Ignition

An ignition event will occur if the flammable liquid air mixture receives enough energy to break the chemical bonds and release the chemical energy within the liquid [2], [21] and [58]. An example of such an event along with high speed photography is provided below.

Frame (a) in Figure 3, shows the flow configuration and the hot surface geometry viewed by high speed camera before injection. Frame (b) in Figure 3 shows the change in color upon the flammable liquid contacting the hot surface as a dark mark. The drop vaporizes and mixes with the air and travels to form the initial plume which can be seen in the same frame. Kernel formation is visible to the naked eye on frame (c) and more kernels continue to form and agglomerate to form a sustainable flame as can be seen in frame (d).

Flames propagate towards the point of ignition. It is shown that ignition takes a longer time with increasing air velocity as more of the ignitable mixture is advected away from the hot surface. Increased air velocity limits the flammable vapors' contact time with the hot surface and reduces exposure time, which increases the temperature required for ignition within the allotted time window provided by the flow conditions [11], [21].

High-speed videos showed that ignition always initiated by small kernels at the hot surface. If flow conditions are right for ignition and an ignitable mixture is present in the surrounding air, these kernels agglomerate and become a sustainable flame. If the airflow dominates over the heat transfer between the hot surface and the ignitable mixture, surrounding kernels won't form into a sustainable flame.
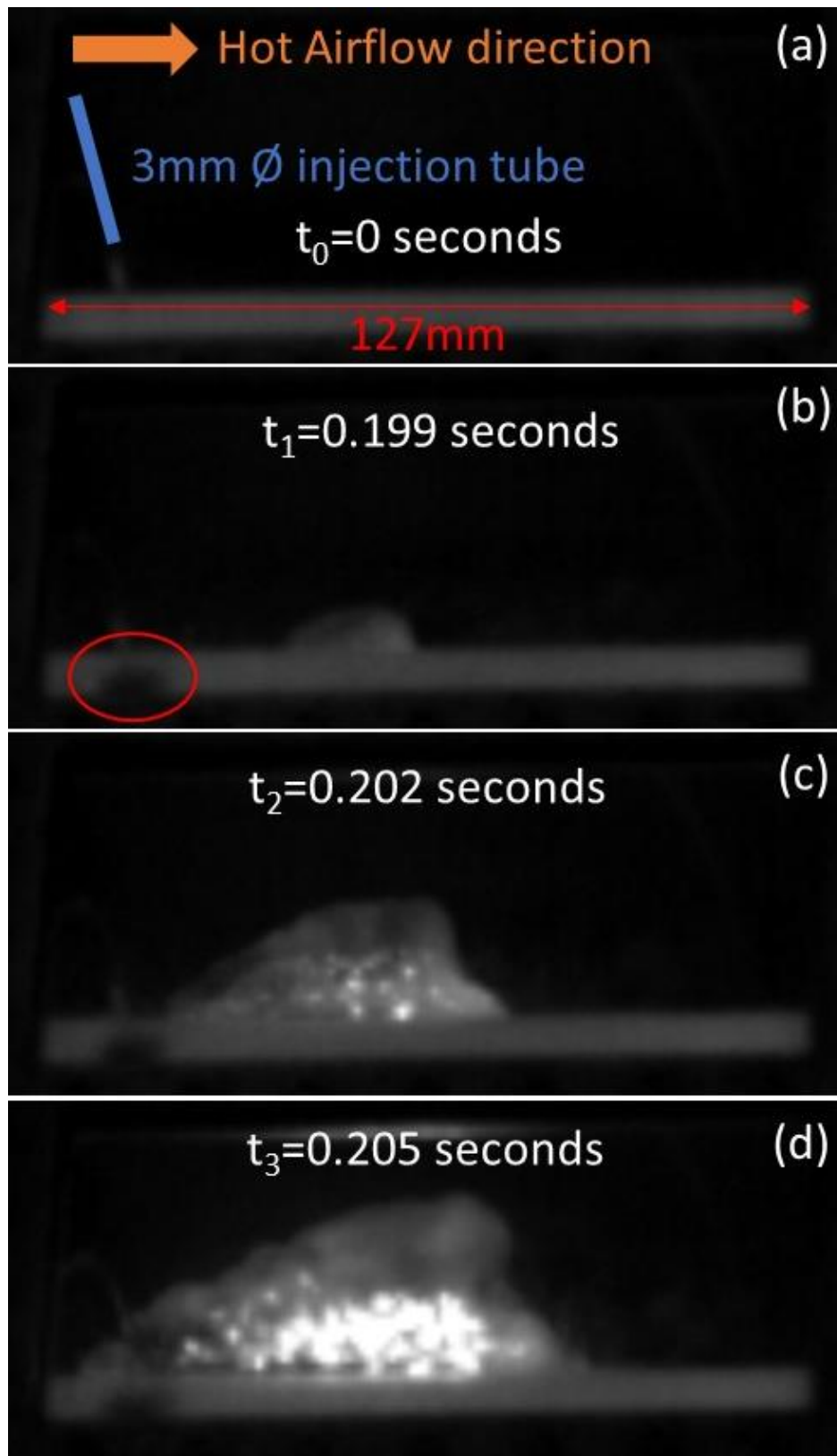
Figure 4-1 Sample high-speed video images of ignition process

Non-sustainable flames will be advected out by the airflow before they can propagate into a larger flame front. This will happen at higher airflow rates, due to the reduced contact time of the ignitable mixture at the hot surface. If no ignition at all is observed it is called non-ignitable, in which case a kernel will not form. Either vaporized flammable liquid or the liquid itself will be advected over the hot surface without ignition.

Hot surface ignition temperatures depend on multiple parameters associated with the fuel, the air, and the geometry of the passage. The MHSIT is not a property of the flammable substance like the autoignition temperature [15]. A fuel/air mixture ignites at the hot surface, when the mixture's equivalence ratio is between the flammability limit. The evaporation rate of the liquid drop is important for controlling heat transfer characteristics between the drop and the hot surface. Liquid drops breakup upon contacting the hot surface. Flammable liquid drops break into smaller drops as the contacting surface temperature increases [59].
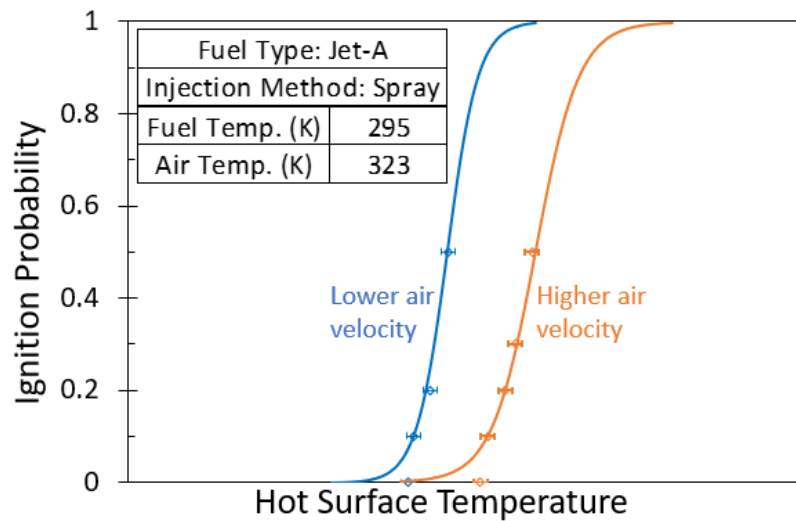
Figure 4-2 Ignition probability vs. hot surface temperature graph for jet fuel

Figure 4-2 shows ignition probability plotted as a function of the hot surface temperature for jet fuel. The symbols indicate the experimental data whereas the solid curves represent an inverse exponential function (S-curve) fitted to the data. MHSIT clearly increases with increasing air velocity as shown in Figure 4-2 and as observed over the entire experimental campaign described in this section.

4.2   Ignition Regime Classifications Based on Airflow Rate

Heat transfer between the ignitable fuel/air mixture and the hot surface can be calculated using the convective heat transfer coefficient. Reynolds (Re) number controls the Nusselt number of the heat transfer between the hot surface and the mixture. Therefore, Re number is relevant in the regime definition. Re number is calculated using the (1) mean velocity in the annulus (flow passage), (2) the hydraulic diameter of the flow passage, and (3) the kinematic viscosity of the air at the film temperature.

Air velocity was varied for a constant surface and air temperature, while maintaining a constant flammable liquid flow rate. Increasing the air velocity effectively changed the global equivalence ratio. Results from 560 injections are shown in Figure 4-3. Four regimes are proposed based on the results of these experiments. The ignition event is a balance between the conductive heat transfer between the hot surface to the ignitable mixture, convective heat loss to the surrounding air, and turbulent mixing of the ignitable vapors [58].

4.2.1   Ignition Regimes

Regime 1 – Conduction Regime: Laminar to turbulence transition occurs between Re = 2100 to 4000 depending on the flow conditions [60]. The bulk velocity in the flow passage featuring a concave octagonal annular outer surface and a convex cylindrical inner surface. The resulting bulk flow Reynolds number was used for evaluation of turbulence properties in the present ignition regime classifications. A total of 80 injections were examined. Out of these, 60 injections ignited. The fuel flow rate in these experiments leads to relatively rich mixtures and results in rapid and high (75%) probability ignition. The time for ignitions for this set of tests is shorter than all the other tests for reasons that are discussed in conjunction with previously developed ignition model [58].
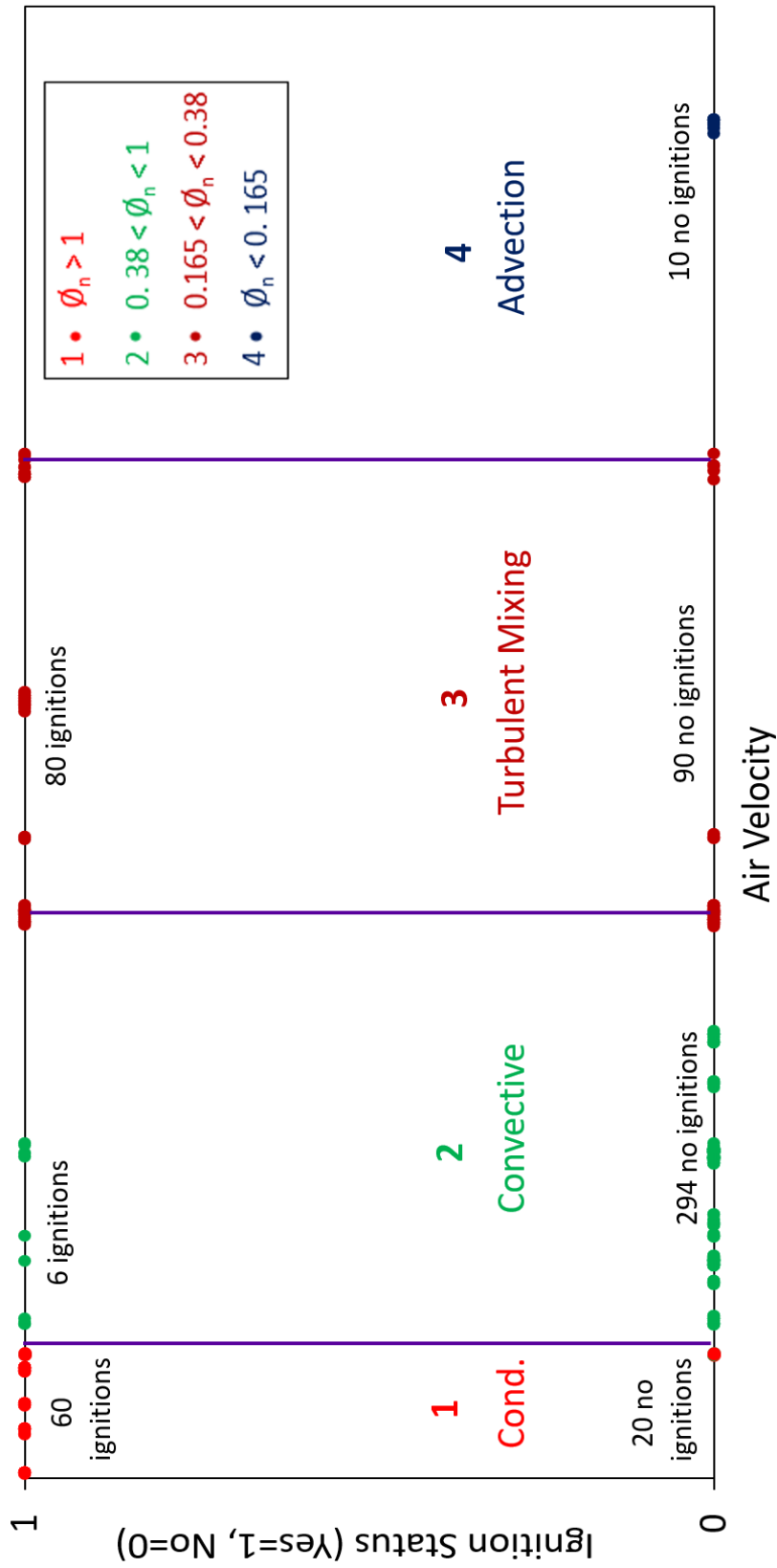
Figure 4-3 Ignition regimes based on global equivalence ratio.

Regime 2 – Convective Cooling Regime: A total of 300 injections led to an analysis of this regime. Only 6 set of conditions led to ignitions for the present experiments within this regime. The airflow transitions from laminar to turbulent based on the bulk Reynolds number. Leaning of the fuel air mixture occurs prior to the advective heating and leads. These effects are conjectured to lead to the lower probabilities of ignition and are captured by the present bulk model. Additional injections were performed to confirm the low probability of ignition in this regime. The overall ignition probability of 2% with 6 ignitions out of 300 leaks was found to be a repeatable characteristic of the convective cooling regime designated as regime 2 in Figure 4-3.

Regime 3 – Turbulent Mixing Regime: Turbulent mixing along with increased airflow rates enhance the probability of occurrence of flammable Kernels near the hot surface and it is conjectured that this caused a larger number of ignitions during the experiments in this regime. Reynolds numbers are above 18000 for the flow conditions categorized in this regime and 80 out of the 170 injections ignited, resulting either in sustainable or non-sustainable flames. These ignitions occurred despite the increased airflow rates and lower global equivalence ratios. The ignition probability is ~47% in this regime.

In the instances when ignition occurs in Regime 3, it is conjectured that the heat transfer from the hot surface to the ignitable mixture was adequate and along with the air speed resulting in a sustained flame front. However, it is also conjectured that stronger vortices with increasing air velocity in turbulent flow resulted in non-sustained flames, mainly due to the larger air speeds. Increased air velocity intensified the turbulence, hence cooler air entrained from the surrounding cold mixtures and reduced the local flammability [57].

Time for ignitions observed in Regime 3 were longer compared to those in Regime 1. This is due to the increased convective cooling. The turbulence enhanced the mixing and formed enough ignitable mixtures around the hot surface to cause chain reactions to form the flame. The ignition flame front propagates primarily due to sequential reactions of the neighboring ignitable mixtures and their varying reactivities.

Regime 4 – Advection Regime: Injections performed at air velocities beyond Regime 3 did not result in any ignitions at all. The bulk Reynolds numbers are all above 33000 for this regime. Ignitable mixtures were either advected out with the strong airflow or extinguished by the convective cooling at the hot surface.

Figure 4-4 shows high-speed images every 34 milliseconds for a selected air velocity from the conduction, turbulent mixing and non-sustainable flames regimes. Images from regime 2: convective cooling and advection regimes are not of interest because very few to none ignitions occurred. The hot surface is installed on the cylindrical body. The cylindrical body is in the center of each image as seen on frame (a.1). The ignition kernels always form around the hot surface and propagate where there is ignitable fuel/air mixture.
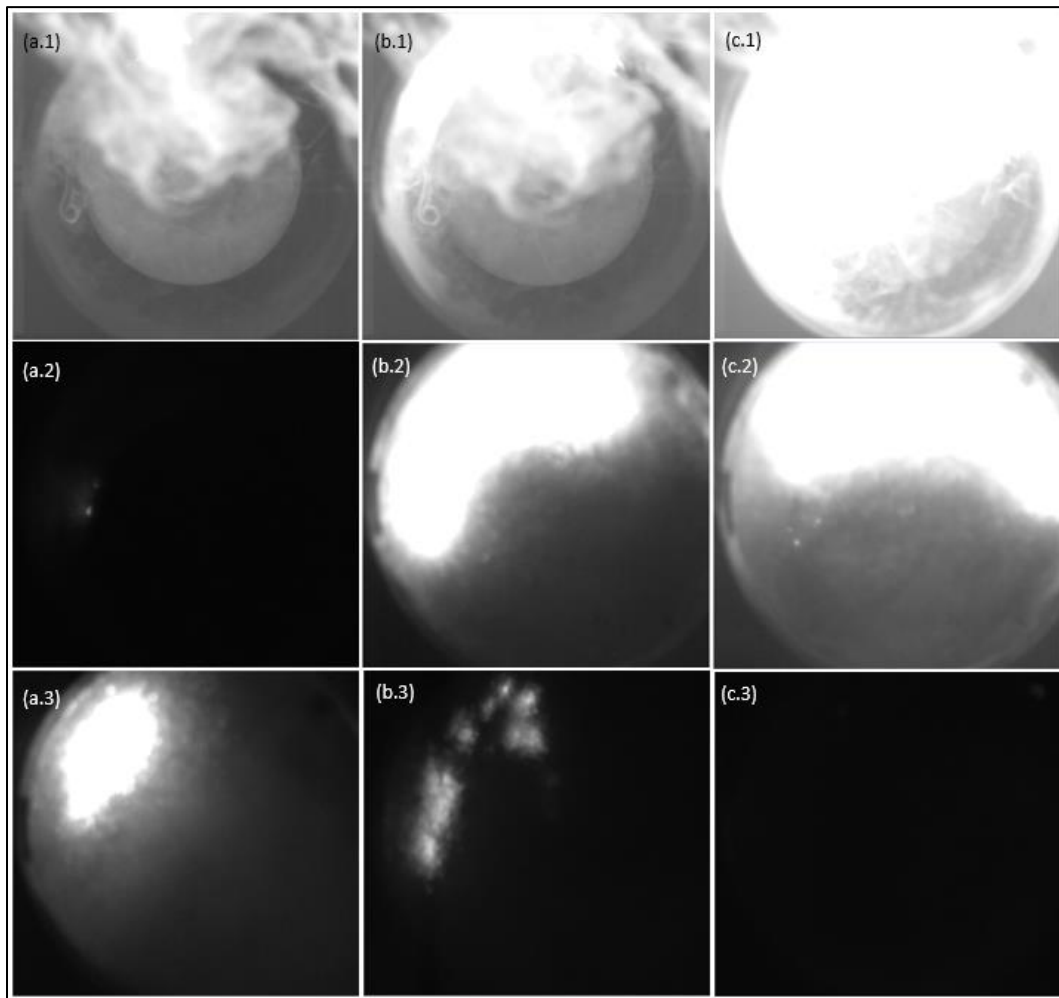
Figure 4-4 High-speed image description. (a.1) – (c.1) conduction regime. (a.2) – (c.2) sustainable flame. (a.3) – (c.3) non-sustainable flames.

Vaporization of the flammable liquid by the hot surface is visible and may block the view of the initial kernel formation in the conduction regime. Vaporization and smoke generation can be seen between frames (a.1) – (c.1). In ~60 milliseconds, the flames from the rich ignition encompass the entire view from the mirror and the image from the high-speed camera looks completely white. This rich ignition and bright flames lasted ~230 milliseconds. This is when flammable liquid injection was stopped, and the system purge was engaged to halt flame propagation. Another characteristic of this type of ignition is that it is sustained with the availability of the ignitable mixtures from the leaks; so long as the flammable liquid is continually leaking the flames sustain themselves.

Convective cooling regime involves low ignition probabilities and is not discussed in Figure 4-4. Overall ignition probability for this regime is 2%. Only 6 ignitions were observed out of 300 injections. The images of a sustained flame from Regime 3 are shown between frames (a.2) – (c.2) on Figure 4-4. The small kernel formation is barely seen on frame (a.2) on the left of the hot surface. Also noted is the lack of visible vaporization of the fuel in frames (a.2 and b.2). This may be an indication of a leaner fuel/air mixture because of the higher airflow rates. Also noted is the propagation of the flame around the surface as mixtures from other portions of the hot surface are ignited by the first ignition kernel. These types of events will be studied further with the help of significant Diesel engines literature related to knocking by premature ignition at the wrong crank angles.

The frames (a.3) – (c.3) of Figure 4-4 illustrate non-sustainable flames from Regime 3. The images show flames that extinguish most likely by convective cooling and/or turbulent mixing. Apparently, sustainable flame initiated from a kernel seen in frame (a.3) became progressively weaker as seen in frame (b.3) and finally vanished in frame (c.3) even though the fuel is continuously leaking into the duct. Flame extinction and non-sustainable flames occur multiple times during the 10-second injection period. (a.3) – (c.3) show an example of non-sustainable flames lasting for ~85 milliseconds. This sequence was somewhat randomly followed by 4 additional non-sustainable flames, each lasting for 29, 83, 145 and 66 milliseconds respectively.

.

5. CONCLUSIONS AND RECOMMENDATIONS

A generic experimental apparatus was designed to test various leakage scenarios relevant to aircraft engine conditions. The three decades old MHSIT database is expanded by increasing airflow rates to capture high pressure ratios seen in the modern engines as well as newer aviation liquids. An empirical model was developed based on the experimental study and delivered to the sponsors of this research as a desktop design tool. Effects of air, flammable fluid, hot surface temperatures, and obstacles were studied.

5.1 Summary of Scientific Contributions

A generic experimental apparatus was built and used to investigate minimum hot surface ignition temperatures over a range of air flow, surface temperature and fluid leak conditions representative of a gas turbine engine environment. A robust experimental technique for evaluating MHSIT was developed and refined over the course of several thousand ignition experiments. Key aspects of the improved experimental technique include: use of a high-speed camera to observe ignition events; tight control of hot surface temperature steadiness and uniformity; small increments of surface temperature to identify small changes in ignition probability, and a sufficient number of injections at each temperature to capture an accurate hot surface ignition probability. As a result, the uncertainty of the MHSIT results claimed by the improved technique is ±5 K, compared to +14 K and -42 K from a referee AFRL study.

Hot surface ignition temperatures are estimated using the empirical model described for a range of air velocities based on the experimental data both from the current study and the available ignition data from the literature. Estimations from the empirical model are within ±5% of the data. Estimations are also capturing the monotonic trends seen in the experiments. Hot surface ignition temperature increases with increasing air velocity. The empirical model can be improved with more experiments covering a larger range of flow conditions. The heat transfer between heat lost to the surroundings from the hot surface and the energy released due to chemical reaction from the ignition can be used to estimate the MHSIT as outlined in this study to avoid costly experiments. Ignition regimes in internal flows are described and explained by three competing factors to affect the hot surface ignition events in continuous flow propulsion devices like gas turbines. Based on

the local flow conditions: (1) conduction heat transfer between the ignitable mixture and the hot surface at low airflow rates; (2) convective heat transfer between the mixture and the airflow, and (3) turbulent mixing of the ignitable vapors and the surrounding air. Four regimes are categorized based on these three competing factors. A total of 560 injections were performed at constant air and surface temperature while maintaining a fixed Jet-A flowrate. Definitions of sustainable and non-sustainable flames as well as non-ignitable leaks are provided. High-speed video images are shown to verify the various ignition regimes based on changes in the airflow rates, and consequently the global equivalence ratio. Ignition regime categorization identifies some false positive MHSIT temperature estimates leading to the wrong increased ignition probability estimates in regime 3. The contributions are expected to allow engineers to improve upon the safety of the already fire resilient aviation systems even further.

5.2   Recommendations for Future Work

The experimental apparatus and the hot surface ignition knowledge accumulated through the project can be utilized to accomplish the following tasks in the future.

- Utilize ANN-based modeling to estimate MHSIT and the relevant ignition probability. More experiments will strengthen the ANN-based models and determine complex interactions between different design parameters, which otherwise would be more difficult
- Study the effect of pressure on MHSIT at relevant aircraft engine conditions (1 – 5 bars)
- Study the effect of hydraulic oil temperature on MHSIT
- Improve the empirical ignition model to estimate low air velocities and natural convective dominant regimes more accurately, based on the recent findings from ignition regime classification in internal flows for hot surface ignition
- Measure experimentally and model numerically and/or computationally, the flow field above the hot surface (thermal and velocity fields)
- Experiments with gaseous mixture (hydrogen) to measure hot surface ignition temperature of flammable gaseous

5.3   Acknowledgements

APPENDIX: MHSIT APPARATUS DRAWINGS
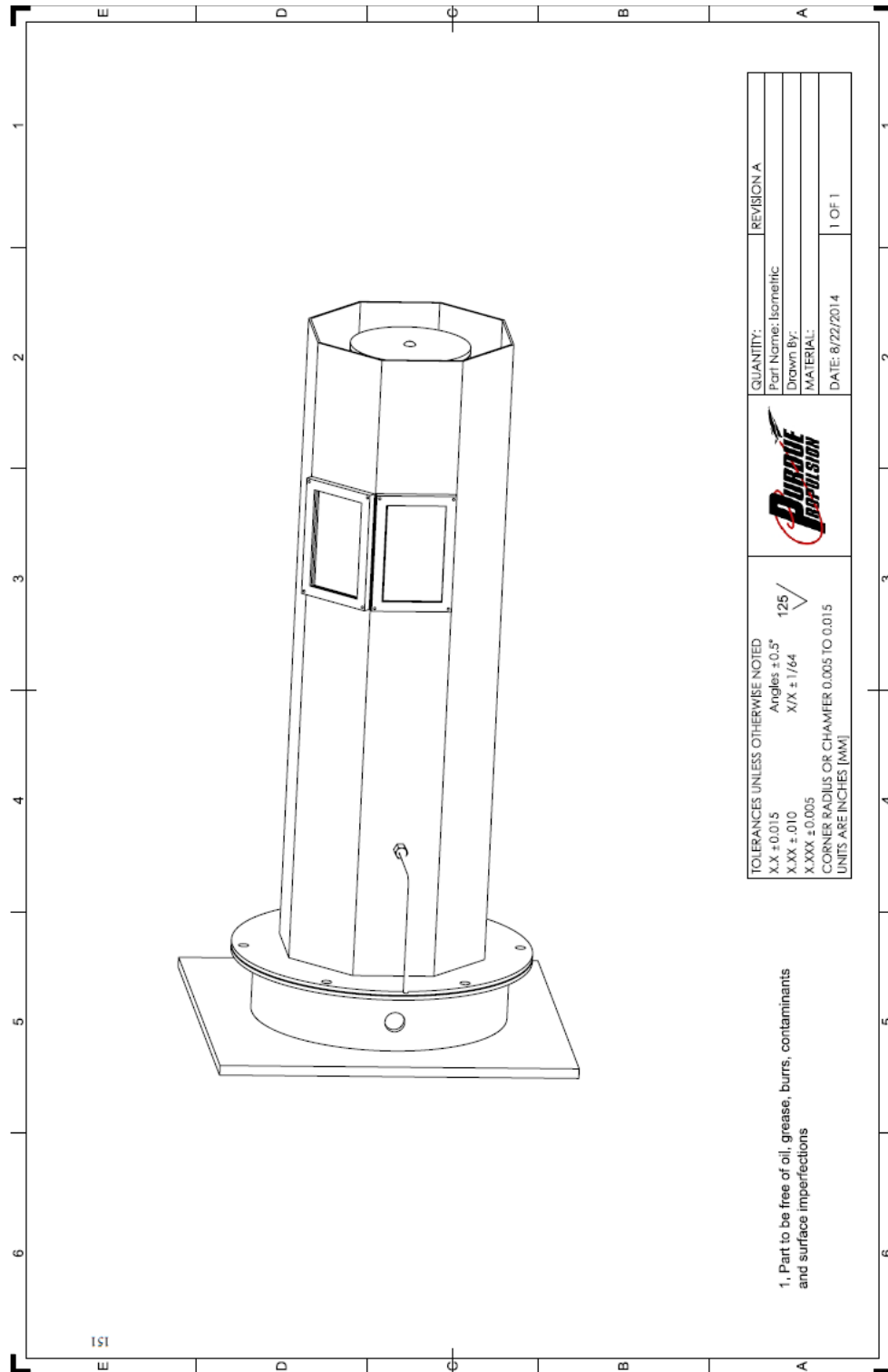
Figure A.1 Test article drawing-1
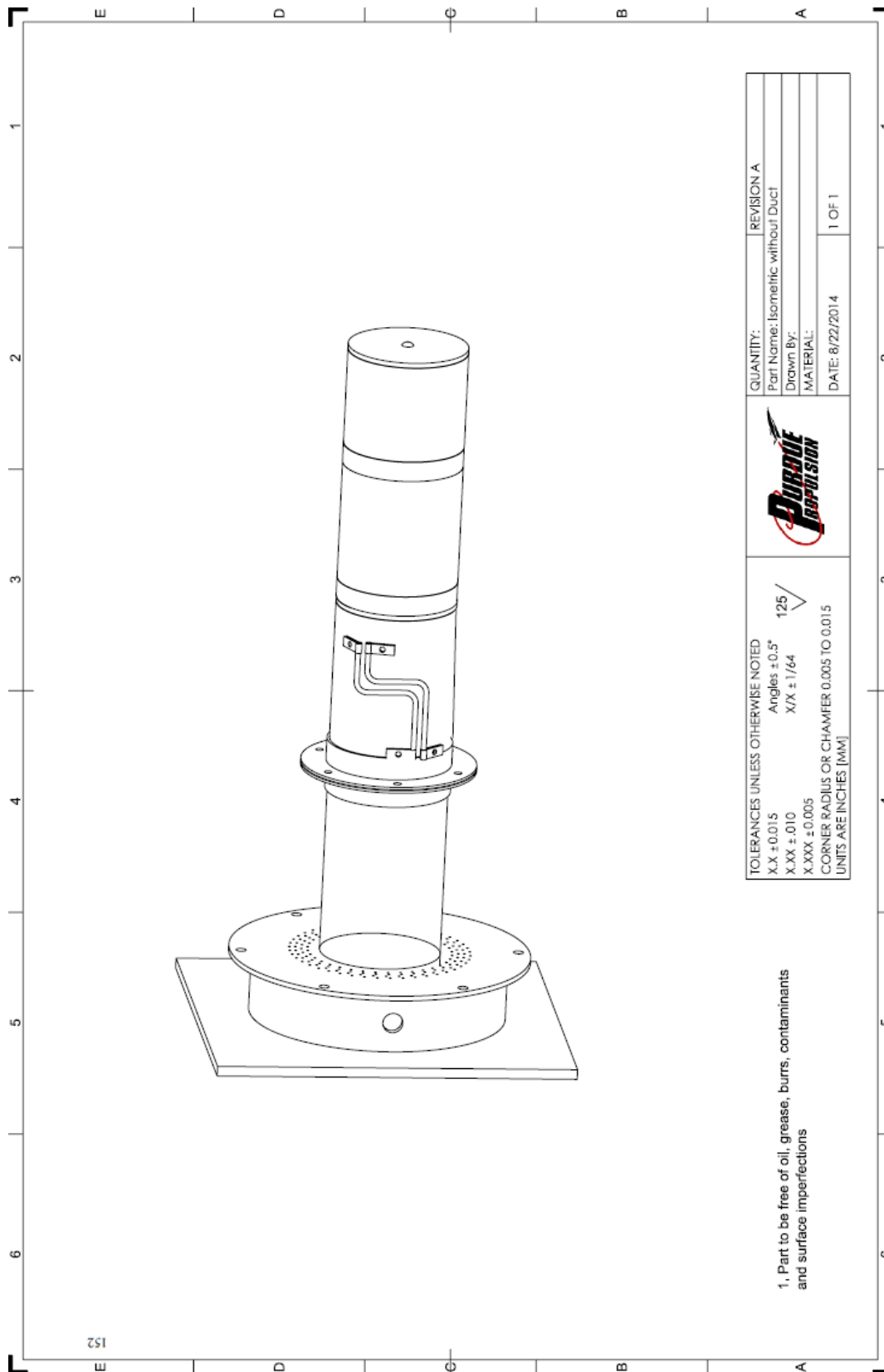
Figure A.2 Test article drawing-2

PC NO	PART NAME	QTY
1	BASE	1
2	PLENUM VESSEL	1
3	ORIFICE PLATE	1
4	CENTER CYLINDER	1
5	CANTILEVER BASE PLATE	1
6	CERAMIC END	2
7	HOT CENTERBODY	1
8	END PIECE ASSEMBLY	1
10	CERAMIC SLEEVE	1
11	CANTILEVERED SUPPORT	1
12	BOLT	1
14	WINDOW FLANGE	2
15	WINDOW	2

TOLERANCES UNLESS OTHERWISE NOTED
X.X ±0.015   Angles ±0.5°
X.XX ± .010   X/X ± 1/64
X.XXX ±0.005
CORNER RADIUS OR CHAMFER 0.005 TO 0.015
UNITS ARE INCHES [MM]

125

QUANTITY: REVISION A
Part Name: Exploded_View_Without Duct
Drawn By:
MATERIAL:
DATE: 8/22/2014   1 OF 1

Figure A.3 Test article drawing-3

95

PC NO	PART NAME	QTY
1	BASE	1
2	PLENUM VESSEL	1
3	ORIFICE PLATE	1
4	CENTER CYLINDER	1
5	CANTELIEVER BASE PLATE	1
6	CERAMIC END	2
7	HOT CENTERBODY	1
8	END PIECE	1
9	FLANGE FEATURE	2

TOLERANCES UNLESS OTHERWISE NOTED
X.X ±0.015   Angles ±0.5°
X.XX ±.010   X/X ±1/64
X.XXX ±0.005
CORNER RADIUS OR CHAMFER 0.005 TO 0.015
UNITS ARE INCHES [MM]

125

PURDUE PROPULSION
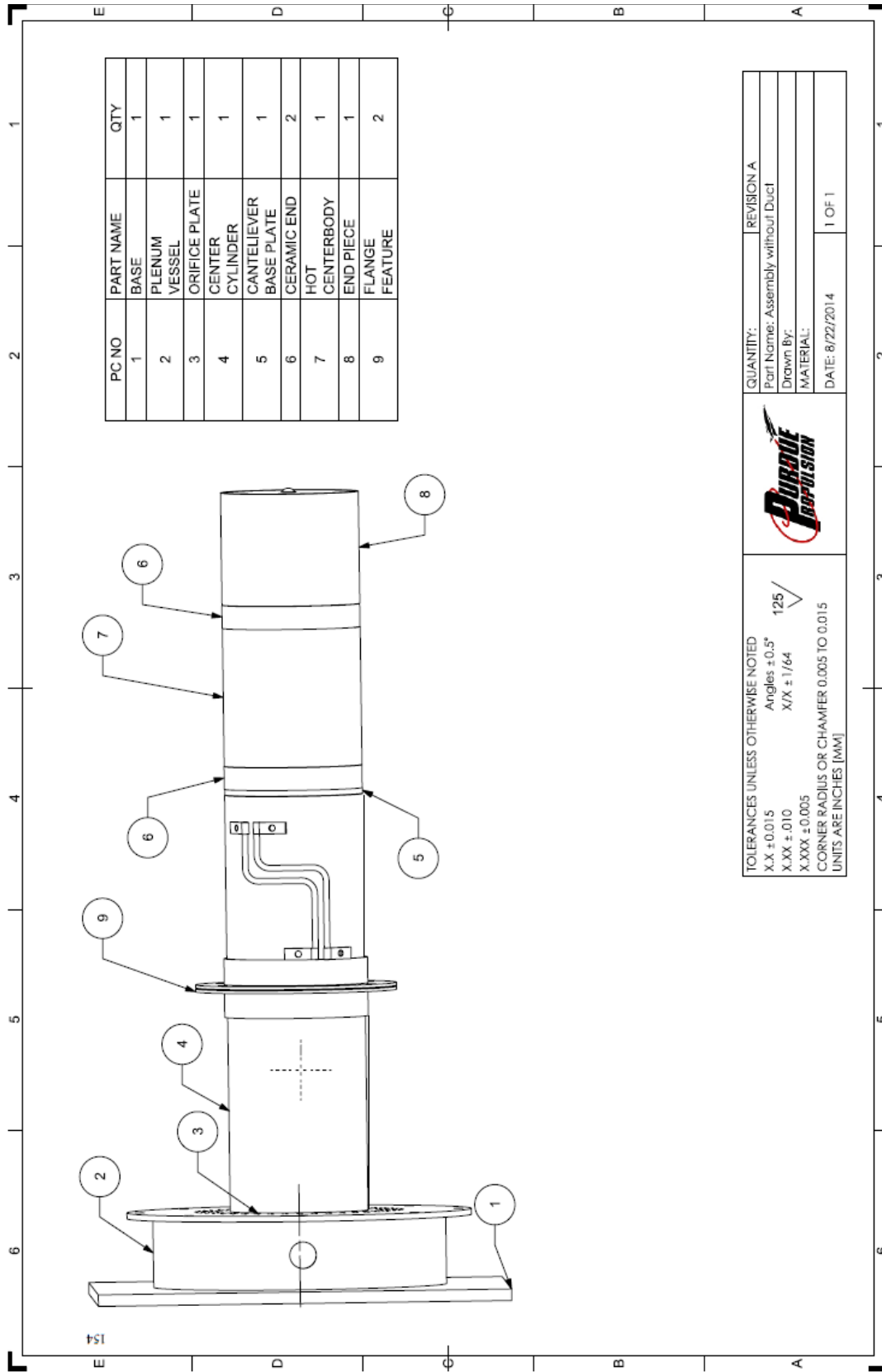
Figure A.4 Test article drawing-4

PC NO	PART NAME	QTY
10	CERAMIC SLEEVE	1
11	CANTILEVERED SUPPORT	1
12	BOLT	1

TOLERANCES UNLESS OTHERWISE NOTED
X.X ±0.015   Angles ±0.5°
X.XX ±.010   X/X ±1/64
X.XXX ±0.005
CORNER RADIUS OR CHAMFER 0.005 TO 0.015
UNITS ARE INCHES [MM]

125

QUANTITY: REVISION A
Part Name: Assembly without Hot Surface
Drawn By:
MATERIAL:
DATE: 8/22/2014   1 OF 1

Figure A.5 Test article drawing-5

PC NO	PART NAME	QTY
13	OCTAGONAL DUCT	1
14	WINDOW FLANGE	2
15	WINDOW	2

TOLERANCES UNLESS OTHERWISE NOTED
X.X ±0.015
X.XX ±.010
X.XXX ±0.005
CORNER RADIUS OR CHAMFER 0.005 TO 0.015
UNITS ARE INCHES [MM]

Angles ±0.5°
X/X ±1/64

125

QUANTITY:
Part Name: Assembly with Duct
Drawn By:
MATERIAL:
DATE: 8/22/2014

REVISION A

1 OF 1

156

Figure A.6 Test article drawing-6

98

Figure A.7 Test article drawing-7

Figure A.8 Test article drawing-8

Figure A.9 Test article drawing-9

Figure A.10 Test article drawing-10

Figure A.11 Test article drawing-11

Figure A.12 Test article drawing-12

Figure A.13 Test article drawing-13

Figure A.14 Test article drawing-14

Note: Cantilever Base Plate is welded to the free end of the center cylinder.

TOLERANCES UNLESS OTHERWISE NOTED
X.X ±0.015
X.XX ±.010
X.XXX ±0.005
Angles ±0.5°
X/X ±1/64
125
CORNER RADIUS OR CHAMFER 0.005 TO 0.015
UNITS ARE INCHES [MM]

QUANTITY:
Part Name: Phase 3
Drawn By:
MATERIAL:
DATE: 8/22/2014
REVISION A
1 OF 1

165

Figure A.15 Test article drawing-15

Ø3.068

Ø3.50

10.0

TOLERANCES UNLESS OTHERWISE NOTED
X.X ±0.015   Angles ±0.5°
X.XX ±.010   X/X ±1/64   125
X.XXX ±0.005
CORNER RADIUS OR CHAMFER 0.005 TO 0.015
UNITS ARE INCHES [MM]

QUANTITY: REVISION A
Part Name: Cantilever_Support
Drawn By:
MATERIAL: Stainless Steel 304
DATE: 8/22/2014   1 OF 1

PURDUE PROPULSION

1, Part to be free of oil, grease, burrs, contaminants
and surface imperfections

991

Figure A.16 Test article drawing-16

108

Note: Cantilevred Support is welded to the Cantilevere Base Plate

TOLERANCES UNLESS OTHERWISE NOTED
X.X ± 0.015
X.XX ± .010
X.XXX ± 0.005
CORNER RADIUS OR CHAMFER 0.005 TO 0.015
UNITS ARE INCHES [MM]

Angles ±0.5°
X/X ± 1/64

125

QUANTITY:
Part Name: Phase 4
Drawn By:
MATERIAL:
DATE: 8/22/2014

REVISION A

1 OF 1

167

Figure A.17 Test article drawing-17

109

Ø3.50

Ø4.00

8.0

TOLERANCES UNLESS OTHERWISE NOTED
X.X ±0.015   Angles ±0.5°
X.XX ±.010   X/X ± 1/64   125
X.XXX ±0.005
CORNER RADIUS OR CHAMFER 0.005 TO 0.015
UNITS ARE INCHES [MM]

QUANTITY: REVISION A
Part Name: Ceramic_Sleeve
Drawn By:
MATERIAL: Alumina Silicate, Grade "A" Lava
DATE: 8/22/2014   1 OF 1

1, Part to be free of oil, grease, burrs, contaminants
and surface imperfections

891

Figure A.18 Test article drawing-18
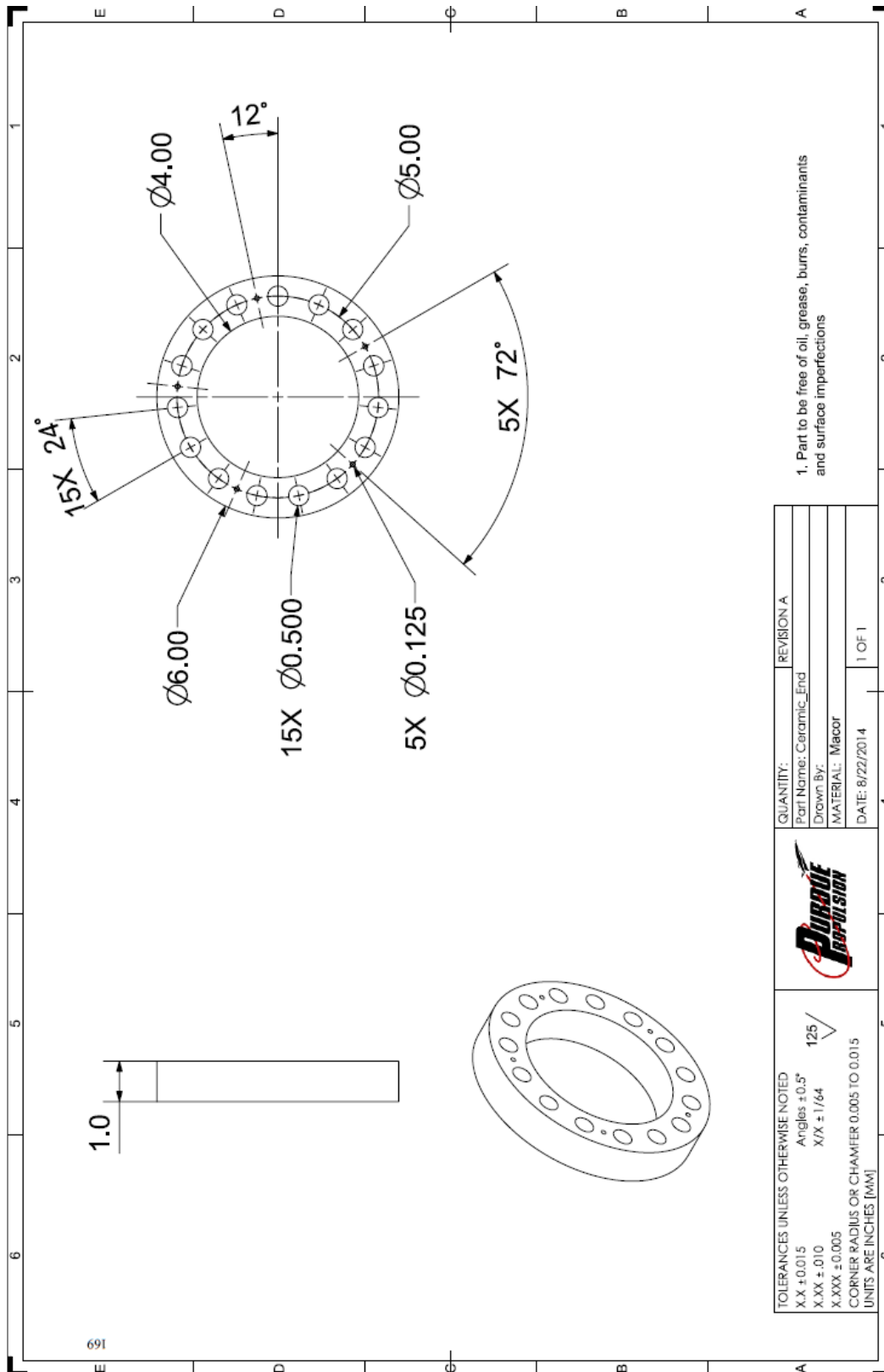
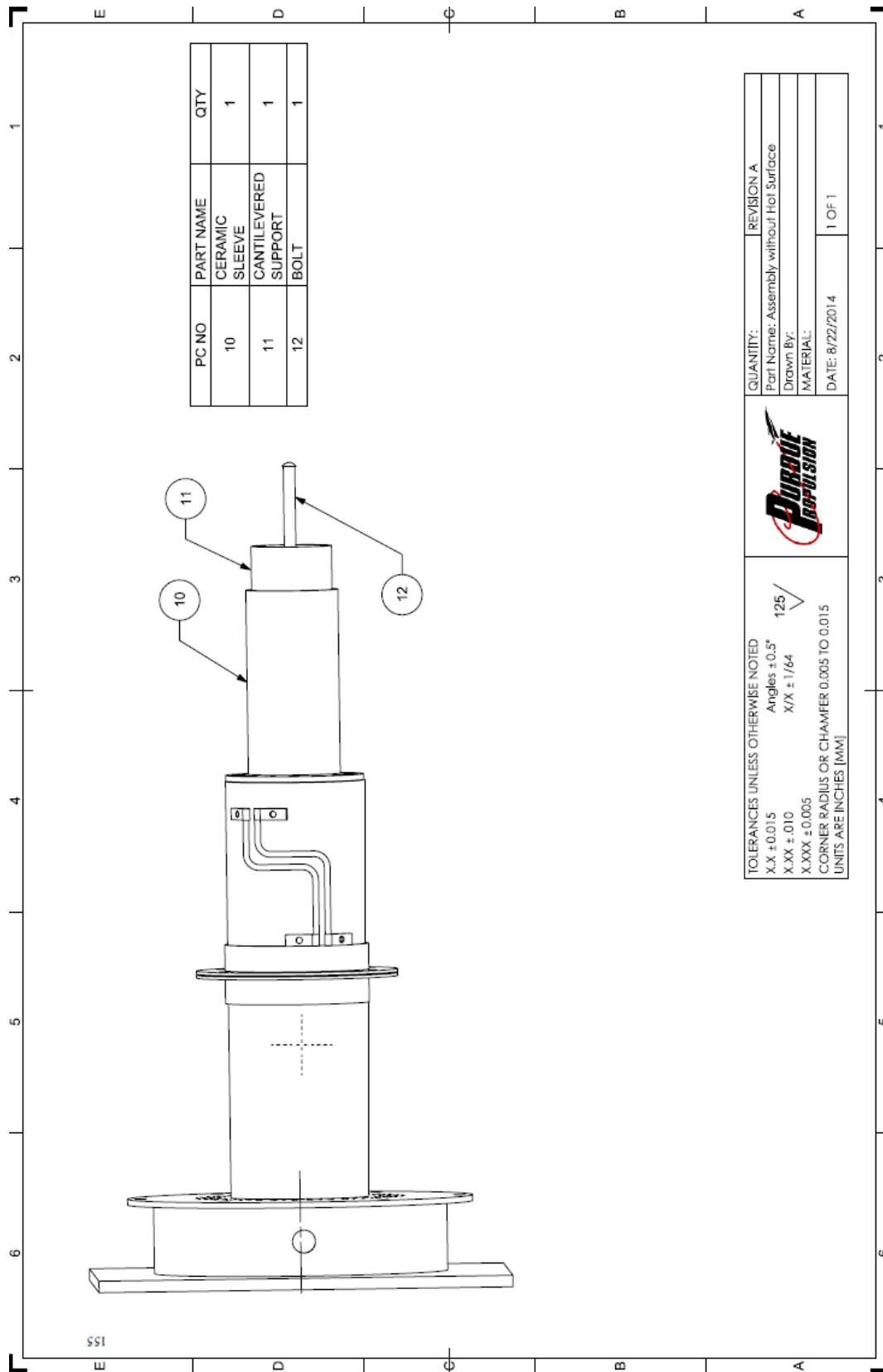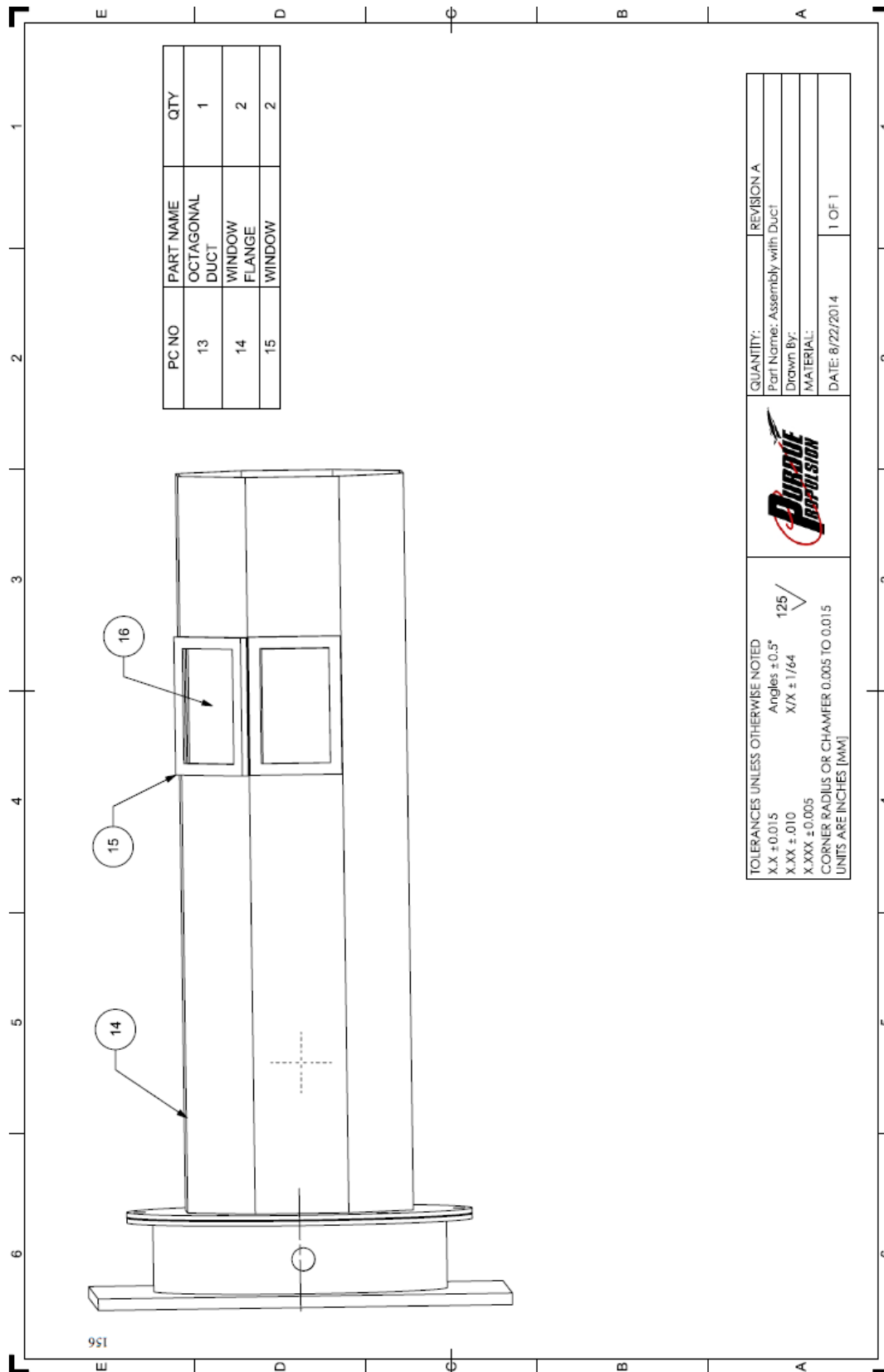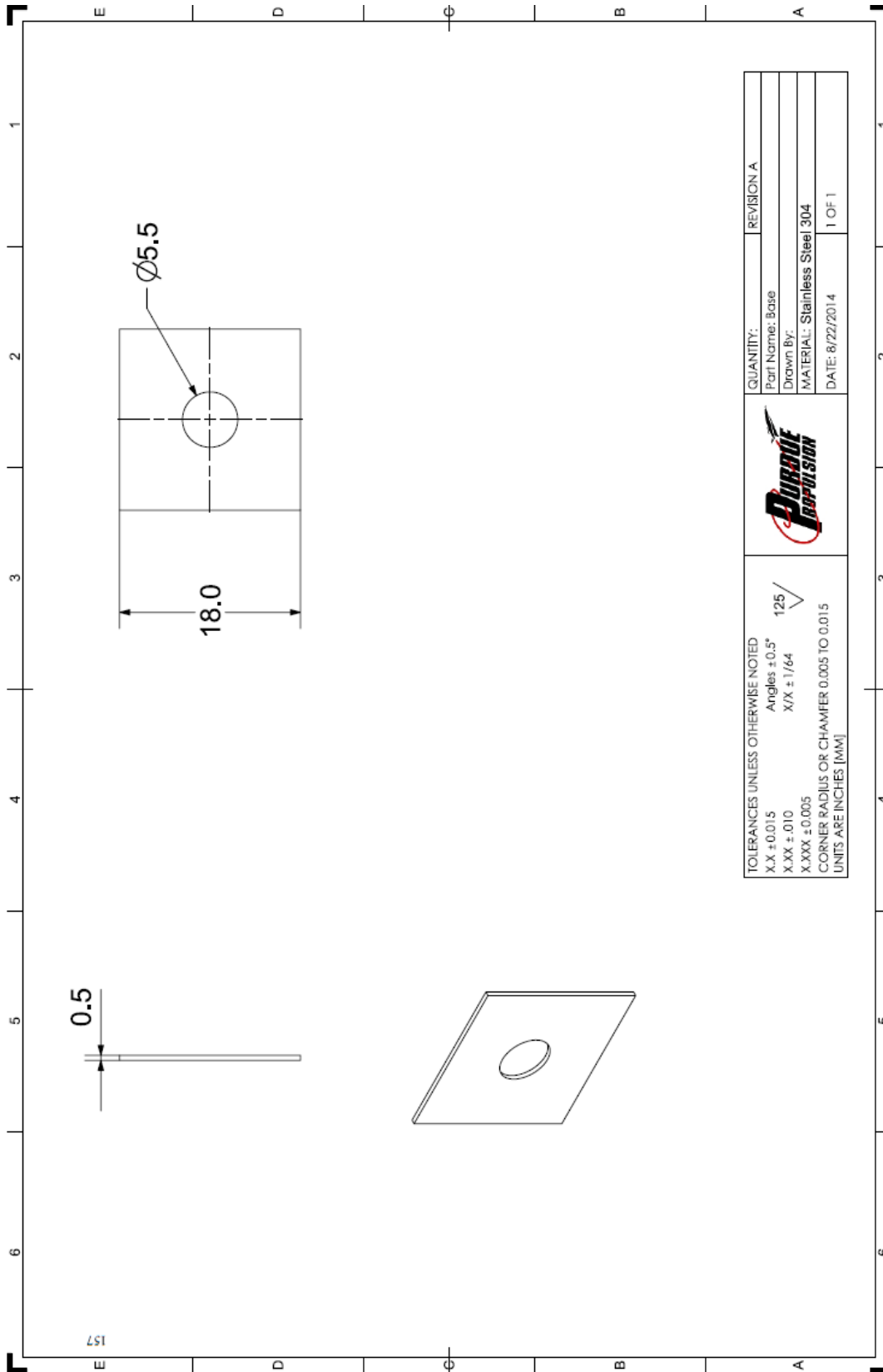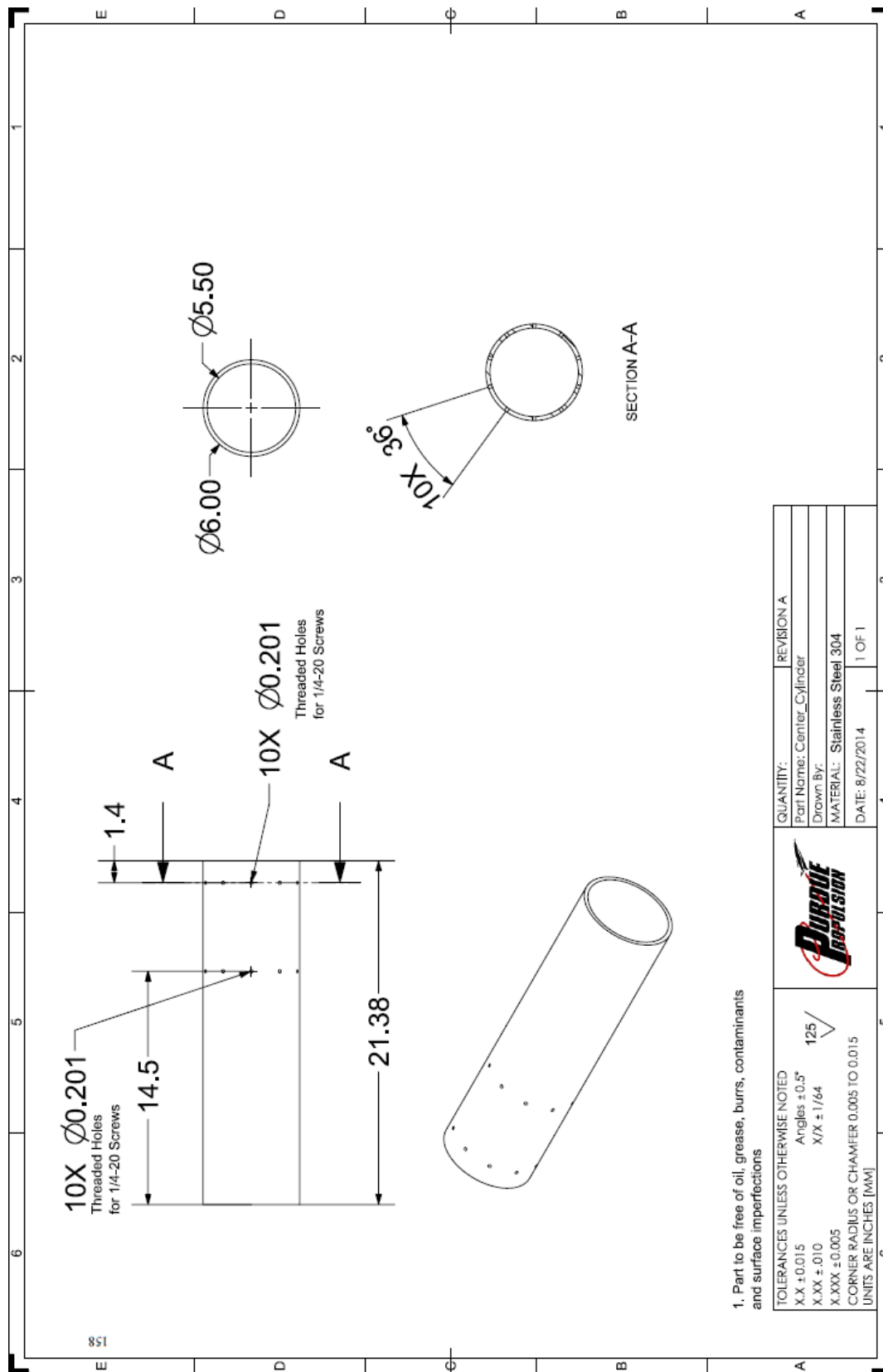Figure A.19 Test article drawing-19
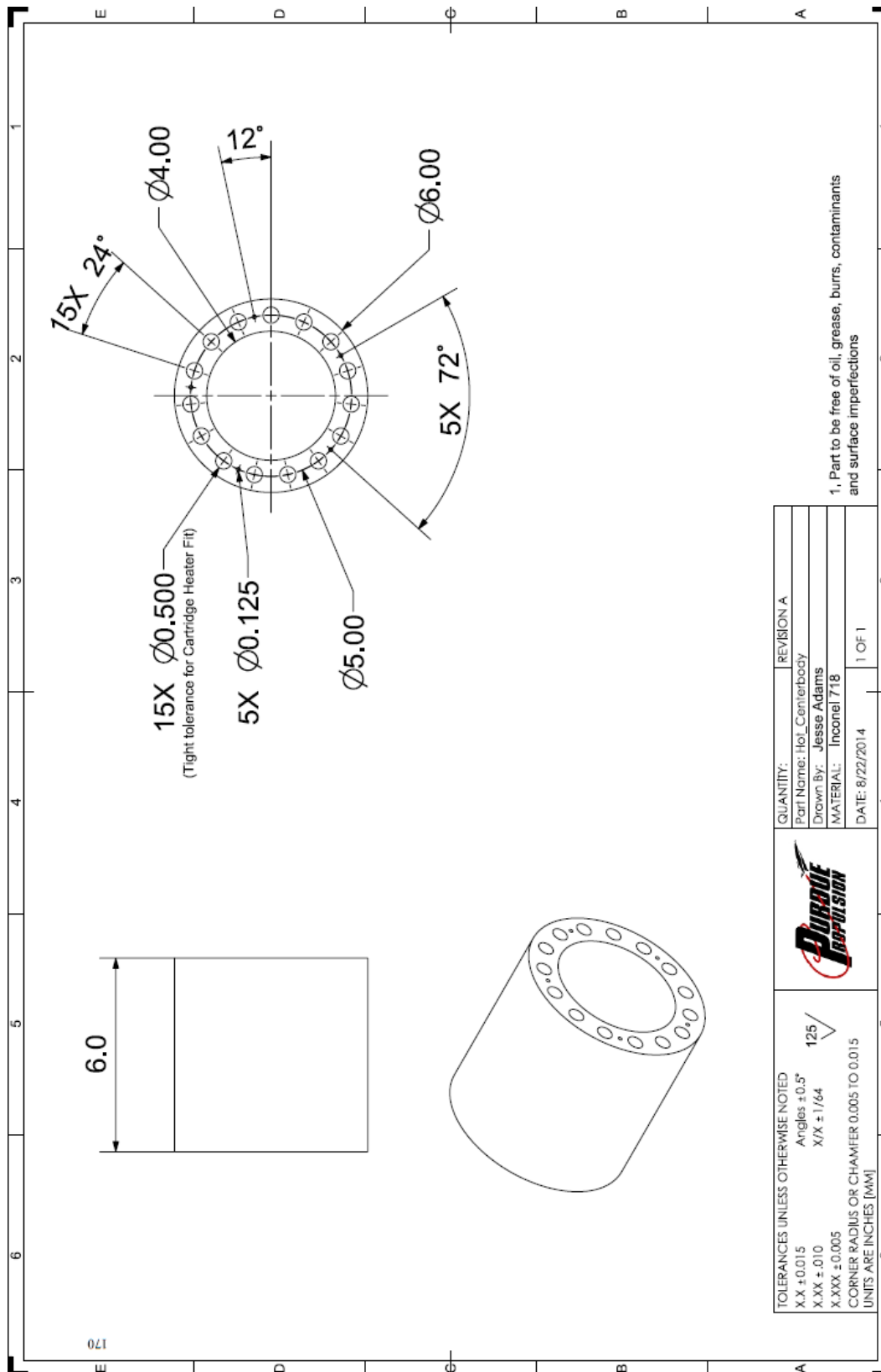
Figure A.20 Test article drawing-20

PC NO	PART NAME	QTY
8a.	END LIP	1
8b.	END VESSEL	1
8c.	END FACE	1

TOLERANCES UNLESS OTHERWISE NOTED
X.X ±0.015   Angles ±0.5°
X.XX ±.010   X/X ±1/64
X.XXX ±0.005
CORNER RADIUS OR CHAMFER 0.005 TO 0.015
UNITS ARE INCHES [MM]

125

QUANTITY: REVISION A
Part Name: End Piece_Assembly
Drawn By:
MATERIAL:
DATE: 8/22/2014   1 OF 1
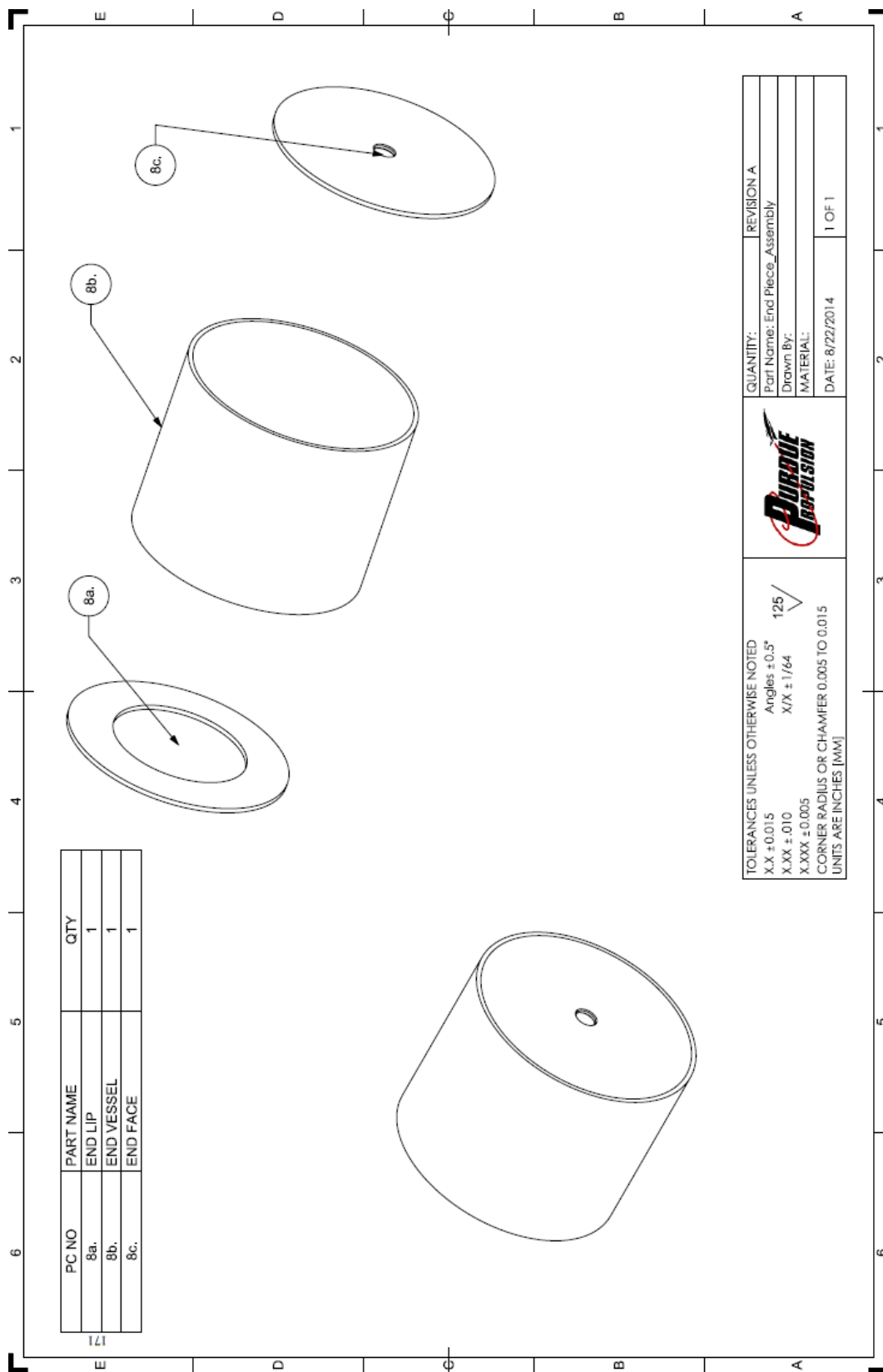
Figure A.21 Test article drawing-21
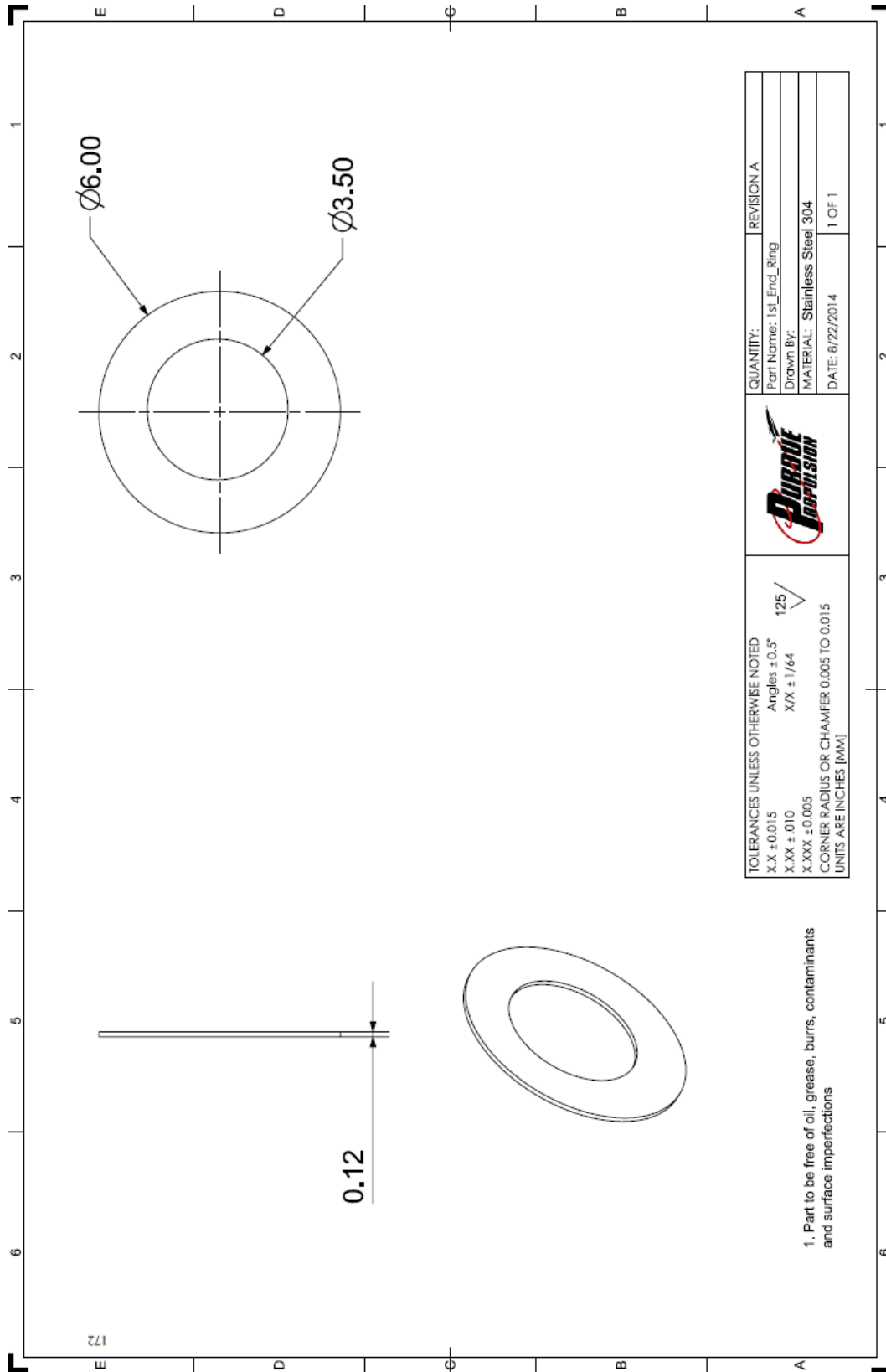
Figure A.22 Test article drawing-22

4.88

Ø6.0

0.250
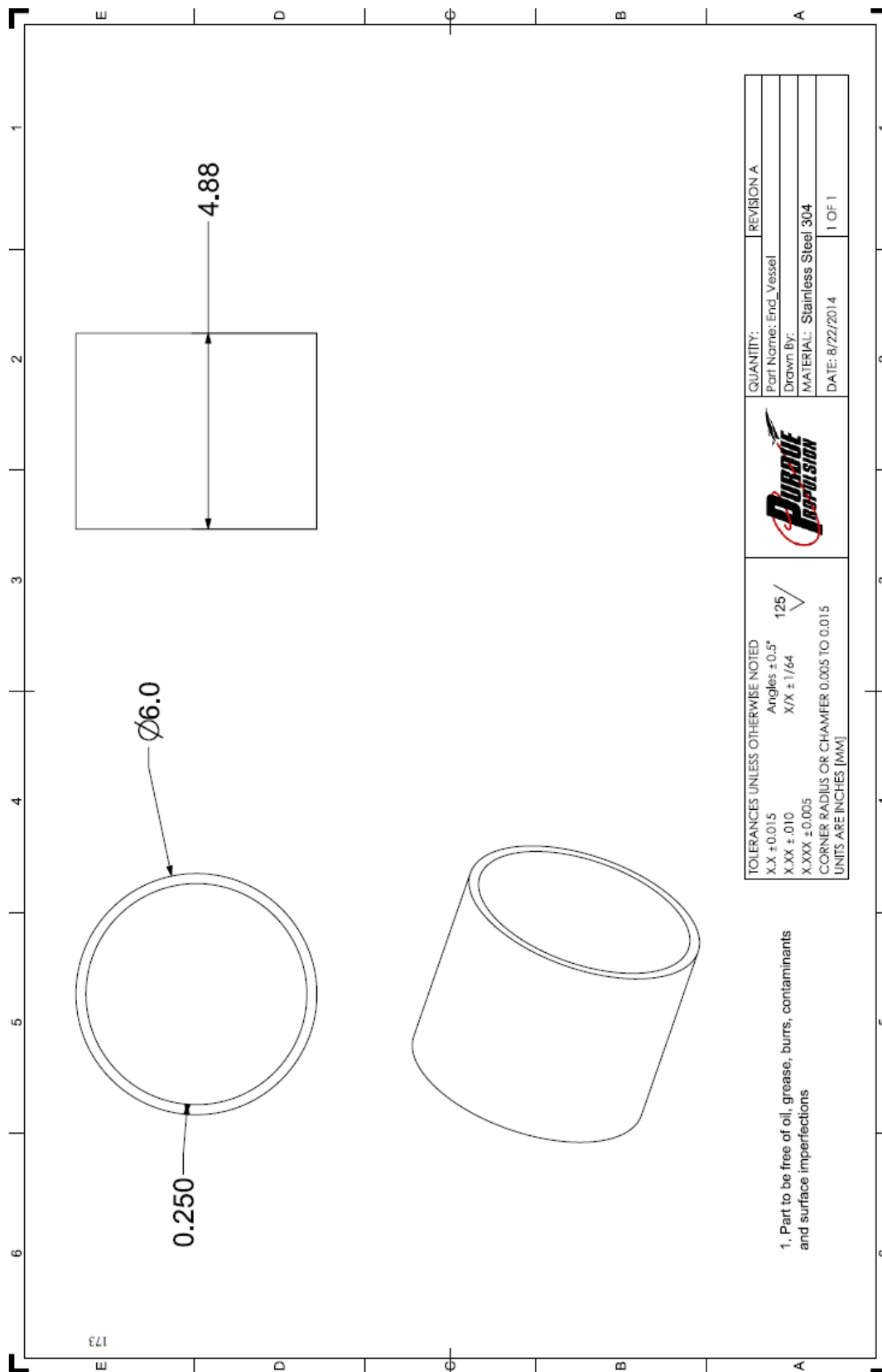
Figure A.23 Test article drawing-23
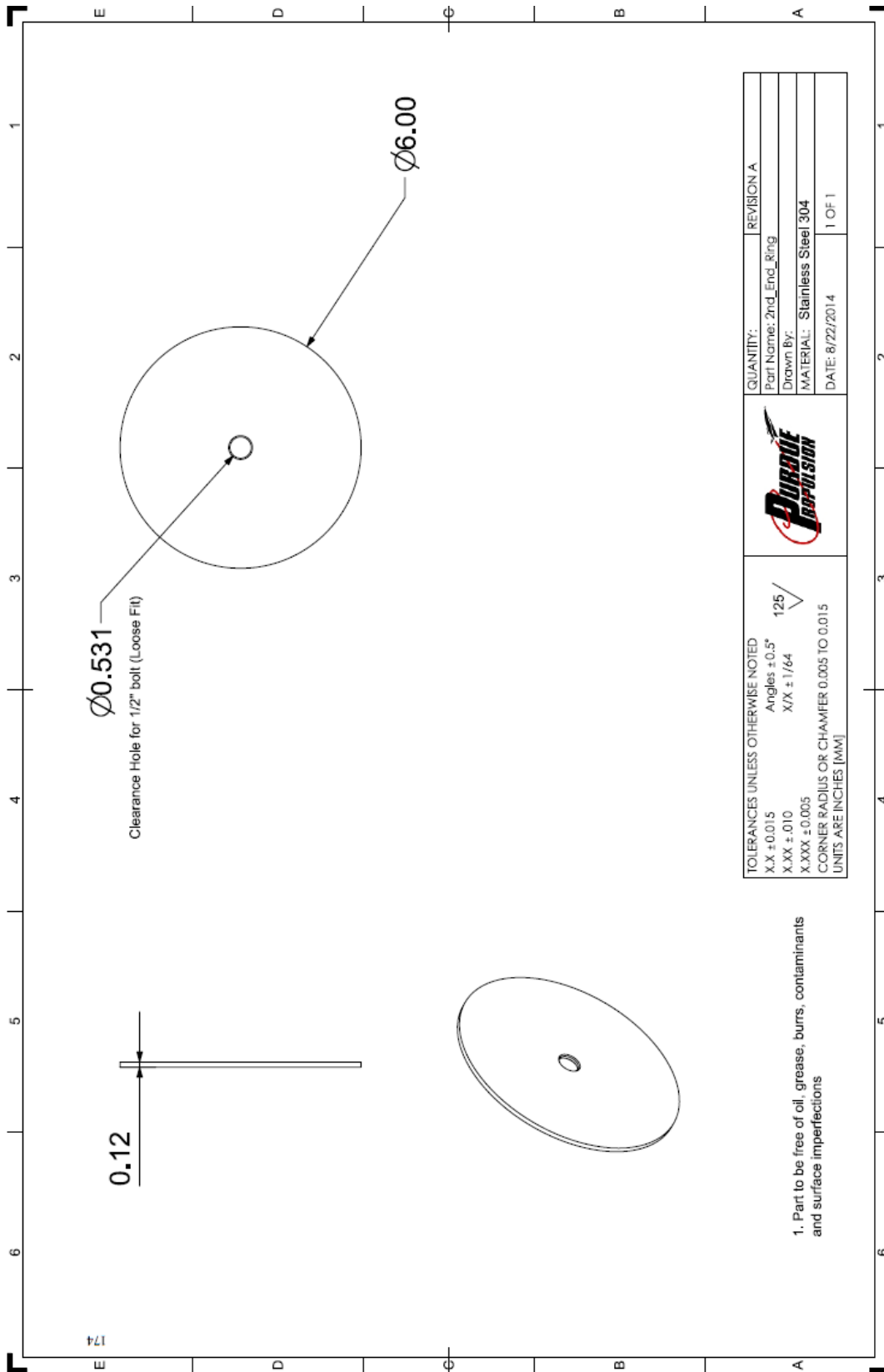
Figure A.24 Test article drawing-24

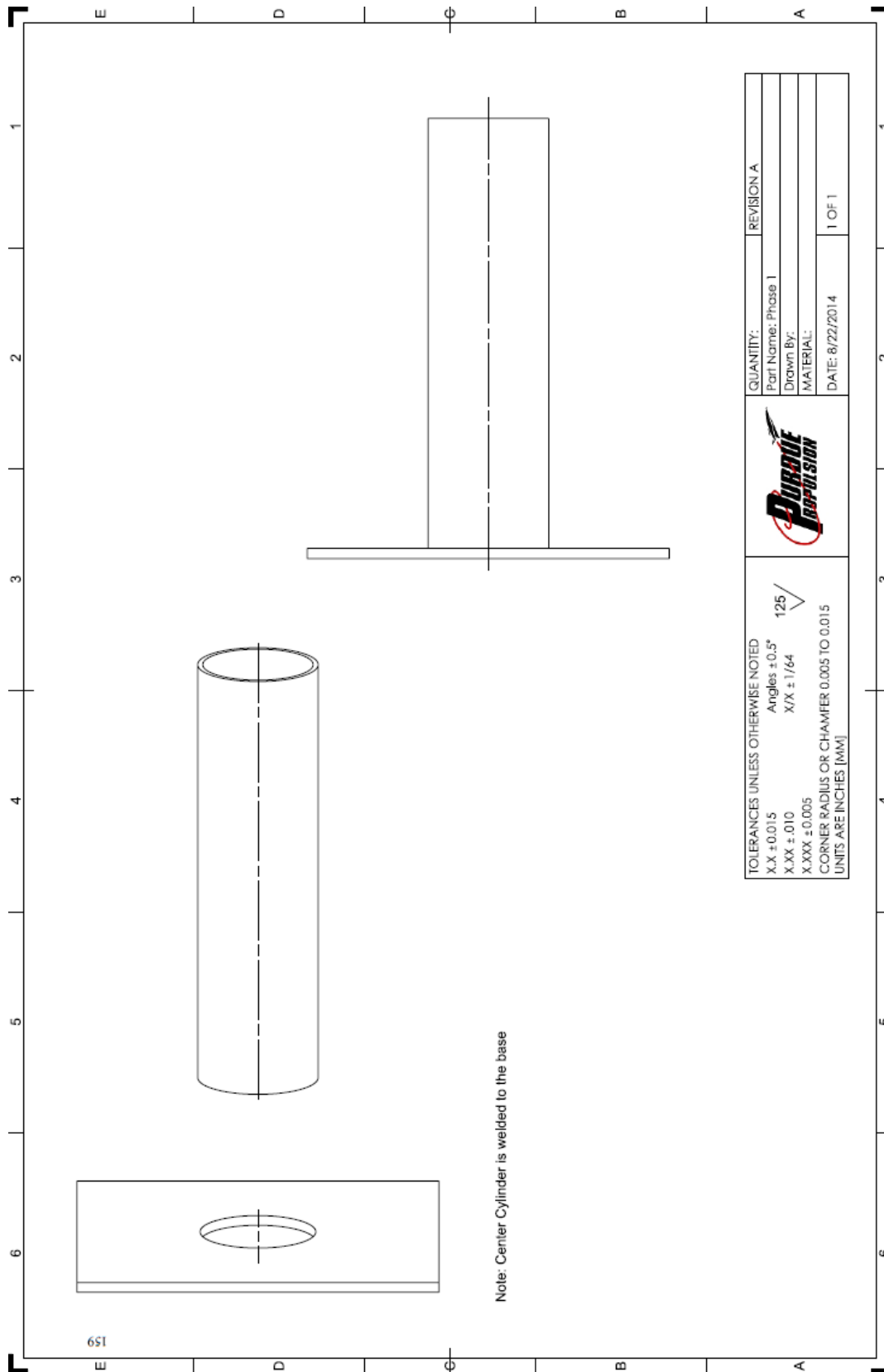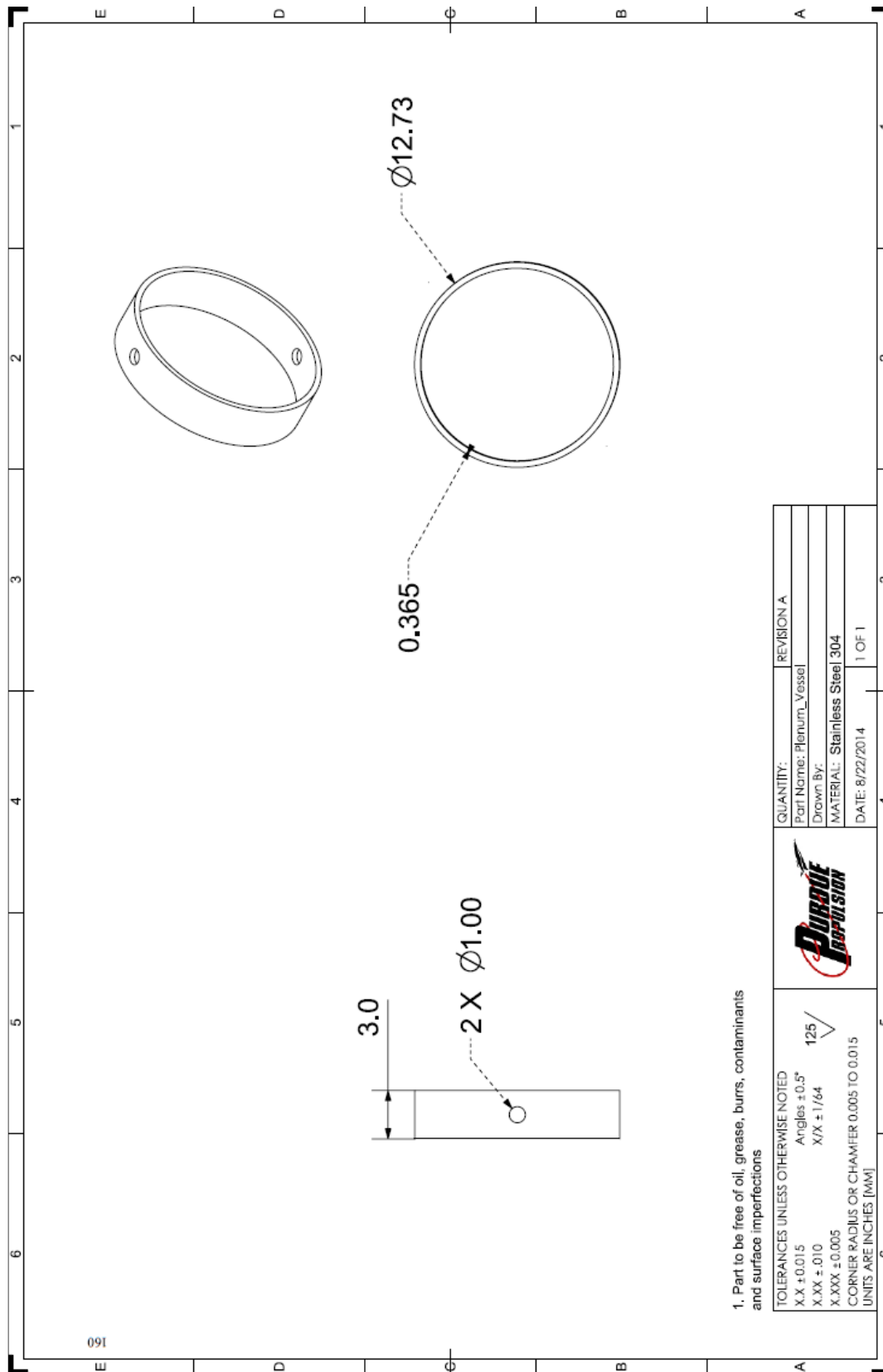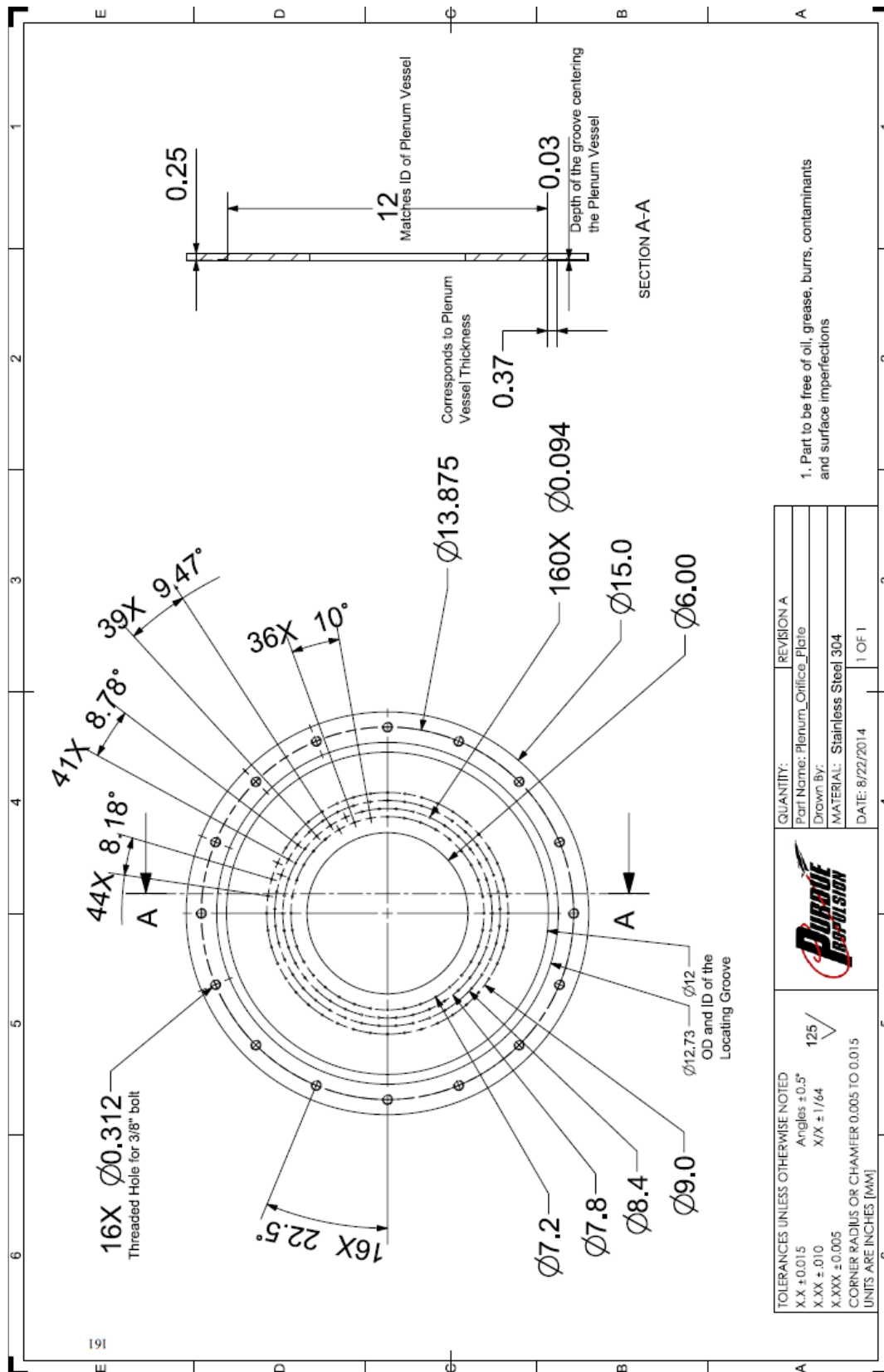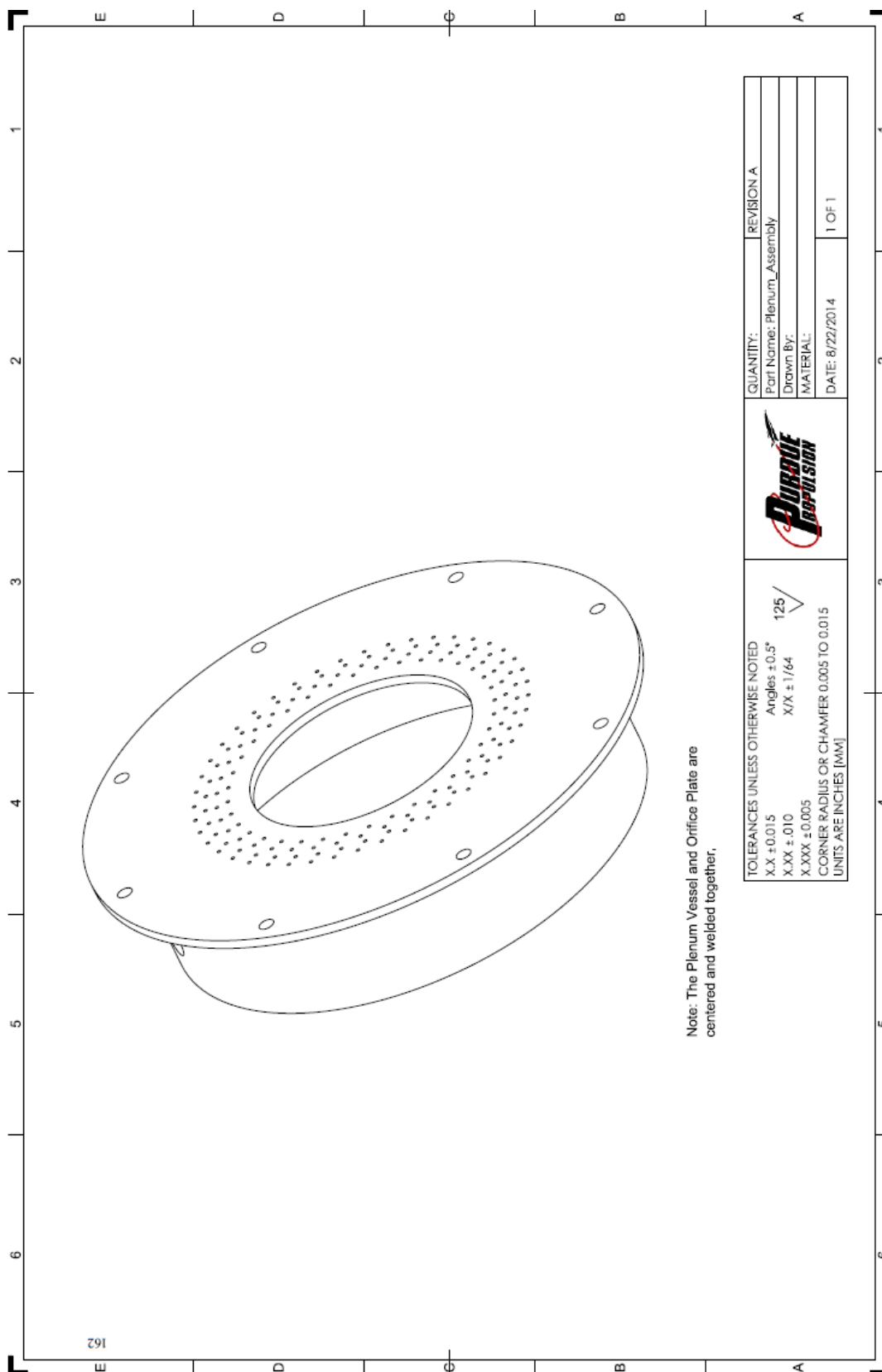Figure A.25 Test article drawing-25

Figure A.26 Test article drawing-26

4X R0.15
Corner Radius

View from the interior of the widow flange

TOLERANCES UNLESS OTHERWISE NOTED
X.X ±0.015   Angles ±0.5°
X.XX ±.010   X/X ±1/64
X.XXX ±0.005
CORNER RADIUS OR CHAMFER 0.005 TO 0.015
UNITS ARE INCHES [MM]

125/

QUANTITY: REVISION A
Part Name: Window_Flange_pg2
Drawn By:
MATERIAL: Stainless Steel 304
DATE: 8/22/2014   1 OF 1

1, Part to be free of oil, grease, burrs, contaminants
and surface imperfections

Figure A.27 Test article drawing-27

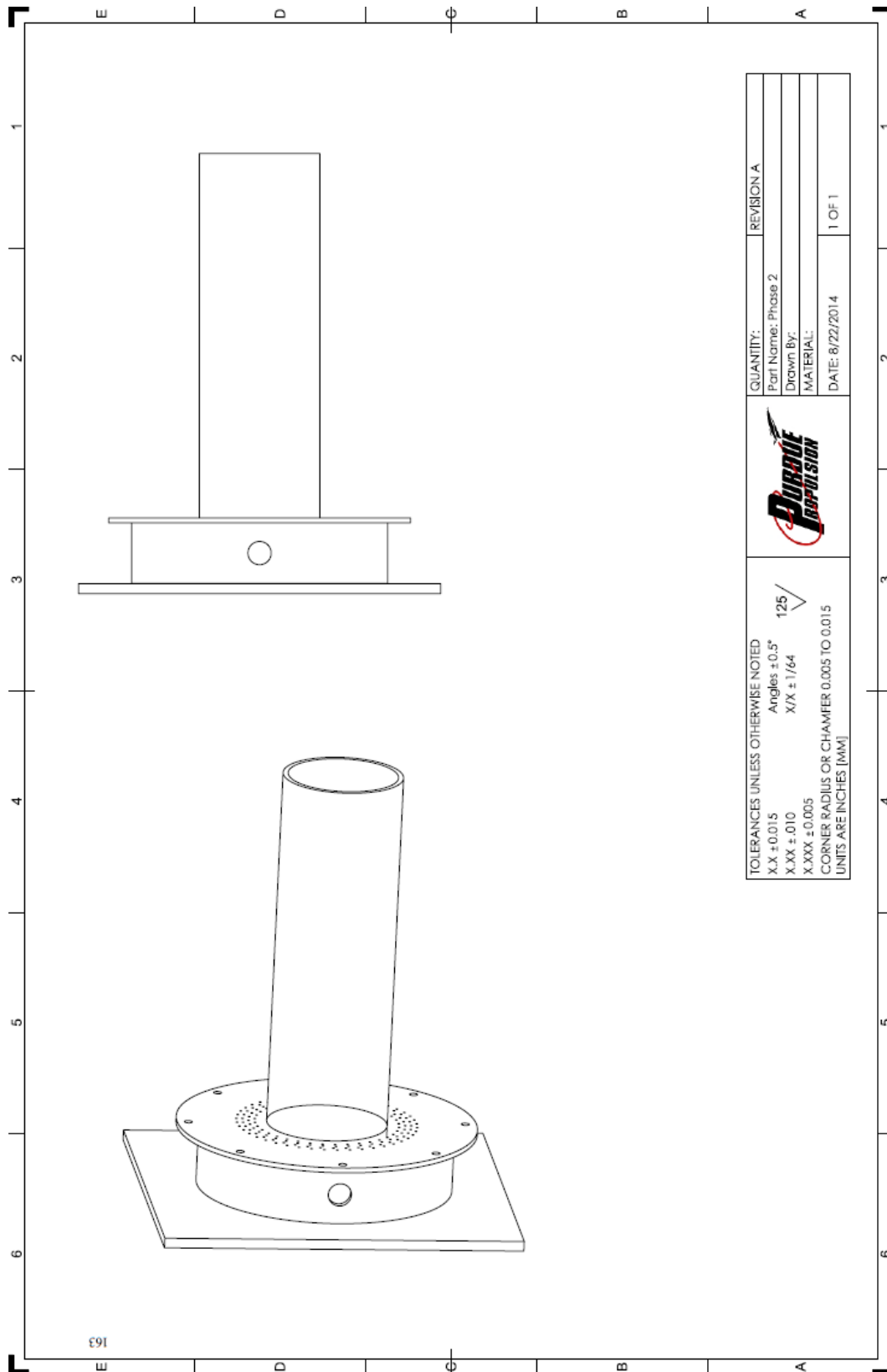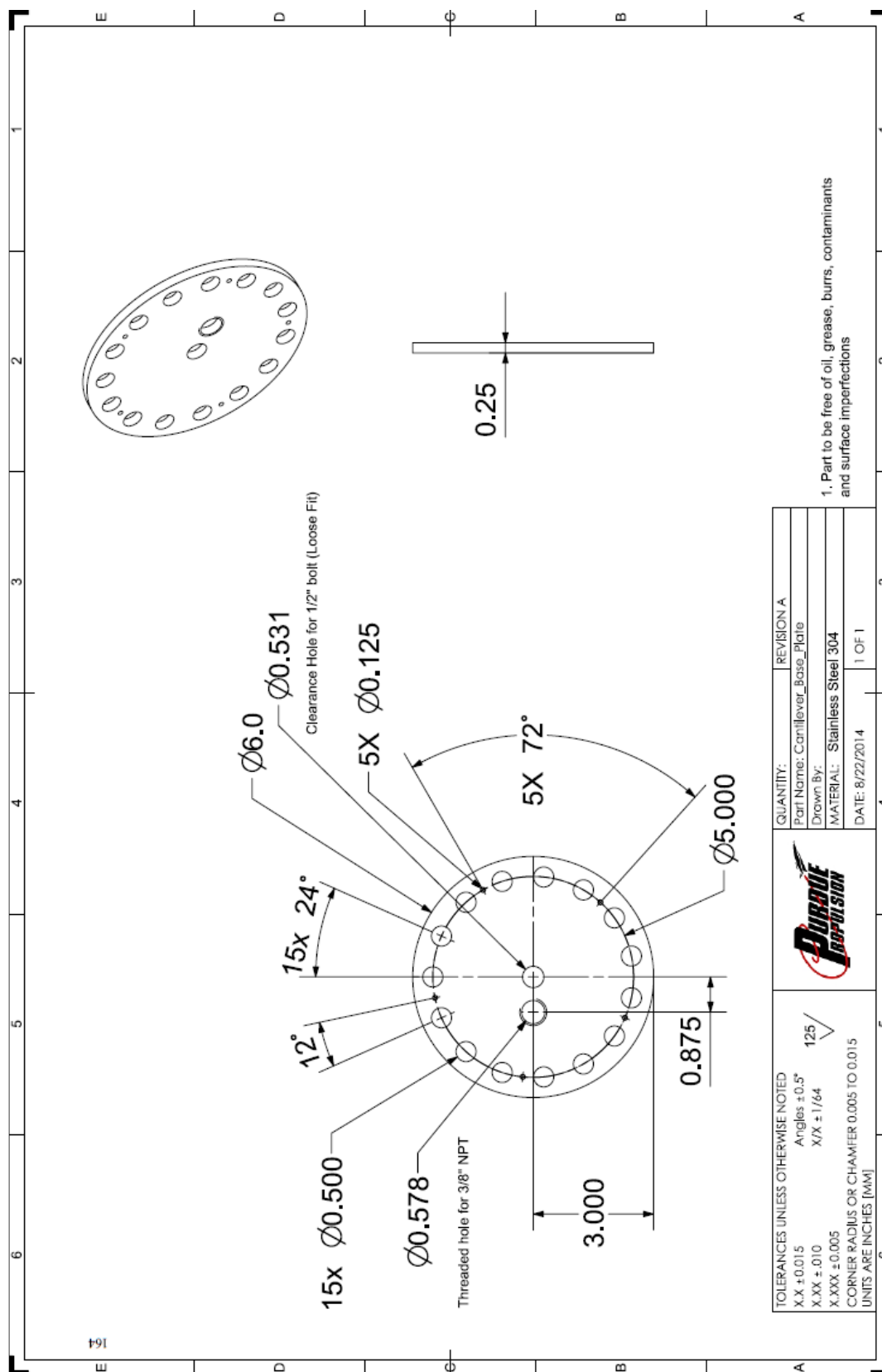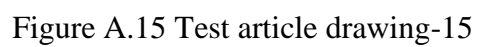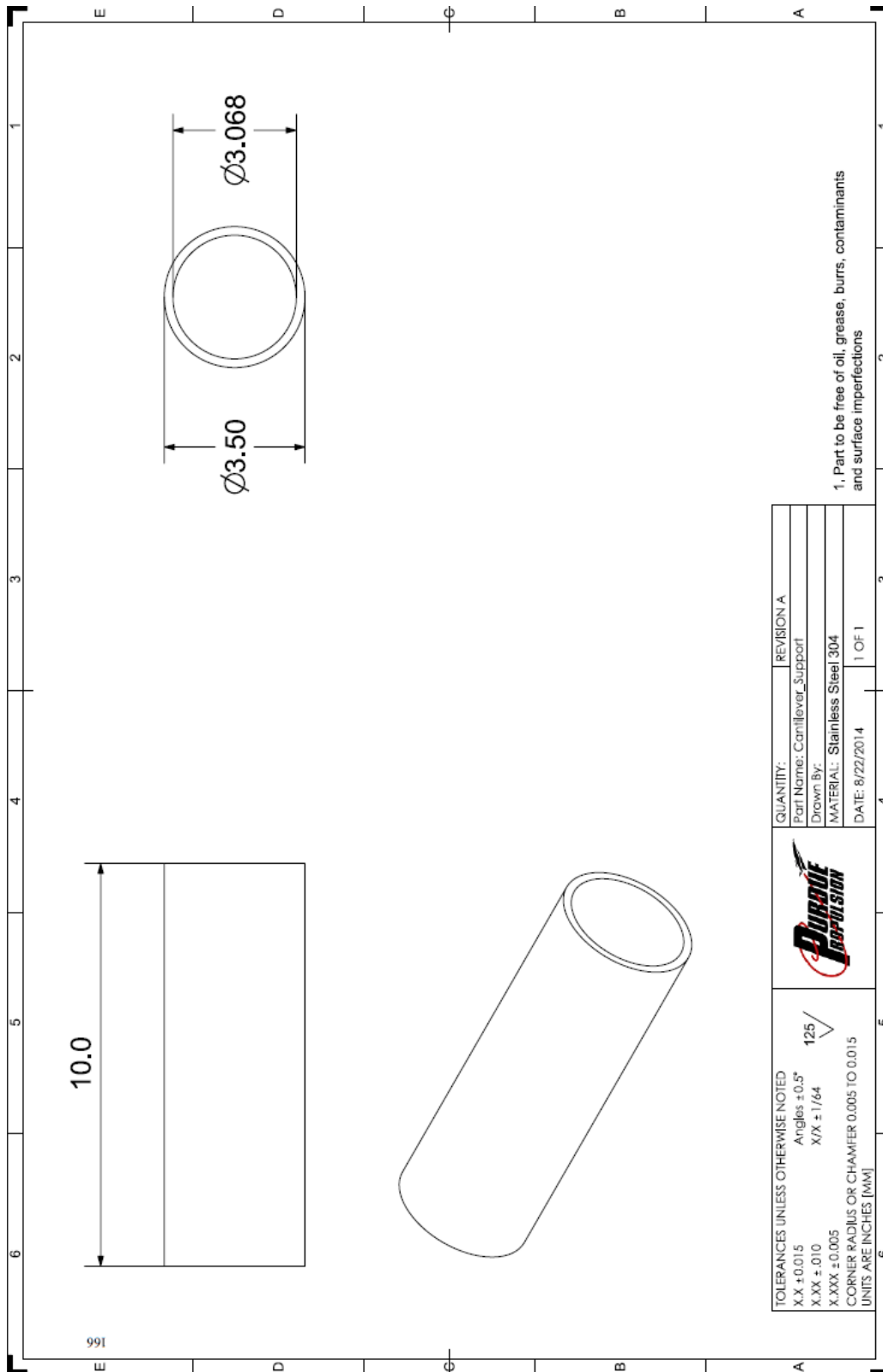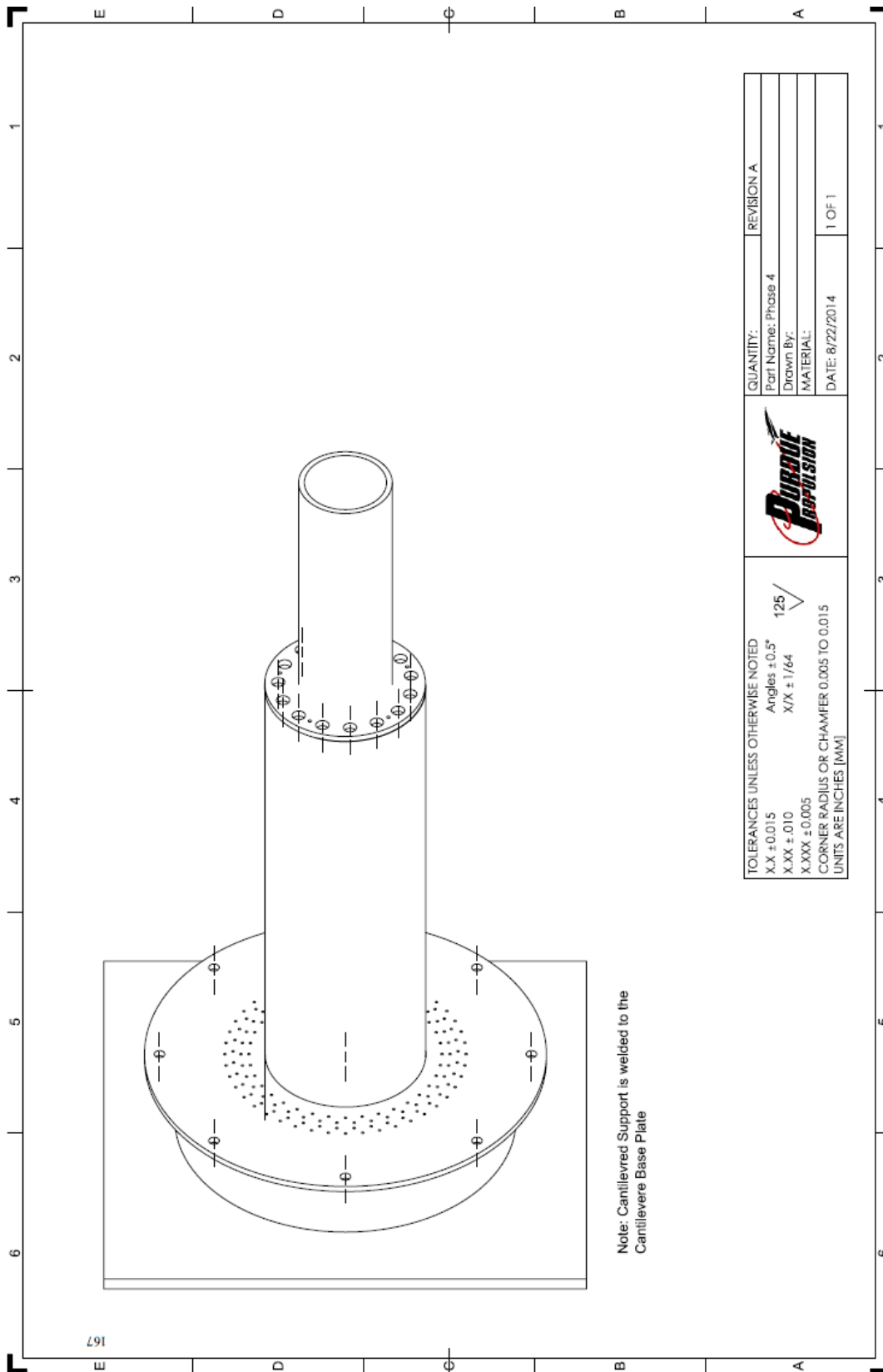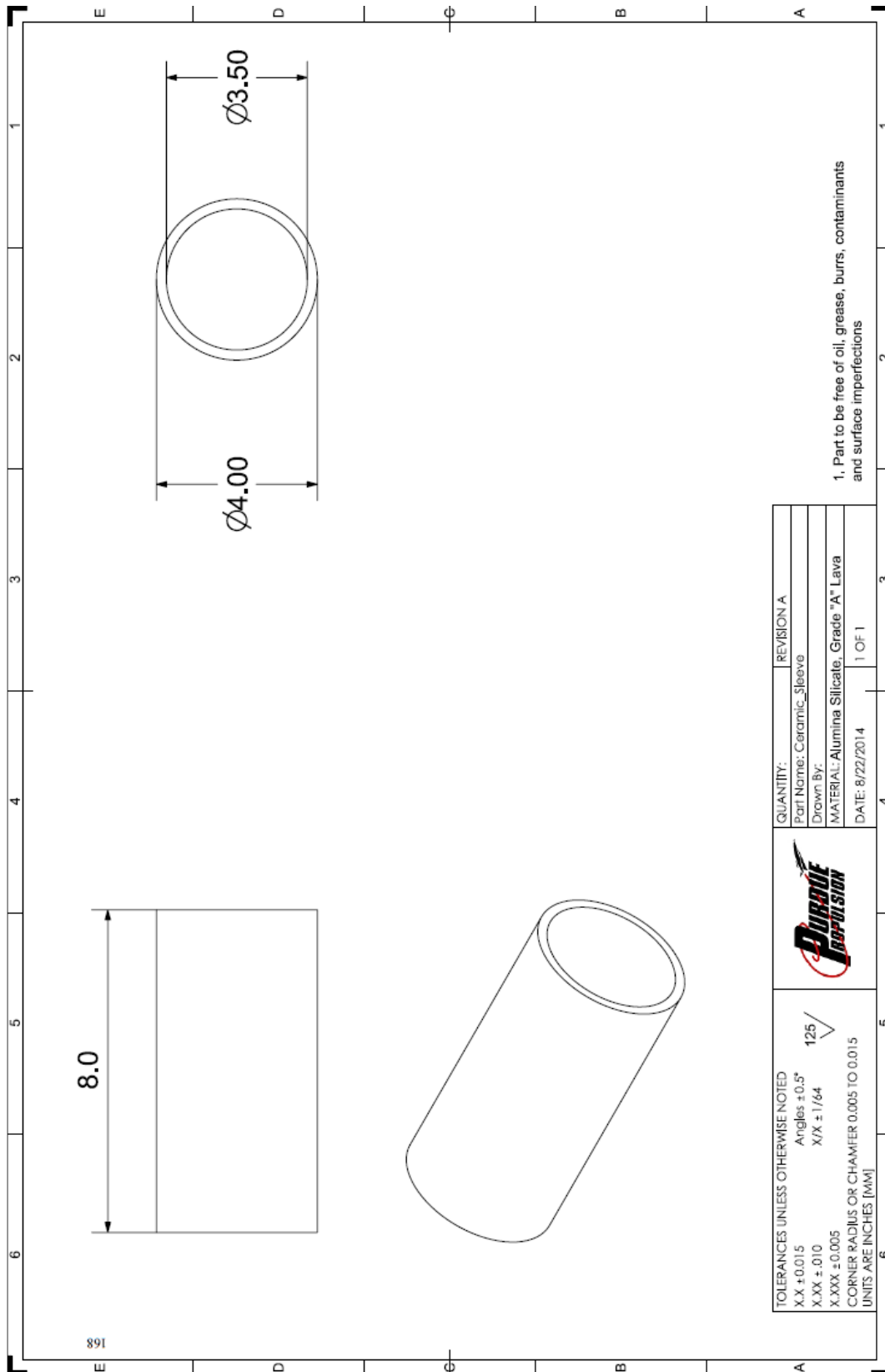Figure A.28 Test article drawing-28

Figure A.29 Test article drawing-29

PC NO	Part Name	QTY
1	Vertical Support	2
2	Elevated Crossbar	2
3	Front Floor Crossbar	1
4	Longitudinal Floor Bar	2
5	Floor Crossbar	1
6	Slanted Support	2

TOLERANCES UNLESS OTHERWISE NOTED
X.X ±0.015   Angles ±0.5°
X.XX ±.010   X/X ±1/64
X.XXX ±0.005   125/
CORNER RADIUS OR CHAMFER 0.005 TO 0.015
UNITS ARE INCHES [MM]

QUANTITY: REVISION A
Part Name: Test_Stand_3
Drawn By: Jesse Adams
MATERIAL: Stainless Steel 304
DATE: 8/22/2014   1 OF 1

1. Part to be free of oil, grease, burrs, contaminants and surface imperfections

081

Figure A.30 Test article drawing-30

122

2.0

2.0

0.25

55.0

4X 4.0

1.0

5X Ø0.397
Clearance Hole for 3/8" bolt

TOLERANCES UNLESS OTHERWISE NOTED
X.X ±0.015   Angles ±0.5°
X.XX ±.010   X/X ±1/64
X.XXX ±0.005
CORNER RADIUS OR CHAMFER 0.005 TO 0.015
UNITS ARE INCHES [MM]

125

1. Part to be free of oil, grease, burrs, contaminants and surface imperfections

REVISION A
QUANTITY:
Part Name: Vertical_Support
Drawn By: Jesse Adams
MATERIAL: Stainless Steel 304
DATE: 8/22/2014   1 OF 1

Figure A.31 Test article drawing-31

TOLERANCES UNLESS OTHERWISE NOTED
X.X ±0.015   Angles ±0.5°
X.XX ±.010   X/X ±1/64
X.XXX ±0.005
CORNER RADIUS OR CHAMFER 0.005 TO 0.015
UNITS ARE INCHES [MM]

125

1. Part to be free of oil, grease, burrs, contaminants and surface imperfections

3X ⌀0.397
Clearance Holes for 3/8" Bolts

2.0
2.0
0.25
1.0
10.5
7.0
3.5
14.0

QUANTITY:		REVISION A
Part Name: Elevated_Crossbar		
Drawn By: Jesse Adams		
MATERIAL: Stainless Steel 304		
DATE: 8/22/2014		1 OF 1

Figure A.32 Test article drawing-32

Clearance Hole for 1/2" Drill
⌀0.562

1.0

14.0

7.0

2.0

2.0

0.25

125

TOLERANCES UNLESS OTHERWISE NOTED
X.X ± 0.015   Angles ± 0.5°
X.XX ± .010   X/X ± 1/64
X.XXX ± 0.005
CORNER RADIUS OR CHAMFER 0.005 TO 0.015
UNITS ARE INCHES [MM]

1. Part to be free of oil, grease, burrs, contaminants
   and surface imperfections

Purdue Propulsion

QUANTITY:	REVISION A
Part Name: Front_Floor_Crossbar	
Drawn By: Jesse Adams	
MATERIAL: Stainless Steel 304	
DATE: 8/22/2014	1 OF 1

183

Figure A.33 Test article drawing-33

Figure A.34 Test article drawing-34

Clearance Holes for 1/2" Drill
2X Ø0.562

1.0

3.5

7.0

14

2.0

2.0

0.25

TOLERANCES UNLESS OTHERWISE NOTED
X.X ± 0.015   Angles ± 0.5°
X.XX ± .010   X/X ± 1/64   125
X.XXX ± 0.005
CORNER RADIUS OR CHAMFER 0.005 TO 0.015
UNITS ARE INCHES [MM]

1. Part to be free of oil, grease, burrs, contaminants
   and surface imperfections

QUANTITY: REVISION A
Part Name: Floor_Crossbar
Drown By: Jesse Adams
MATERIAL: Stainless Steel 304
DATE: 8/22/2014   1 OF 1

Figure A.35 Test article drawing-35

127

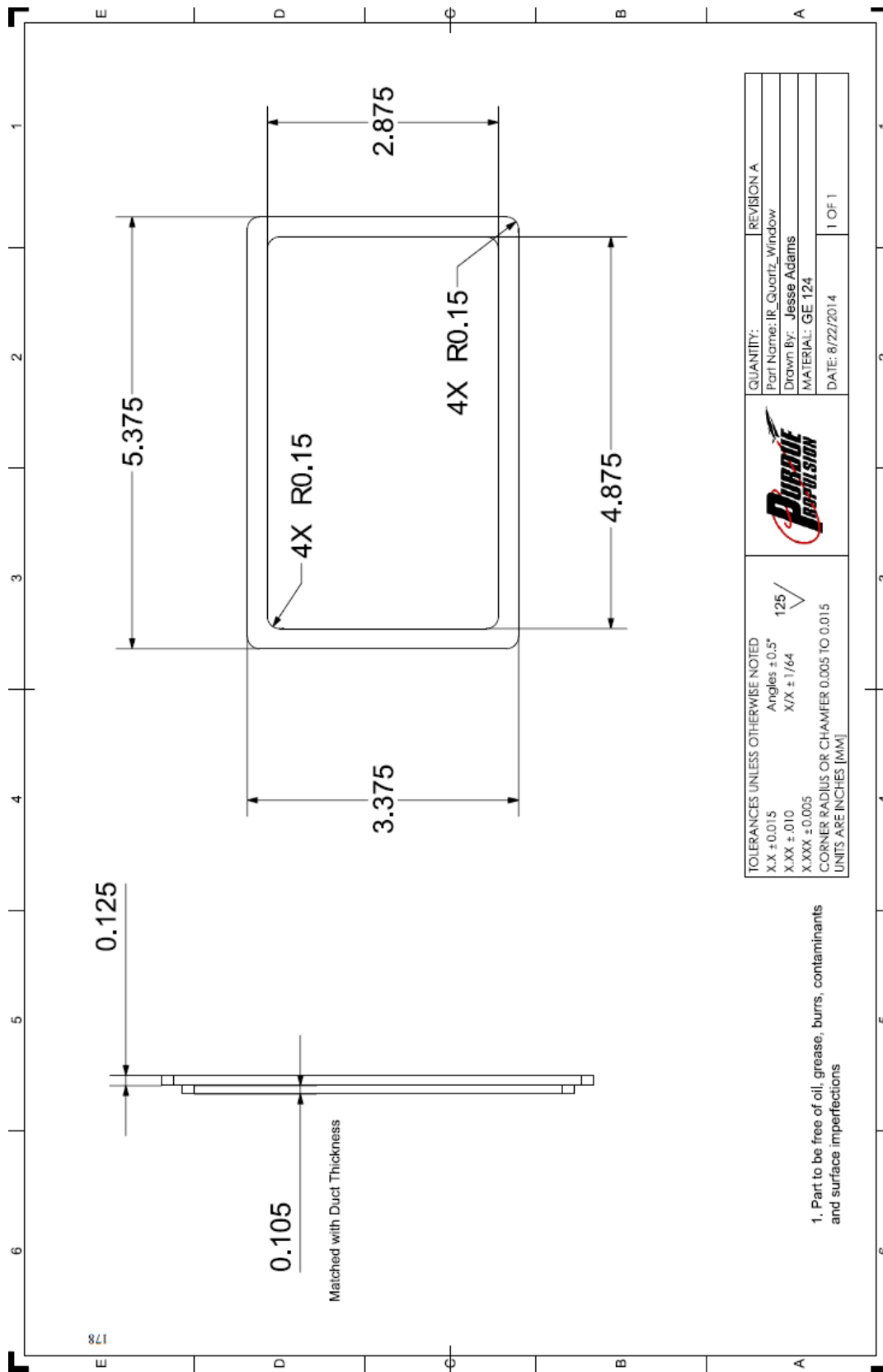Figure A.36 Test article drawing-36

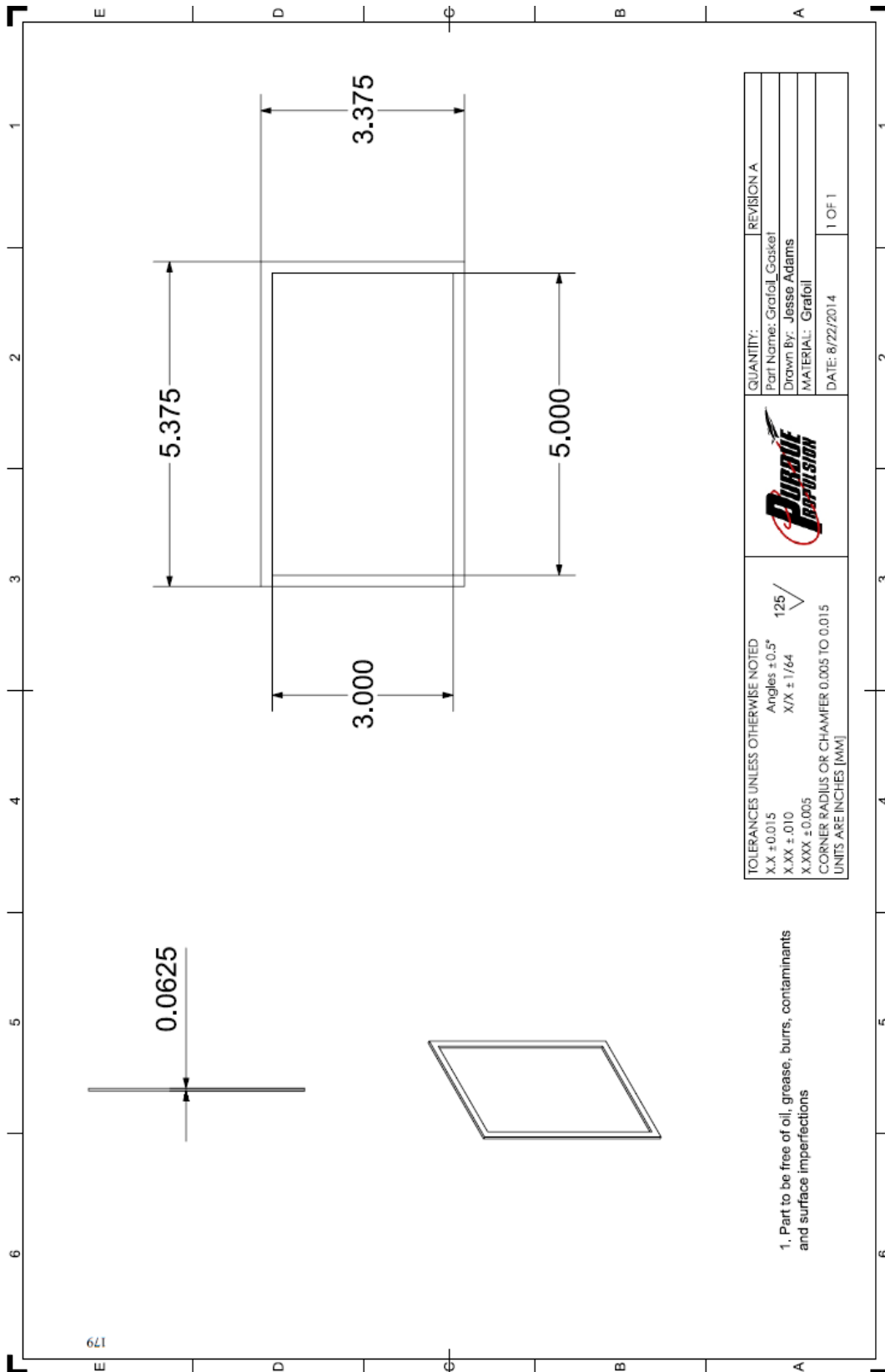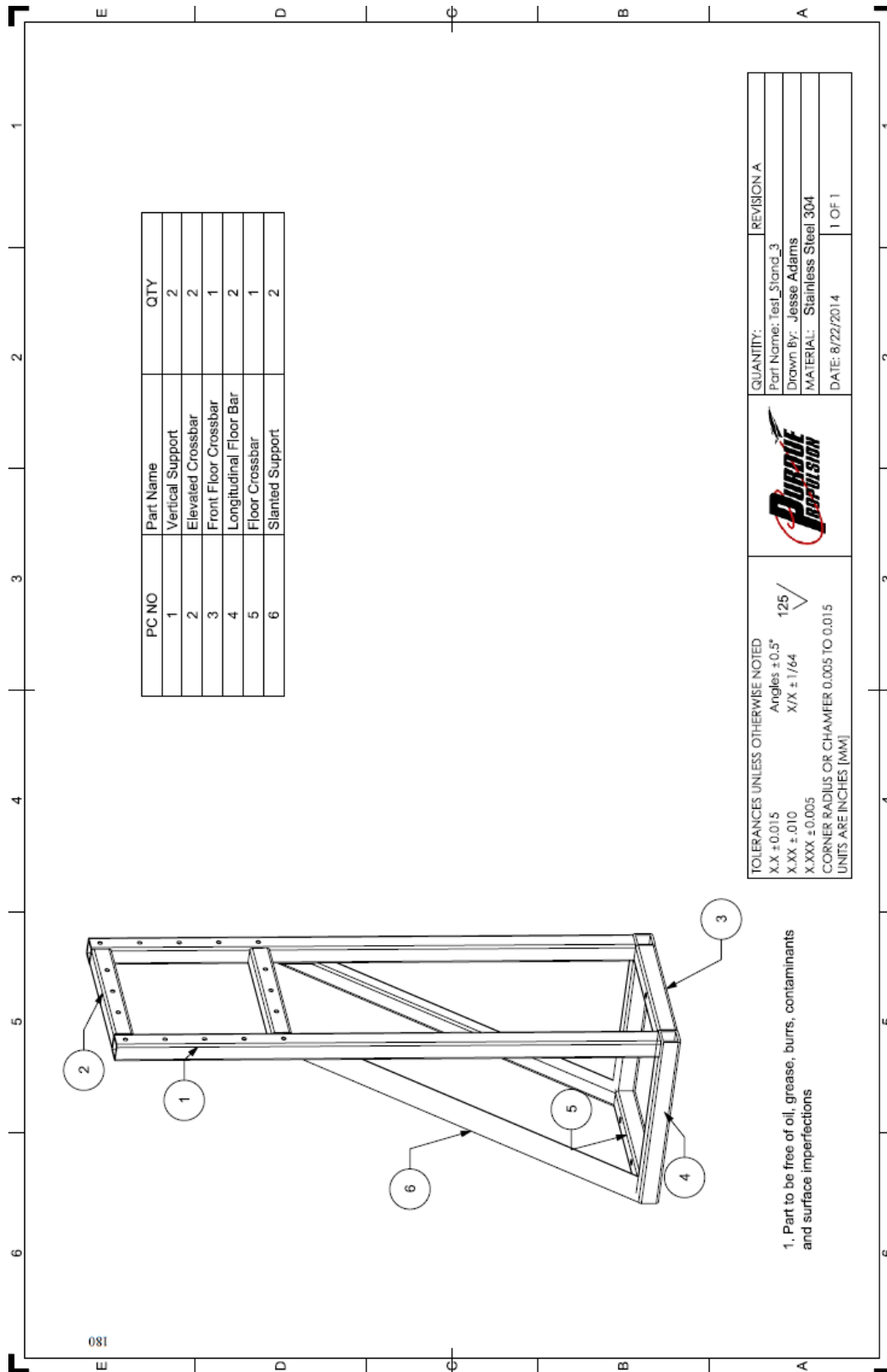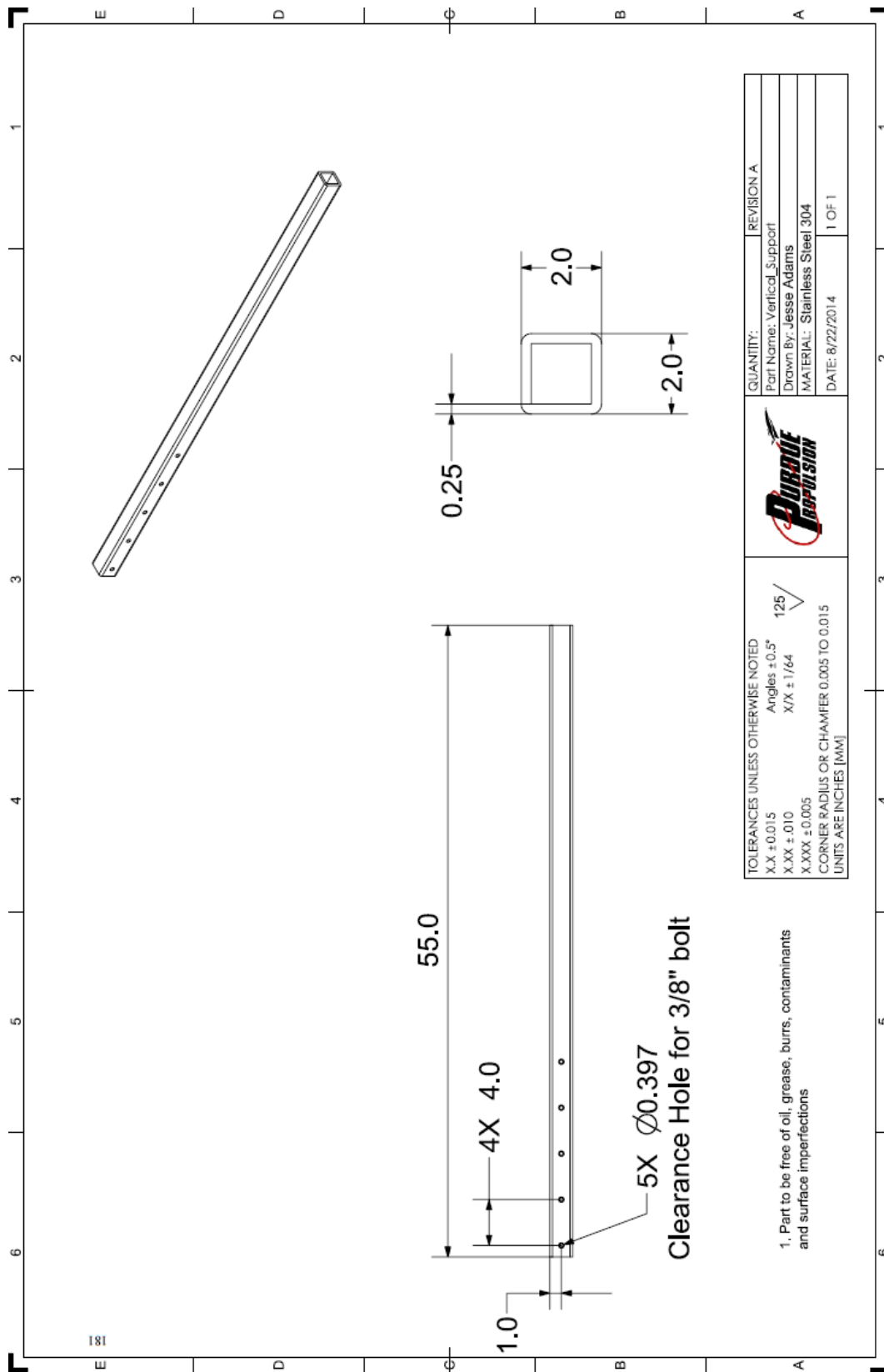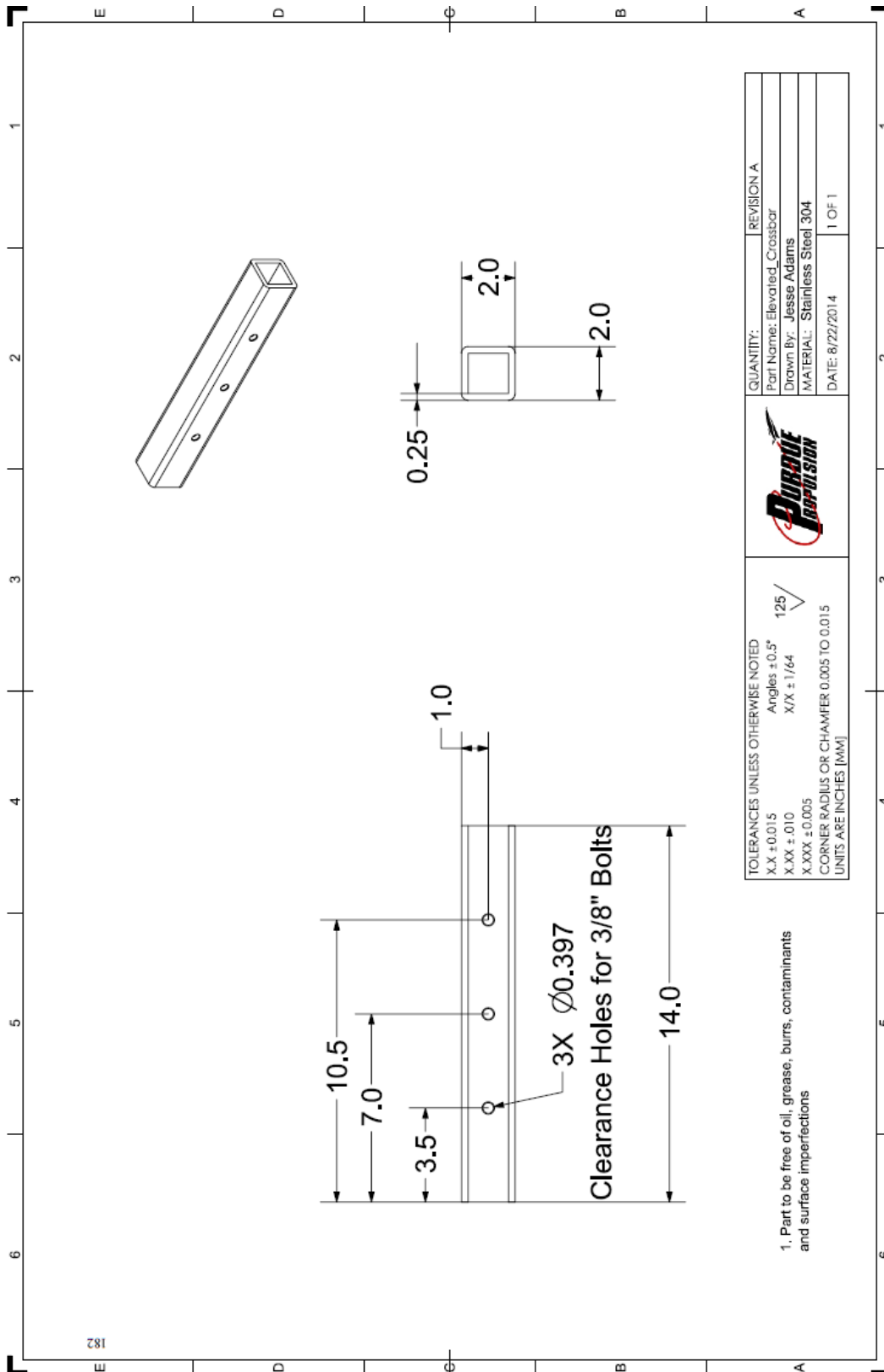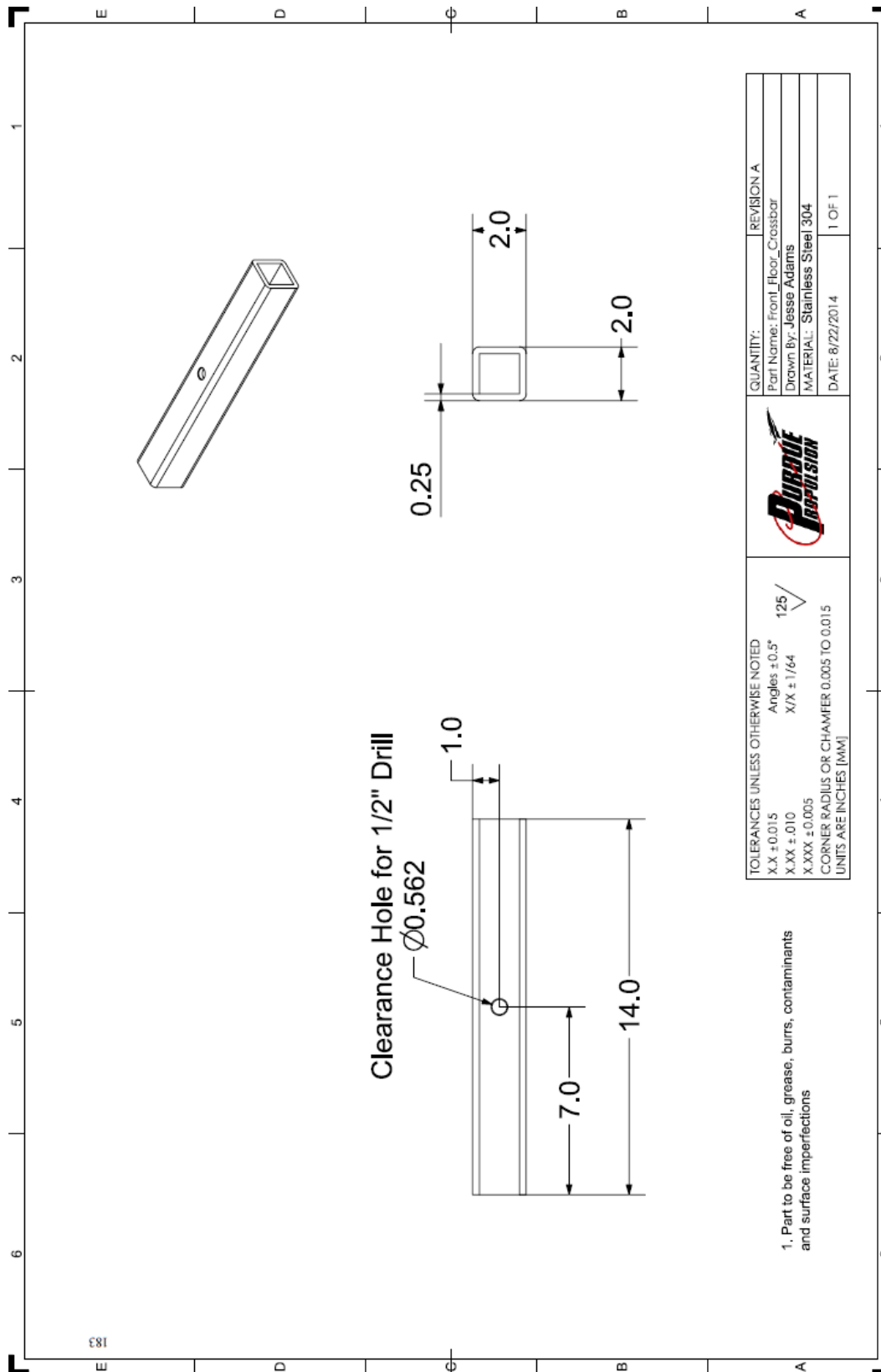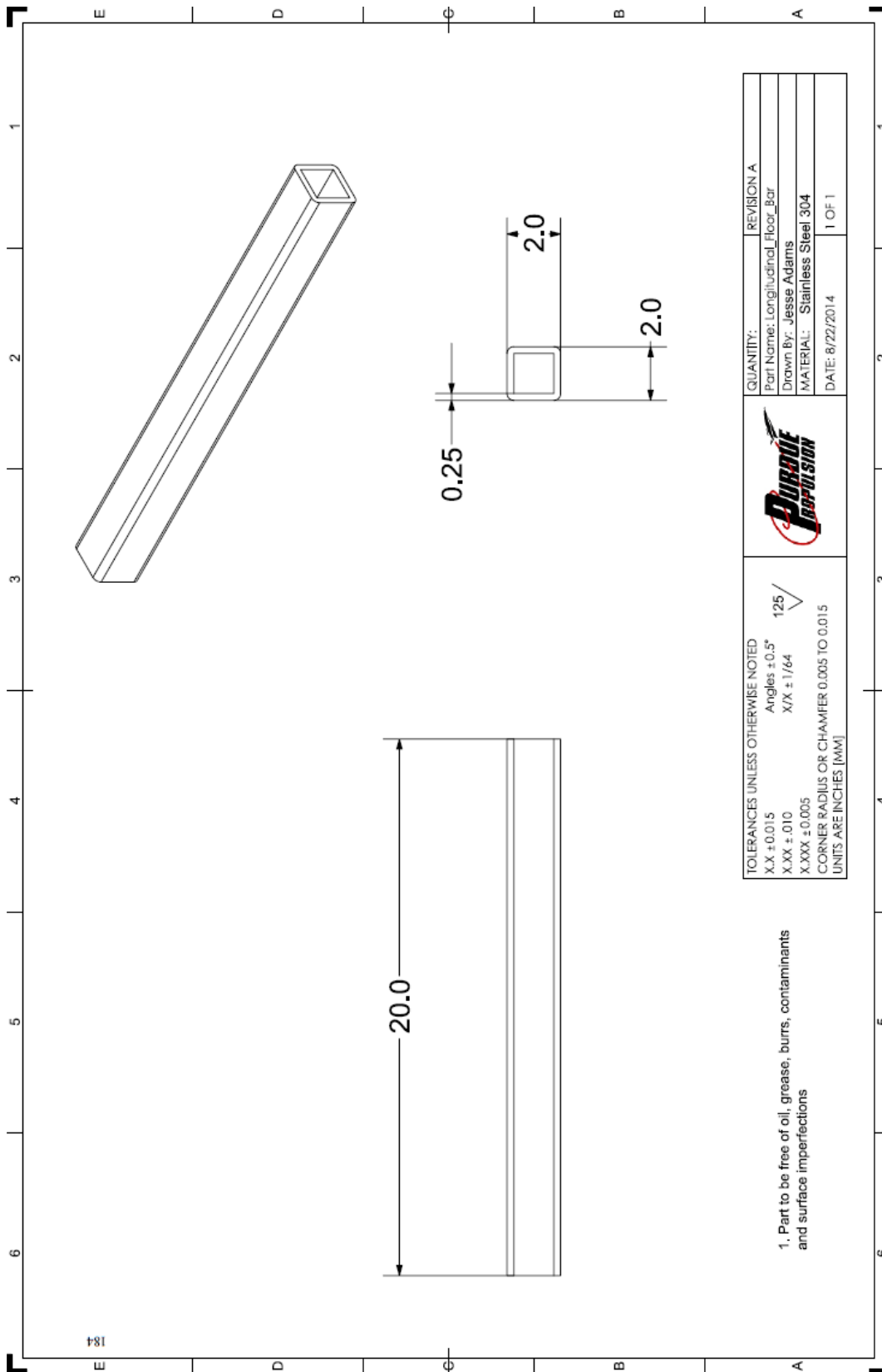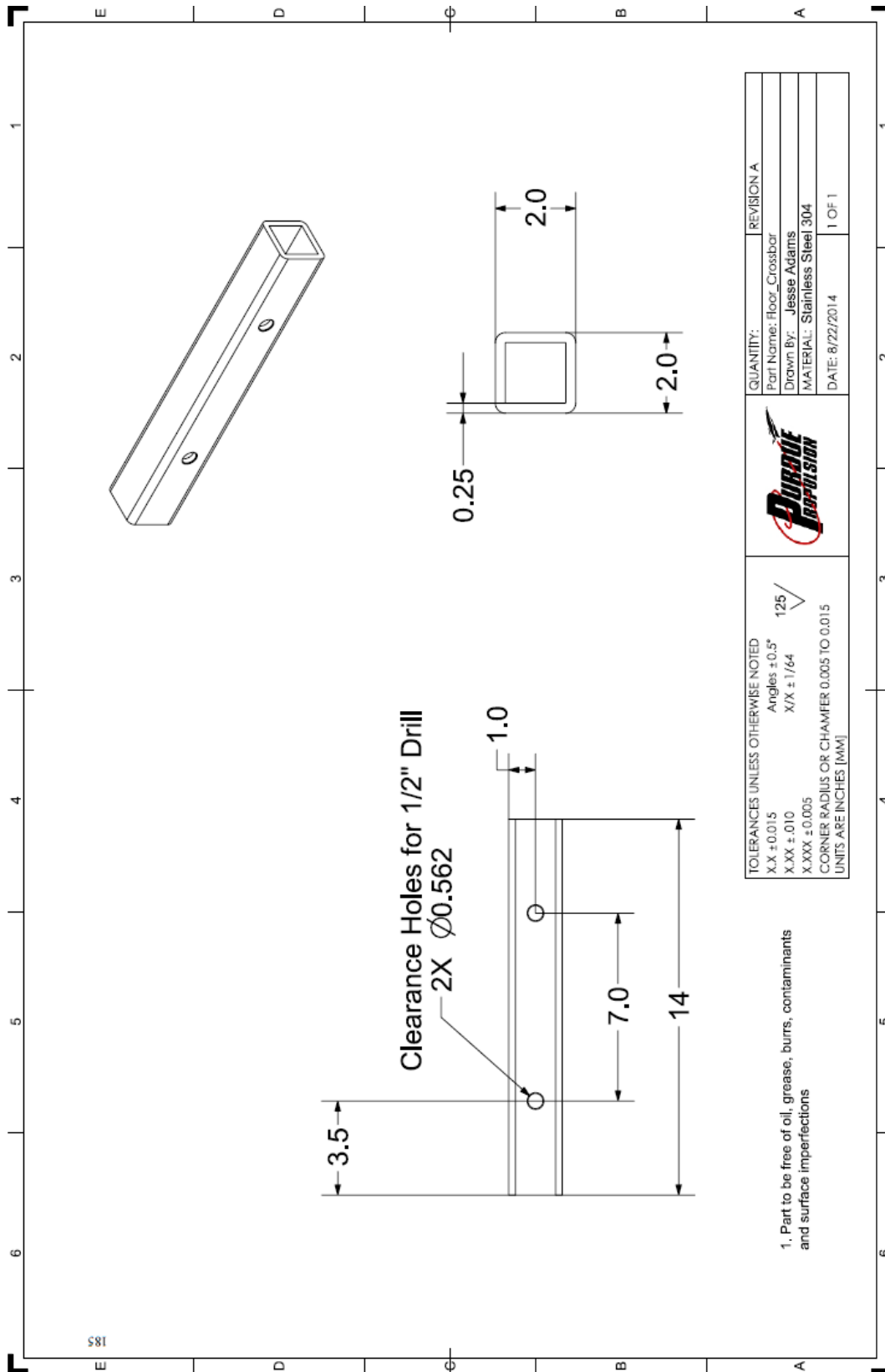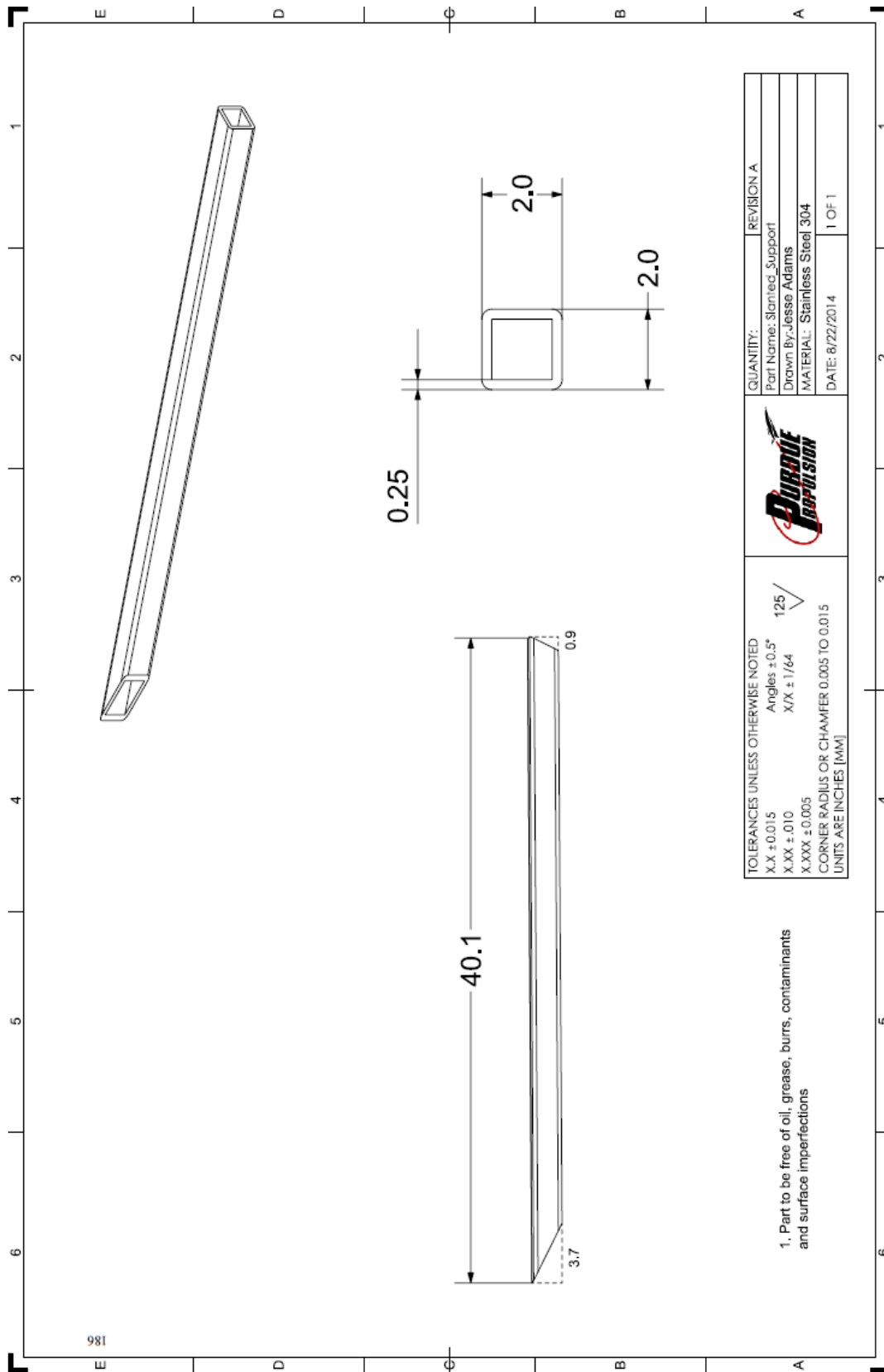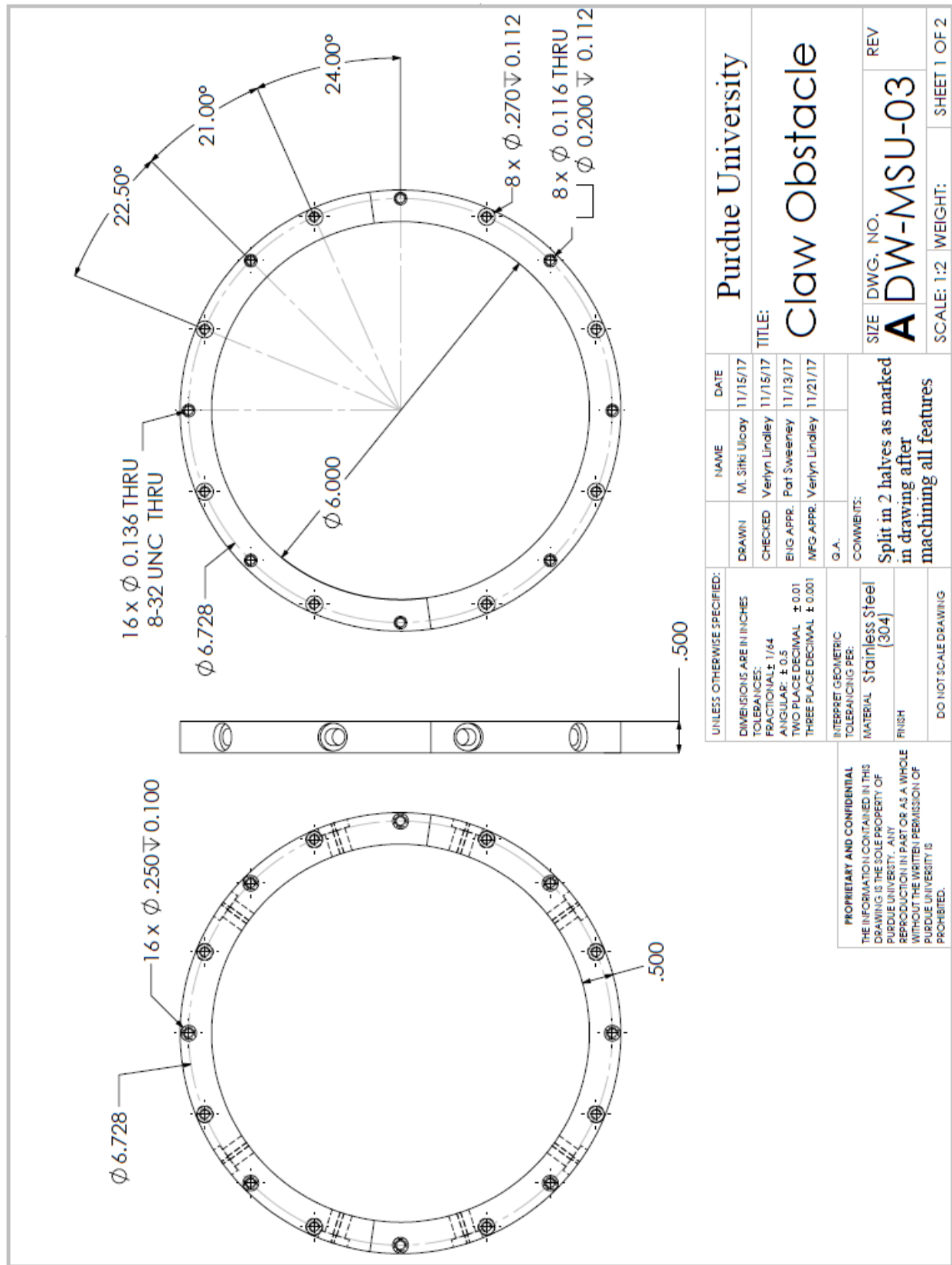Figure A.37 Test article drawing-37

Figure A.38 Test article drawing-38

REFERENCES

[1] V. Goyal, A. B. Carayon, S. Meyer, J. Gore and R. Simmons, "Hot Surface Ignition Temperatures of Hydrocarbon Fuels," in *55th AIAA Aerospace Sciences Meeting*, Grapevine, TX, 2017.

[2] P. A. Boettcher, "Thermal Ignition," California Insititute of Techology, Pasadena, 2012.

[3] L. Strawhorn, Motor Vehicles, Quincy, MA: National Fire Protection Association, 2003.

[4] A. M. Johnson, A. J. Roth and A. N. Moussa, "Hot Surface Ignition Tests of Aircraft Fluids," AF Wright Aeronutical Laboratories, Wright-Patterson Air Force Base, OH, 1988.

[5] N. T. S. Board, "Aircraft Accident Report: In-flight breakup over the Atlantic Ocean Trans World Airlines Flight 800," 2000.

[6] A. T. S. Report, "In-flight uncontained engine failure overhead Batam Island, Indonasio," Australina Transport Safety Bureau, Canberra, 2013.

[7] Advisory Group for Aerospace Research and Development (AGARD), Aircraft Fire Safety, 1989: Specialised Printing Services Limited , May.

[8] "Philippine Airlines flight to Manila engine caught on fire," Twitter, 21 11 2019. [Online]. Available: https://twitter.com/KrisAnkarlo/status/1197652212509364224.

[9] "Thai B773 at Bangkok," Avherald, 20 10 2019. [Online]. Available: http://avherald.com/h?article=4ce47f3f.

[10] J. M. Kuchta, B. A. and M. G. Zabetakis, "Hot Surface Ignition Temperatures of Hydrocarbon Fuel Vapor-Air Mixtures," *Journal of Chemical and Engineering Data,* vol. 10, no. 3, pp. 282-288, 1965.

[11] J. D. Colwell and A. Reza, "Hot Surface Ignition of Automative and Aviation Fluids," *Fire Technology,* vol. 41, no. 2, pp. 105-123, 2005.

[12] Department of Defense, MIL-STD-810G, Environmental Engineering Considerations and Laboratory Tests, 2008.

[13] A. S. E659-15, "Standard Test Method for Autoignition Temperature of Chemicals," ASTM International, 1978.

[14] Y. Khamliche, "Flammable Fluid Hot Surface Ignition," Rolls Royce Corporation, Indianapolis, IN, 2014.

[15] N. M. Laurendeau and R. N. Caron, "Influence of Hot Surface Size on Methane-Air Ignition Temperature," *Combustion and Flame,* vol. 46, pp. 213-218, 1982.

[16] W. H. Geyer and N. A. Moussa, "Hot Surface Ignition and Fire Suppression Tests in an Aircraft Engine Bay," in *AIAA, 27th Joint Propolsion Conference*, Sacramento, CA, 1991.

[17] R. G. Clodfelter, "Hot Surface Ignition and Aircraft Safety Criteria," in *Aerospace Technology Conference and Exposition*, Long Beach, California, 1990.

[18] S. K. Aggarwal, "A Review of Spray Ignition Phenomena: Present Status and Future Research," *Progress in Energy and Combustion Sciences,* vol. 24, pp. 565-600, 1998.

[19] D. Ballal and A. Lefebvre, "Ignition and Flame Quenching of Qiescent Fuel Mists," *Proceedings of the Royal Society,* vol. A, no. 364, pp. 277-294, 1978.

[20] N. M. Laurendeau and R. N. Caron, "Influence of Hot Surface Size on Methane-Air Ignition Temperature," *Combustion and Flame,* vol. 46, pp. 213-218, 1982.

[21] N. M. Laurendeau, "Thermal Ignition of Methane-Air Mixtures by Hot Surfaces: A Critical Examination," *Combustion and Flame,* vol. 46, pp. 29-49, 1982.

[22] M. Mizomoto, H. Hayano and S. Ikai, "Evaporation and Ignition of a Fuel Droplet on a Hot Surface (Part 1, Evaporation)," *Bulletin of the JSME,* vol. 21, no. 162, 1978.

[23] J. M. Bennett, "Ignition of Combustible Fluids by Heated Surfaces," *Process Safety Progress,* vol. 20, no. 1, pp. 29-36, 2001.

[24] J. M. Bennett and D. R. Ballal, "Ignition of Combustible Fluids by Heated Surfaces," in *41st Aerospace Sciences Meeting and Exhibit*, Reno, Nevada, USA, 2003.

[25] F. Khaled, J. Badra and A. Farooq, "Ignition delay time correlation of fuel blends based on Livengood-Wu description," *Fuel,* vol. 209, pp. 776-786, 2017.

[26] FAA, "AC 33.17-1A- Engine Fire Protection Document Information," FAA, 2009.

[27] S. Davis, D. Chavez and H. Kytomaa, "Hot surface ignition of flammable and combustible liquids," in *SAE Technical Paper Series, Fire Safety*, Detroit, Michigan, 2006.

[28] S. Davis, S. Kelly and V. Somandepalli, "Hot Surface Ignition of Performance Fuels," *Fire Technology,* vol. 46, p. 3630374, 2010.

[29] K. C. Smith and N. P. Bryner, "Short-Duration Autoignition Temperature Measurements For Hydrocarbon Fuels Near Heated Metal Surfaces," *Combustion Science and Technology,* vol. 126, pp. 225-253, 1997.

[30] H. Kopecek, H. Maier, G. Reider, F. Winter and E. Wintner, "Laser ignition of methane - air mixtures at high pressures," *Experimental Thermal and Fluid Science,* vol. 27, no. 4, pp. 499-503, 2003.

[31] S. K. Menon, P. A. Boettcher, B. Ventura and G. Blanquart, "Hot surface ignition of n-hexane in air," *Combustion and Flame,* 2016.

[32] L. D. Pederson, K. K. Nielsen, C. Yin, H. Sorensen and I. Fossan, "Modeling of hot surface ignition wihtin gas turbines subject to flammable gas in the intake," in *Proceedings of ASME Turbo Expo, Turbo machinary Technical Conference and Exposition*, 2017.

[33] G. McTaggart-Cowan, J. Huang, M. Turcios, A. Singh and S. Munshi, "Evaluation of a Hot-Surface Ignition Systems for a Direct-Injection of Natural Gas Engine," in *ASME Internal Combustion Engine Division Fall Technical Conference*, San Diago, CA, 2018.

[34] J. F. Adams, "Minimum Hot Surface Ignition Tmeperature Diagnostics including Infrared Imagery," Purdue University, West Lafayette, IN, 2015.

[35] C. A. Bryce, "An Investigation of Nonequilibrium Effects on Combustion in Supersonic Streams," Purdue University, West Lafayette, IN, 1969.

[36] Anonymus, "NASA Glenn Research Center," NASA, 08 April 2018. [Online]. Available: https://www.grc.nasa.gov/www/k-12/airplane/mflchk.html. [Accessed 2018].

[37] Coordinating Research Council, Inc., Handbook of Aviation Fuel Properties, Warrendale, Pennsylvania: DTIC, 1983.

[38] E. M. Aviation, "World Jet Fuel Specifications with Avgas Supplement," 2005. [Online]. Available: https://web.archive.org/web/20160409022632/http://www.exxonmobil.com/AviationGlobal/Files/WorldJetFuelSpecifications2005.pdf. [Accessed 2018].

[39] A. S. Lubricants, "Safety Data Sheet ROYCO 500 MIL-PRF-23699," chemtura.com, 2015.

[40] A. S. Lubricants, "Dafety Data Sheet Royco 756 MIL-PRF-5606H," chemtura.com, 2017.

[41] T. Edwards, "Reference Jet Fuels for Combustion Testing," in *55th AIAA Aerospace Sciences Meeting*, Grapevine, TX, 2017.

[42] N. B. Siccama and R. K. Westerterp, "Modeling of the Ignition of Ethene-Air Mixtures with a Hot Surface under Flow Conditions," *Industrial and Engineering Chemical Research,* vol. 34, no. 5, pp. 1755-1768, 1995.

[43] S. Sazhin, "Modelling of Heating, Evaporation and Ignition of Fuel Droplets: Combined Analytical, Asymptotic and Numerical Analysis," *Journal of Physics,* vol. 22, 2005.

[44] M. Mizomoto, S. Ikai and A. Morito, "Evaporation and Ignition of a Fuel Droplet on a Hot Surface (Part 2, Ignition)," *Bulletin of the JSME,* 1978.

[45] M. Mizomoto, A. Morito and S. Ikai, "Evaporation and Ignition of a Fuel Droplet on a Hot Surface (Part 3, Effects of Initial Droplet Diameter)," *Chemical Pharmaceutical Bulletin,* vol. 22, no. 171, p. 2091, 1979.

[46] M. Mizomoto, S. Ikai and A. Morita, "Evaporation and ignition of a fuel droplet on a hot surface (Part 4, model of evaporation and ignition)," *Combustion and Flame,* vol. 51, pp. 95-104, 1983.

[47] F. A. Williams, Combustion Theory, Menlo Park, CA: The Benjamin/Cummings Publishing Company Inc., 1985.

[48] A. S. L. F. P. I. a. D. P. D. Theodore L. Bergman, Fundamentals of Heat and Mass Trasnfer, John Wiley and Sons Inc., 2002.

[49] N. M. Laurendeau, "Thermal Ignition of Methane-Air Mixtures by Hot Surfaces: A Critical Examination," *Combustion and Flame,* vol. 46, pp. 29-49, 1982.

[50] M. S. Ulcay, L. N. Dillard, J. P. Gore and P. C. Sweeney, Design of an Experimental Apparatus to Measure Hot Surface Ignition Temperature (MHSIT) of Aviation Fluids, Pasedena, CA: 11th U.S. National Combustion Meeting, 2019.

[51] Coordianted Resaerch Council, Inc., Handbook of Aviation Fuel Properties, Atlanta, Georgia: Coordinated Research Council Incorporated, 1983.

[52] Anonymus, Petroleum UK, 2015. [Online]. Available: http://www.petroleum.co.uk/oil-as-a-lubricant. [Accessed 2018].

[53] S. S. A. a. H.-N. S. Bagherzadeh-Namazi A., "Biodefradation of Used Engine Oil Using Mixed and Isolated Cultures," *International Journal of Environmental Research,* vol. 2, no. 4, pp. 431-440, 2008.

[54] Y. B. Zeldovich, "Regime Classification of an Exothermic Reaction with Nonuniform Initial Conditions," *Combustion and Flame,* vol. 39, pp. 211-214, 1980.

[55] S. Gupta, H. G. Im and M. Valorani, "Classification of Ignition Regimes in HCCI Combustion Using Computational Singular Perturbation," *Proceedings of the Combustion Institute,* vol. 33, pp. 2991-2999, 2011.

[56] K. P. Grogan, S. S. Goldsborough and M. Ihme, "Ignition Regimes in Rapid Compression Machines," *Combustion and Flame,* vol. 162, pp. 3071-3080, 2015.

[57] A. U. S. Takamori, "Behavior of a Flame Ignited By a Hot Spot in a COmbustible Vortex (Vortex-Bursting Initiation Revisited)," *Proceedings of Combustion Institute,* vol. 29, pp. 1729-1736, 2002.

[58] M. S. Ulcay, L. N. Dillard and J. P. Gore, "Empirical Modeling of Minimum Hot Surface Ignition Temperature (MHSIT) of Aviation Fluids," in *AIAA Propulsion and Energy Forum*, Indianapolis, IN, 2019.

[59] A. Chausalkar, S. Kong and a. J. Michael, "Multicomponent drop breakup during impact with heated walls," *International Journal of Heat and Mass Transfer,* vol. 141, pp. 685-695, 2019.

[60] D. A. Kaminski and M. K. Jensen, Introduction to Thermal and Fluid Engineering, Hoboken, NJ: John Wiley & Sons, Inc., 2005.

[61] S. Rehman, "Hot Surface Ignition and Combustion Characteristics of Sprats in Constant Volume Combustion Chamber Using Various Sensors," *Cogent Engineering,* vol. 5, 2018.

[62] S. Takamori and A. Umemura, "Behaviors of a Flame Ignited By a Hot Spot in a Combustible Vortex (Vortex-Bursting Initiation Revisited)," *Proceedings of the Combustion Institute,* vol. 29, pp. 1729-1736, 2002.

[63] A. M. Johnson, A. J. Roth and M. N. Albert, "Hot Surface Ignition Tests of Aircraft Fluids," AF Wright Aeronutical Laboratories, Wright-Patterson Air Force Base, OH, 1988.

VITA

Mehmed Sitki Ulcay received Associates degree from Hudson Valley Community College in Engineering Science and holds Bachelor of Science (B. Sc.) and Master of Engineering (M. Eng.) degrees in mechanical engineering from Rensselaer Polytechnic Institute. He worked as a mechanical engineer at Pro Solution, GMR and GRTC contracting companies for projects at General Electric Global Research Center in Niskayuna, NY ranging from heat transfer applications of microscale electronics cooling projects to high pressure aircraft sealing technologies between 2006 – 2014. He also taught at Hudson Valle Community College (HVCC) as an instructor in Mechanical Engineering Technology department between 2012 – 2015. He taught CAD, Instrumentation, Electricity, Manufacturing Processes, and Senior Design classes while at HVCC.

PUBLICATIONS

1. Ulcay M. S., Dillard L. N., Gore J. P. *"Global Equivalence Ratio Based Hot Surface Ignition in Internal Crossflows"* – manuscript ready, submission in progress

2. Ulcay M. S., Dillard L. N., Gore J. P., Sweeney P. C., *"Machine Learning based Calculations of Minimum Hot Surface Fluid Ignition Temperature"*, 2020 Spring Technical Meeting Central States Section of The Combustion Institute, Huntsville, AL, May 2020

3. Roncancio R., Ulcay M. S., Gore J. P., Arango J. E., *"Experimental study of CO_2 corn stover char gasification using iron nitrate as a catalyst under a high-pressure environment"*, Fuel, Volume 267, May 2020
   doi: 10.1016/j.fuel.2020.117237

4. Ulcay M. S., Dillard L. N., Gore J. P. *"Empirical Modeling of Minimum Hot Surface Ignition Temperature (MHSIT) for Aviation Fluids"*, AIAA Propulsion and Energy Forum, Indianapolis, IN, August 2019
   doi: 10.2514/6.2019-4458

5. Ulcay M. S., Dillard L. N., Gore J. P., Sweeney P. C., *"Design of an Experimental Apparatus to Measure Hot Surface Ignition Temperature (MHSIT) of Aviation Fluids"*, 11th U.S. National Combustion Meeting Organized by the Western States Section of Combustion Institute, Pasadena, CA, March 2019

6. Roncancio R., Ulcay M. S., Gore J. P., Arango J. E., *"Experimental study of CO_2 biomass gasification using iron nitrate as a catalyst under high pressure environment"*, Central States Section Combustion Institute Technical Meeting, Minnesota, USA, May 2018

7. Ulcay, M. S., *"CHF Enhancement of Al2O3, TiO2 and Ag Nanofluids and Effect of Nucleate Pool Boiling Time"*, Proceedings of IEEE ITHERM Conference, Florida, USA, May 2014.

8. Arik M., Ulcay M., *"Sweeping Flow Heat Transfer with Piezoelectric Fans over Vertical Flat Surfaces"*, Proceedings of ASME Summer Heat Transfer Conference, California USA, July 19-23, 2009

9. Thermal Management of Programmable Logic Controllers and Light Emitting Diodes with Synthetic Jets" for Energy and Propulsion Technologies at Thermal Systems Lab, GE GRC publication, 2007. (GE internal publication)

10. Thermal Management of LEDs with Synthetic Jets" for Energy and Propulsion Technologies at Thermal Systems Lab, GE GRC publication, 2006. (GE internal publication)